1/27K

THE AMERICAN MINERALOGIST

JOURNAL OF THE MINERALOGICAL SOCIETY OF AMERICA

Vol. 42 JANUARY–FEBRUARY, 1957 Nos. 1 and 2

STUDIES ON THE CHRYSOTILE AND ANTIGORITE COMPONENTS OF SERPENTINE

George L. Kalousek[1] and Lawrence E. Muttart.[1]

Abstract

The fiber (chrysotile) and adjoining layer of matrix of several specimens of serpentine were compared for differences in chemical compositions, *x*-ray diffraction, specific volume, loss on heating, differential thermal analysis, thermal balance analysis and electron microscopy. The significant difference in composition was a lower Al_2O_3, and also generally Fe_2O_3 and FeO, content of the fiber compared to the matrix. Results of computation of the structural formulas using the method of Duncan McConnell suggested that a small difference occurs in the distribution of the extraneous ions (Al^{3+}, Fe^{3+}, etc.) in the structure of chrysotile and the matrix. The computations indicated that in the case of the fiber, the only extraneous substituent in the silica layer was tetrahedral water ($(H^+)_4$ for Si^{4+}), the other ions apparently assuming octahedral coordination. The silica layer of the matrix, on the other hand, contained small amounts of ions together with the tetrahedral water. Thermal balance and static loss-on-heating results indicate clearly that a small portion of the water is liberated at a higher temperature than that from the brucite layer, and this high-temperature water could be the tetrahedral water suggested by results of the computations.

Electron microscope examinations showed that specimens of the matrix contained "fibers" in form of laths of probably different degrees of curvature, including tubes. The occurrence of chrysotile in tubular crystals was confirmed with a variation not previously reported. The specimen from Eden Mills exhibited curling of lath-like crystals from both edges which apparently resulted in formation of twin tubes. Results of specific volume measurements on a massive sample of this mineral indicated negligible voids precluding a tubular morphology. Since the subdivided fibers occurred in form of tubes it may be assumed that these form during the grinding of the specimen.

I. Introduction

Results of investigations in recent years (1, 2, 3, 4, 5, 6) on the morphology of chrysotile show that the fibers occur in the form of tubular crystals. Antigorite on the other hand in microscopically detectable particles occurs in platy crystals. Bates and Mink (7) advanced the hypothesis, on the basis of Pauling's (8) theory of "misfit" between layers as being the fundamental cause of curvature; that the crystals of antigorite tended to be flat because of the presence of extraneous ions which relieved the stress. Roy and Roy (9) studied the effects of substitutions of ions on the morphology of synthetic serpentines and showed that the crystal habit, platy or tubular, was related to the size of the substituent ion.

---

[1] Research Department, Owens-Illinois Glass Company, Toledo, Ohio.

The present study was undertaken to examine the possible effects of the extraneous constituents in mineral serpentines on their properties. The specimens, from different localities, consisted of veins of chrysotile between adjoining layers of the matrix. The results of complete chemical analysis, *x*-ray diffraction, electron microscopy, differential thermal analysis, thermal balance analysis, static loss on heating and specific volumes are given in this report.

II. MATERIALS AND PROCEDURES OF TEST

1. Materials

The minerals used in this study and related information on them are given in Table 1. As noted, most of the fiber and matrix pairs were obtained from the National Museum, others were purchased from Ward's Natural Science Establishment. Fibers for special tests were purchased on the open market. The specimens from Quebec varied considerably one from the other in physical characteristics.

TABLE 1. MINERALS USED IN PRESENT STUDY

Designation or name	Locality	Supplier and supplier's No.
Fiber and Matrix	Eden Mills, Vt.	Wards[a]
Fiber and Matrix	Delaware Co., Pa.	N.M.[b] R 4658
Fiber and Matrix	Aboutville, N. Y.	N.M. 9143
Fiber and Matrix	Globe, Arizona	N.M. R 4654
Fiber and Matrix	———, Quebec	N.M. 18,879
Fiber and Matrix	———, Quebec	N.M. 107,853
Fiber and Matrix	Montville, N. J.	N.M. R 4656
Yu Yen Stone	Manchuria, China	N.M. 94356

[a] Ward's Natural Science Establishment.
[b] National Museum, Washington, D. C.

The matrix immediately adjoining the veins of fibers was cut to a thickness of $\frac{1}{4}$ inch and then crushed finely. These are the samples, with one exception, to be mentioned, used in the present study.

2. Procedures

X-ray diffraction was recorded with either a North American Philips wide angle Geiger-counter unit or with cameras of 57.3 mm. radius. Filtered CuKα radiation obtained with excitation of 35 K.V.P. at tube current of 17 ma. was used exclusively. Rates of scan for Geiger-counter recording ranged from 1° to 1/8° per minute, in 2θ.

The matrix specimen for the electron microscope mounts were finely subdivided by repeated grinding in a mortar with a pestle. The fibers for this purpose were dispersed in aqueous suspension with a Waring Blendor. The photographs were taken using an R.C.A., Universal Model, Electron Microscope at magnifications up to 9,900 ×.

Specific volumes were determined with Gay Lussac flasks of 10 ml. and 100 ml. capacity in water at 35° C., controlled to ±0.05° C. Water and CCl_4 were used alternately as density media, and the samples ranged from one to five grams in weight. Temperatures were recorded to ±0.025° C. and weighings to about 0.1 mg.

Precautions, as follows, were observed in this phase of the study. Each flask was standardized with both density media, at the temperature used. To insure surface wetting of the samples, one drop of "Tergitol"[a] was added to the water in each determination. The liquids were admitted to the flasks containing the specimen under partial vacuum. A stoppered desiccator provided with a thistle tube and stopcock was used for filling the flasks. The fiber-matrix pairs were always tested concurrently.

Specimens used for determining the specific volume of massive chrysotile (in compact condition as occurring in the vein) were cut into pieces of 0.7 to 1.0 inch-square cross sections parallel to the fibers, the fibers being held intact by the layers of matrix still present at the extremities of the fibers. The matrix was then trimmed back so that the fibers had a protective layer of about 1/16 to 3/32 inch of the matrix. The veins ranged from 5/8 to 7/8 inch in thickness. The specimens, after overnight drying at 100° C., were exposed to the laboratory air for about two weeks before weighings and measurements were taken. After completion of these tests, the specimens, wrapped in glazed paper, were crushed carefully in a vise in order to separate matrix from fibers. The volume of the matrix, assumed to be void free, was computed from its weight and density and the value obtained subtracted from the measured volume of the composite specimen.

The differential thermal analysis (*DTA*) equipment used in the present study has been described (10). In order to obtain results that could be compared without need of allowing for variations due to equipment, all samples were tested in the same cell starting with a cold furnace. The same weight of fiber and matrix obviously could not be used at a fixed volume due to the bulking effects inherent in the fibers. The samples for tests, amounting to 1.00±0.10 g. of matrix (passing a No. 20 sieve and

[a] Sulfate derivative of 3.9 diethyl tridecanol-6.

retained on No. 50 sieve) and 0.60±0.05 g. of fibers were packed in the cell with a minimum of crushing of "bundles" about 0.02 to 0.05 inches in diameter, following a set procedure to minimize possible variations in degree of compaction from sample to sample.

Chemical analyses were made according to standard methods.

Loss-on-heating curves were determined in a laboratory furnace, the temperatures being obtained with chromel-alumel thermocouples located near the crucibles. A period of twenty-four hours was allowed for attainment of equilibrium at each temperature. Some small deviation from equilibrium may have occurred between temperatures of about 500 to 600° C., but because the samples were heated together, the data are comparable.

III. Results and Discussions

1. Oxide Composition of Minerals

The results of chemical analysis of the serpentines for 19 constituents are given in Table 2. These data show that the Al_2O_3 content of the matrix was always higher than that of the fibers for each serpentine sample. Also, the sum of the moles of the extraneous constituents was invariably higher for the matrix than for the fibers for any given serpentine. One correlation based on the total amounts of Al^{3+}, Fe^{3+} and Fe^{2+} ions is given later in this report.

In order to ascertain how the composition of a given serpentine might vary from one section to another, a specimen consisting of a layer of matrix between two veins was analyzed. The 3.0 inch thick layer of Eden Mills matrix was cut into five sections of equal thickness and these are marked consecutively *M-1* to *M-5*. The results are given in Table 3. The fiber-matrix pairs at the two extremities of the specimen showed the same trends as manifested by those listed in Table 2. The variations in the amounts of the constituents in zones *M-2*, *M-3*, and *M-4* were large, indicating possible presence of some other phase, probably a chlorite. One may note especially the high magnesia and low water contents of samples *M-3* and *M-4*.

In the application of analytical data, the possible presence of impurities becomes a problem. The serpentine specimens from Globe, Arizona, and Eden Mills, Vermont, contained a second phase, possibly chlorite and magnesite, respectively. The Montiville fiber also probably contained an unidentified impurity. The other specimens were assumed to be homogeneous phases, that is, the extraneous ions were considered to be lattice constituents. On such assumption, the following computations were made.

Attempts to calculate structural formulas from the analytical data

TABLE 2. OXIDE COMPOSITIONS OF FIVE PAIRS OF SERPENTINE AND ONE ANTIGORITE

	Delaware Co. Pa. N.M. R 4658		Aboutville, N. Y. N.M. 9143		Globe, Arizona N.M. 4654		Quebec, Canada N.M. 18879		Montville, N. J. N.M. 4656		Antigorra N.M. 96917
	Matrix	Fiber	Matrix	Fiber	Matrix	Fiber	Matrix	Fiber	Matrix	Fiber	Matrix
SiO_2, %	42.40	42.50	41.80	41.80	26.80	43.00	41.52	41.70	42.02	41.88	41.30
Al_2O_3	.74	.32	.19	.11	.42	.27	.57	.24	.49	.19	1.59
Fe_2O_3	.48	.50	.93	.68	1.13	1.08	.36	.30	1.50	.81	3.61
FeO	.043	.010	.06	.05	.22	.17	.06	.05	.057	.05	4.51
MgO	42.70	42.50	42.67	42.82	25.00	40.00	42.80	42.85	42.05	41.38	36.30
Ign., Loss	13.52	13.46	13.88	14.04	14.85	13.17	14.36	14.23	13.74	14.22	11.19[a]
SO_3	.00	.00	.08	.09	.00	.01	.02	.02	.07	.31	.06
TiO_2	.070	.021	.10	.05	.022	.020	.06	.03	.073	.036	.15
CO_2	.11	.14	.04	.01	9.98	.78	.00	.07	.06	.02	.03
Cr_2O_3	.008	.004	.003	.003	.006	.005	.01	.005	.001	.005	.30
CaO	.01	.04	.19	.10	21.00	1.43	.11	.05	.26	.47	.43
MnO	.02	.02	.04	.04	.12	.16	.04	.02	.024	.05	.11
NiO	.00	.00	.00	.00	.00	.00	.00	.00	.002	.00	.26
CuO	.05	.01	.00	.00	.05	.03	.05	.02	.00	.00	nd.
Na_2O	.03	.04	.02	.03	.03	.03	.03	.07	.02	.06	.04
K_2O	.02	.02	.01	.01	.03	.02	.02	.01	.014	.023	.02
Loss at 110° C.	.26	.65	.24	.28	.16	.53	.60	.83	.32	.60	nd.
Total, %	100.55	100.23	100.25	100.11	99.82	100.71	100.55	100.51	100.70	100.10	99.90

[a] Includes loss at 110° C.

Table 3. Oxide Compositions of Serpentine Specimen from Eden Mills Consisting of a Layer of 3 Inches of Matrix between Two Veins of Fibers Cut into Layers .6 Inch Thick

	Fiber	M-1	M-2	M-3	M-4	M-5	Fiber
SiO_2	38.38	36.78	37.96	40.56	40.42	36.88	39.96
Al_2O_3	0.44	1.67	1.47	1.53	0.34	1.48	.64
Fe_2O_3	6.19	6.01	3.83	3.50	1.81	5.87	4.30
FeO	1.30	1.81	2.09	2.78	2.42	1.69	1.30
MgO	39.90	39.75	41.90	43.10	43.90	39.80	41.00
Loss (1100° C.)	13.26	13.26	11.94	8.81	10.21	13.69	12.88
SO_3	0.14	0.14	0.10	0.12	0.11	0.10	0.10
TiO_2	0.03	0.05	0.02	0.02	0.02	0.03	0.072
CO_2	—	—	0.19	0.18	0.18	0.14	0.00
Cr_2O_3	0.11	0.31	0.25	0.26	0.24	0.33	0.12
CaO	—	—	0.03	0.03	0.04	0.03	0.04
MnO	0.08	0.09	0.12	0.15	0.13	0.10	0.08
NiO	0.10	0.22	0.18	0.13	0.12	0.10	0.06
Na_2O	0.02	0.03	0.03	0.04	0.02	0.04	0.02
K_2O	—	—	0.04	0.03	0.03	0.03	0.02
Loss (110° C.)	0.28	0.21	—	—	—	—	.38[a]
Total, %	100.23	100.33	100.15	100.26	99.99	100.31	100.97

[a] Loss at 150° C.

following conventional methods gave unsatisfactory results. Application of the method of McConnell (11) which is based on the assumption that a portion of the water, designated as tetrahedral water, is substituted for the silica ($(H^+)_4$ for Si^{4+}) similarly as in the hydrogarnets, gave some striking results. The data are given in Table 4. In these computations, it is assumed that the silica layer is completely filled, there being 2.000 moles of the cations. Since the analytical results did not give the indicated total, the deficiency was made up by assuming that the excess water, as indicated in the calculations, was substituted in the silica layer. Any further deficiency from the required value of 2.000 was subtracted from the sum of the cations in the brucite layer without regard to kind.

The computed results in Table 4 show that tetrahedral water is the only substituent for Si^{4+} in the silica layer of chrysotile, the total of cations being very close to a value of 2.000. The calculations of the antigorite formula indicate, on the other hand, that a small but apparently real amount of substituents other than the water are present in the silica layer of this mineral.

After the deductions were made, the brucite layer of both minerals

TABLE 4. ION DISTRIBUTIONS IN OCTAHEDRAL AND TETRAHEDRAL POSITIONS IN ANTIGORITE AND CHRYSOTILE CALCULATED BY THE METHOD OF DUNCAN MCCONNELL (11)

Ion	Delaware Co., Pa.		Aboutville, N. Y.		Quebec #18879		Montville, N. J.	
	Matrix	Fiber	Matrix	Fiber	Matrix	Fiber	Matrix	Fiber
Mg^{2+}	2.924	2.937	2.922	2.937	2.915	2.935	2.873	2.820
Fe^{3+}	.017	.017	.032	.024	.012	.010	.052	.021
Fe^{2+}	.002	.003	.003	.001	.003	.002	.002	.001
Al^{3+}	.040	.017	.007	.006	.031	.012	.027	.013
$R \pm R^{4+}$[a]	.009	.007	.026	.016	.027	.017	.034	.064
	2.992	2.981	2.990	2.984	2.988	2.976	2.989	2.919
Tetrah. Reg.[b]	.012	.001	.013	.000	.004	.000	.008	.001
Octah. Total	2.980	2.980	2.977	2.984	2.984	2.976	2.981	2.918
Si^{4+}	1.950	1.961	1.921	1.921	1.900	1.915	1.940	1.914
$(H^+)_4$	.038	.038	.066	.079	.096	.085	.052	.085
Debit[c]	.012	.001	.013	.000	.004	.000	.008	.001
Tetrah. Total	2.000	2.000	2.000	2.000	2.000	2.000	2.000	2.000

[a] Summation of all ions other than those listed in the table.

[b] The amounts of ions required for completing the silica layer are subtracted from the total amount assumed to occupy the octahedral position.

[c] Amount of ion required to fill all tetrahedral positions.

showed a balance very close to a value of 2.980 except for the Montville fiber, this being 2.919. Some uncertainty regarding the computed result occurs because of the relatively large amounts of CaO (0.47%) and SO_3 (0.31%), the SO_3 was not counted in either the fiber or matrix computations. Because of the uncertainty regarding the manner in which the CaO and SO_3 are combined, the computed results on the fiber of the Montville serpentine cannot be interpreted rigorously.

2. *X-ray Data*

The *x*-ray data of five fiber-matrix pairs are given in Table 5. Each result represents the average value of 2 to 5 measurements. A distinguishing feature of these data is a generally richer and sharper pattern for the matrix compared to that of the fiber. Also small spacing differences in the 4.3 to 4.8 Å region are evident in the results of the matrix samples.

A specific feature of the data generally serving to differentiate between the chrysotile and matrix is the ratio of the intensities of the line at 7.3

TABLE 5. X-RAY DIFFRACTION DATA FOR FIBROUS AND MATRIX COMPONENTS OF SERPENTINE FROM DIFFERENT LOCALITIES. EACH PATTERN IS THE AVERAGE OF 2 TO 5 MEASUREMENTS OBTAINED ON FILM OR WITH GEIGER-COUNTER RECORDER

Delaware, Pa.				Aboutville, N. Y.				Globe, Ariz.				(N.M. 18879) Quebec, Canada				Montville, N. J.			
Fiber		Matrix		Fiber		Matrix		Fiber		Matrix[a]		Fiber		Matrix		Fiber		Matrix	
I/103[b]	d, Å	I/77	d, Å	I/36	d, Å	I/80	d, Å	I/35	d, Å	I/45	d, Å	I/108	d, Å	I/125	d, Å	I/138	d, Å	I/158	d, Å
				.15	13.4											.01	11.1	.08	11.1
				.15	10.2			.1	11.3										
		.05	8.1	.06	7.8			.1	8.7							1.0	7.11	1.0	7.25
1.0	7.37	1.0	7.32	1.0	7.28	1.0	7.28	1.00	7.31	1.00	7.31	.91	7.34	1.00	7.35				
vw[c]	6.6	vvw	6.8	.08	6.8			.1	6.6							.04	5.8		
vw	5.75																		
								.1	4.77										
		.25	4.58			.2	4.60					.15	4.60	.25	4.63	.04	4.55	.15	4.55
.15	4.53	.14	4.53					.15	4.53	.13	4.53			.10	4.52				
				.10	4.51	.2	4.52					.10	4.48	.05	4.48				
.15	4.47			.11	4.45							.15	4.45						
.15	4.44					.1	4.42	.2	4.41							.13	4.37		
				.10	4.37														
				.05	4.29	.05	4.31					.15	4.43						
								.1	3.95							.92	3.63	.59	3.63
1.0	3.66	.66	3.64	.88	3.64	.69	3.65	.85	3.63	.67	3.66	.89	3.66	.73	3.63				
								.05	3.20										
vw	2.93							.1	3.02										
								vvw	2.88										
						.01	2.63												
				.05	2.58									.05	2.66	.07	2.61		
						.10	2.54							.05	2.62				
						.25	2.50												
w	2.45	.35	2.46			.20	2.46											.28	2.50
				.10	2.42			ms	2.42					.40	2.51				
				.05	2.37											.10	2.42	.03	2.43
		.1	2.15			.08	2.16					.07	2.44						
																		.12	2.14
w	1.84	.05	1.85	.05	1.82	.06	1.83	m	1.82					.10	2.16				
																.06	1.82	.05	1.86
								ms	1.52			.03	1.83	.05	1.80	.03	1.77		
m	1.54	.2	1.54	.10	1.53			m	1.46									.15	1.58
vw	1.46	.1	1.50	.05	1.46									.05	1.55	.13	1.53	.08	1.57
		w	1.31	.05	1.31			mw	1.22					.25	1.54				
vw	1.22																	.06	1.34
																		.04	1.31

---

[a] Pattern not completely reported because of large amount of impurity

[b] Intensities are given as the ratio of each line to the strongest line, which is designated in counts per second.

[c] The abbreviations: w—weak, m—medium, s—strong, and v—very, apply to the comparative intensities of lines in film recording.

Å to that at 3.6 Å, referred to as the $I_{7.3}/I_{3.6}$ ratio. In Fig. 1 these ratios are plotted against the total number of moles of Al^{3+}, Fe^{3+} and Fe^{2+} for seven fiber-matrix pairs. The values for each pair are connected by a line. The values of the ratios ranged from about 1.0 to 1.2 for the fibers and about 1.3 to 1.8 for the matrix specimens. Four other fiber-matrix pairs of other serpentines, which were not analyzed, were also observed to manifest a similar variation in the $I_{7.3}/I_{3.6}$ ratios. The values for all specimens ranged from 0.80 to 1.40 for the fibers and 1.27 to 2.40 for the matrix. Because of the overlapping of the values for the fiber and matrix in the range between about 1.27 and 1.40, these values alone are not suitable for differentiating between fibers and matrix. However, in every

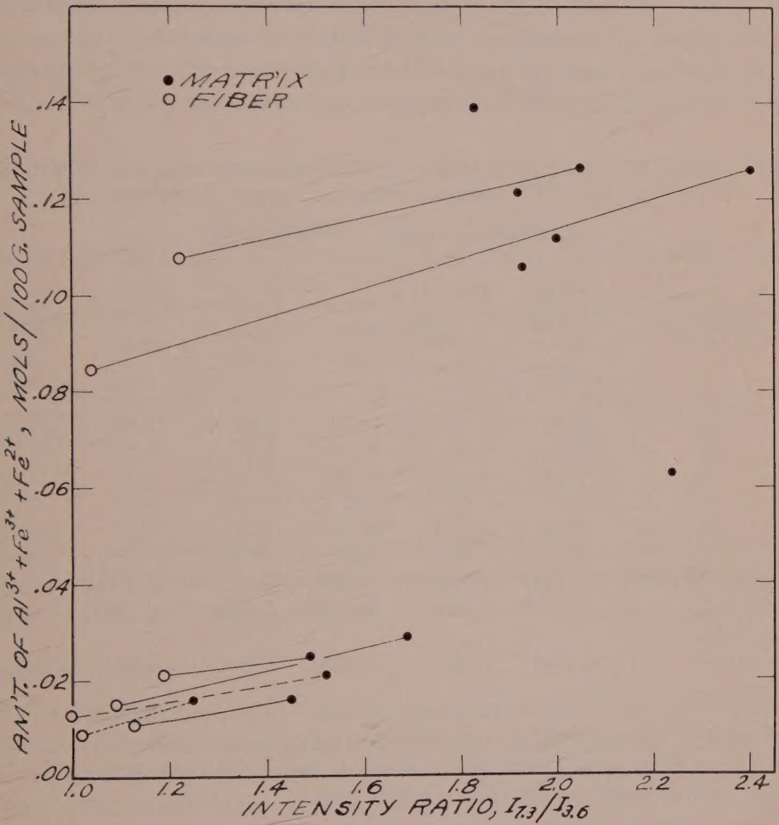

Fig. 1. Plot of the total Al^{3+}, Fe^{3+} and Fe^{2+} contents of serpentine samples and the ratios of the intensities of lines at 7.3 Å and 3.6 Å ($I_{7.3}/I_{3.6}$).

sample of serpentine examined, the value of the $I_{7.3}/I_{3.6}$ ratio was invariably higher for the matrix than for the fiber.

3. *Specific Volume*

The specific volume values for the three fiber-matrix pairs containing the lowest amounts of impurities were consistent and the average value of 15 determinations on the fibers was 0.392, and average of six values on the matrix was 0.398. It appeared worthwhile to compare these values with those calculated from the unit cell on a product of ideal composition, $3MgO \cdot 2SiO_2 \cdot 2H_2O$, and the values so calculated are given in Table 6.

TABLE 6. TABULATION OF UNIT CELL SIZES, IN K*x* UNITS, BY WHITTAKER (12) AND COMPUTED DENSITY FUNCTIONS OF CHRYSOTILE AND ANTIGORITE

(In these calculations, 1 Å = 1.00202 K*x*)

Parameter or function	Warren & Bragg chrysotile	Warren & Hering chrysotile	Aruja chrysotile	Padurow chrysotile	Whittaker chrysotile	Aruja antigorite
a_0	14.66	7.33	14.62	7.36	14.65	7.265
b_0	18.50	9.24	9.2	9.26	9.2	9.238
c_0	5.33	5.33	5.32	5.33	5.33	5.42[a]
α	90°	90°	90°	92°50′	90°	90°
β	93°16′	93°16′	93°12′	93°11′	93°7′	91°24′
γ	90°	90°	90°	89°50′	90°	90°
Calculated Density[b]	2.533	2.535	2.558	2.522	2.548	2.513
Specific Volume	0.3948	0.3945	0.3909	0.3965	0.3925	0.3979
Ratio Specific Volumes Matrix: Fiber	1.008	1.009	1.018	1.004	1.014	(Unity)

[a] The eight-fold multiplication along the c axis gives a value of $c_0=43.39$.

[b] Calculations were performed using Avagadros number, $N=6.06\times10^{-23}$ so that direct comparison with Aruja's original results may be made.

The results of 0.394 and 0.398 for chrysotile and matrix (antigorite) are in good agreement with the experimentally determined values. Results of 0.381 and 0.378 for the specific volume of the fiber and matrix, respectively, of the Eden Mills, Vermont, serpentine are lower than those given because of the higher amounts of iron present in this sample.

The results obtained with water and CCl_4 showed good agreement, within 1.0 per cent, for the fibers only. The matrix specimens gave consistently higher values in CCl_4, by 3.00±0.75 per cent, than in water. The only apparent explanation which can be made is that all voids in fibers and matrix were filled with water, but not all with CCl_4 in the matrix.

The apparent specific volumes of three massive chrysotile specimens are given in Table 7. The Eden Mills fibers contained only 1.0 per cent voids compared to 12.5 per cent for the Globe fibers. One may safely assume that the Eden Mills fiber with so low an amount of voids could not occur as tubular fibers or even solid round rods (the void volume for rods of uniform diameter in closest possible packing amounts to 9.3 per cent). On the other hand, the entire Globe specimen, and a portion of the Delaware specimen could occur as small bore capillaries. Pundsack (13) who used a different technique in preparation of the test specimens than described here for void-volume measurements observed voids amounting to only few per cent of total volume.

TABLE 7. APPARENT AND ABSOLUTE SPECIFIC VOLUMES OF SPECIMENS OF SERPENTINE CONSISTING OF THICK LAYERS OF FIBERS BETWEEN THIN LAYERS OF MATRIX, AND AMOUNTS OF VOIDS IN THE FIBERS

Specimen	Specific volume		Amount fibers % by vol.	Voids by % of app. vol.
	Apparent, cc./g.	Absolute, cc./g.		
Eden Mills	.386	.383	77	1.0
Delaware County	.422	.394	80	8.2
Globe, Ariz.	.440	.394	84	12.5

4. Loss on Heating

Representative loss-on-heating curves are presented for two samples of fiber-matrix components of serpentine in Fig. 2. The losses are referred to a constant weight obtained on drying at 135° C. Two other specimens of fiber and matrix (Globe, Arizona and commercial grade of Quebec chrysotile) showed curves intermediate between the respective ones shown in Fig. 2.

The two matrix specimens manifested a small continuous loss up to about 450° C. and this was followed by a large loss in the temperature interval from 450° to about 550° C. These specimens also showed a second but comparatively small inflection between approximately 550° and 600° C. This suggests that a portion of the water was held somewhat more strongly than that given off at the lower temperature. Such a two-step dehydration was not observed for the fiber. In comparing further the curves of the fiber to those of the matrix, it is seen that the fibers in both pairs of specimens lost the water at higher temperatures than did the matrix specimens. It follows, therefore, that the major amount of water is more tightly bound in the chrysotile component than in the matrix.

The loss-on-heating curves indicate a small but apparently real difference in the binding strength of water in the fiber and matrix.

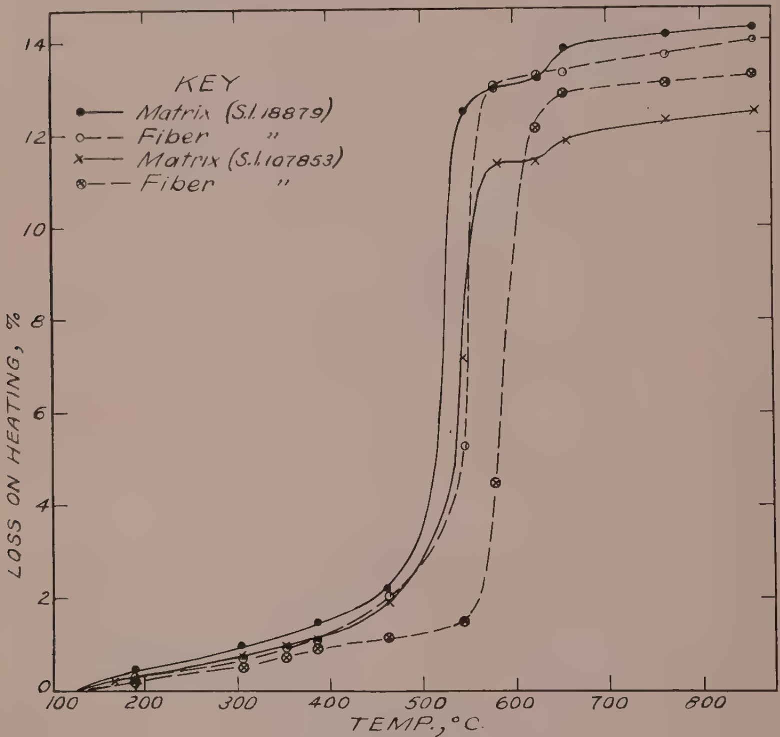

FIG. 2. Loss on heating curves.

5. *Differential Thermal Analysis*

The *DTA* results on six pairs of serpentine specimens did not show any definite trends which could serve to differentiate between fiber and matrix. The principal thermal effects, accompanying the dehydration of the brucite water, and the subsequent exothermic peak, varied about equally among the samples with no relation to sample origin. In general, the temperature interval between completion of dehydration of the brucite water and the start of the exothermic reaction was slightly larger for the fiber than for the matrix. However, due to the uncertainties of definitely measuring this difference, reproduction of the *DTA* results does not appear to be justified.

6. *Thermal-Balance Analysis*

In view of the loss-on-heating results, and the possible difference in the temperature gap, just mentioned, between the fibers and matrix, it seemed desirable to obtain further information on the dehydration of the serpentine pairs in the form of thermal-balance curves. The thermal-balance gives the loss in weight, in a continuously recorded curve, as a function of temperature. The tests were performed on three serpentine pairs at the Bureau of Reclamation, Denver, Colorado, under direction of Dr. R. C. Mielenz. The samples were heated at a temperature-rise rate of 5° C. per minute.

The result of most interest is the amount of water lost at high temperatures. The thermograms were examined for inflections in regions of high temperatures, and the temperature at which the "high-temperature" water started to be driven off was taken at the point where the tangent to the curve first begins a negative (clockwise) rotation. These points generally were not easily located but may be considered to represent fairly closely the temperature at which the liberation of the high-temperature water started. The results are summarized in Table 8 along with the identification of the specimens. The temperatures at which the high-temperature water started to come off were approximately the same for the two components of each serpentine sample, but varied among the serpentines. Dehydration was complete at about 900 to 940° C. The amounts of the high-temperature water ranged from 0.60 to 0.93 per cent by weight of the sample exposed to laboratory air.

The curves for the Quebec serpentine (National Museum 18879) are presented in Fig. 3 in terms of percentage loss in weight in order that

TABLE 8. SUMMARY OF THERMAL BALANCE RESULTS ON SERPENTINE SAMPLES

Sample	Loss on ignition %[a]	Temp. range of "high-temp. water" ° C.	Amount "high-temp. water" %[a]	Calc. amt. of $(H^+)_4$ in mols, (Table 4)
Quebec Matrix N.M. 18,879	14.59	745–1000	.93	.096
Quebec Fibers N.M. 18,879	14.80	763–1000	.74	.085
Delaware Co., Pa. Matrix	13.33	816–1000	.67	.038
Delaware Co., Pa. Fibers	13.58	811–1000	.76	.038
Eden Mills, Matrix	12.77	788–1000	.71	
Eden Mills, Fibers	12.17	796–1000	.60	

[a] The amount of water, in per cent, is based on the weight of the sample in equilibrium with air in the laboratory.

direct comparison to the loss-on-heating curves could be made. These curves, and those of the remaining samples, failed to show a second step dehydration as did two of those shown in Fig. 2 in static loss-on-heating tests. Apparently the rate of heating affects the manner in which the high-temperature water is lost.

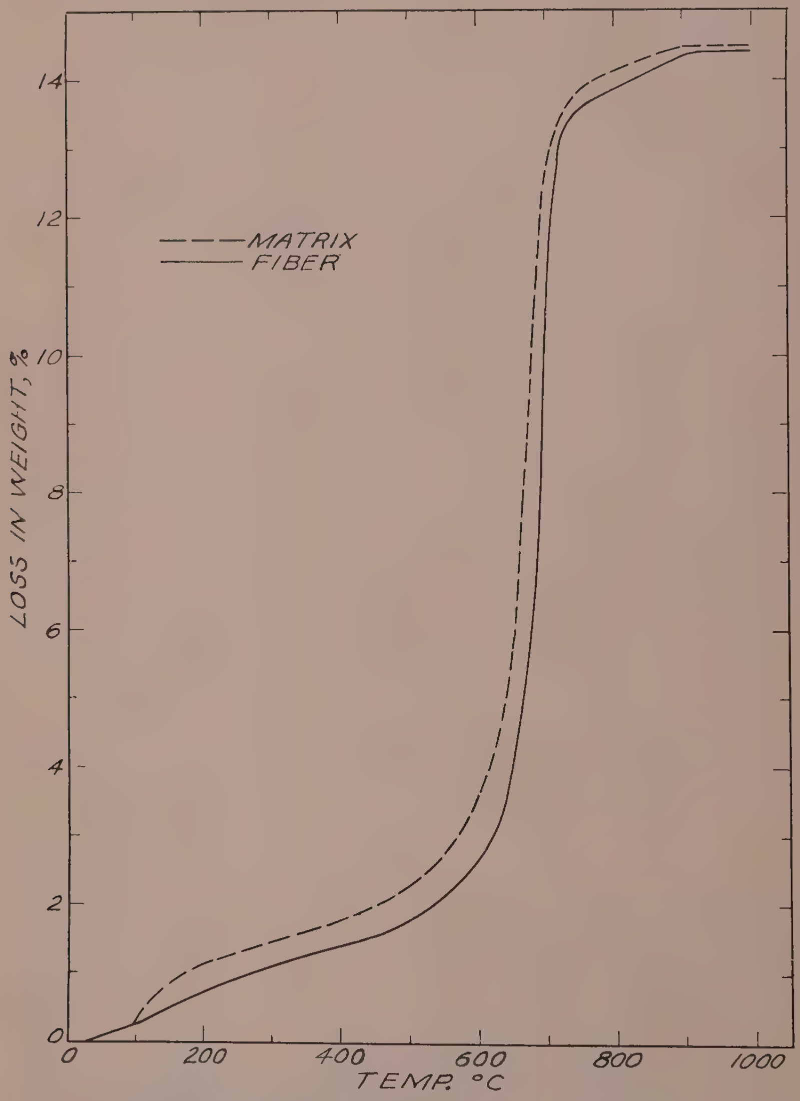

FIG. 3. Thermal-balance results on serpentine (Quebec, N.M. 18879), the loss being expressed in percentage.

The amount of high-temperature water can be determined only approximately because the temperature at which this water starts to be given off probably coincides with that at which loss of the other is still occurring. The possibility that the high-temperature water and tetrahedral water are the same, as suggested by computations based on McConnell's methods would seem to merit further study. Quantitative substantiation of the hypothesis based on the observed and calculated amounts of high-temperature water is not indicated by the present data. This is not surprising because of possible variations in amounts of surface adsorbed water at time of testing the samples, and the possible simultaneous loss of high-temperature water and the principal water of hydration. Nevertheless, there can be little doubt, if any, that the dehydration takes place in two stages and there is a qualitative relationship as indicated by a comparison of the last two columns of Table 8 which suggests the presence of tetrahedral water in the serpentines.

7. *Electron Microscopy*

The pairs of serpentine from Eden Mills, Delaware County, Quebec (N.M. 18879), the Globe fibers and Yu Yen Stone were examined with the electron microscope. The examinations confirmed the previously observed (1, 2, 3, 4, 5, 6) tubular crystalline habit with exception of certain variations in the Eden Mills fibers to be described.

The Yu Yen Stone, microscopically of a clearly platy crystalline habit, was examined after prolonged grinding. The crystals in massive form and in fragments manifested the usual laminar habit. However, crystals having appearance of tubes or curved laths were abundantly present in the lighter fraction of the suspended sample. The electron micrograph in Fig. 4 illustrates the morphology of this mineral. The Eden Mills matrix contained a high proportion of fibrous crystals which at highest magnification appeared like partially curved laths. The fibers also contained some crystals manifesting a trough-like appearance. The required higher resolution for study of this detail was realized by Joseph G. Sayre on the electron microscope at Owens-Corning Glass Company, who examined this specimen and the Globe and Delaware County chrysotile.

The examination of the Globe and Delaware County specimens revealed presence of capillaries of apparently small bore as illustrated in Fig. 5. The specific volumes of massive specimens of these two minerals suggested presence of voids which could be those between fibers and the pores.

In Fig. 6 is shown a fiber, between two others, of the Eden Mills chrysotile which is considered to manifest a cross section similar to a trough. Curvature apparently occurred simultaneously from both edges

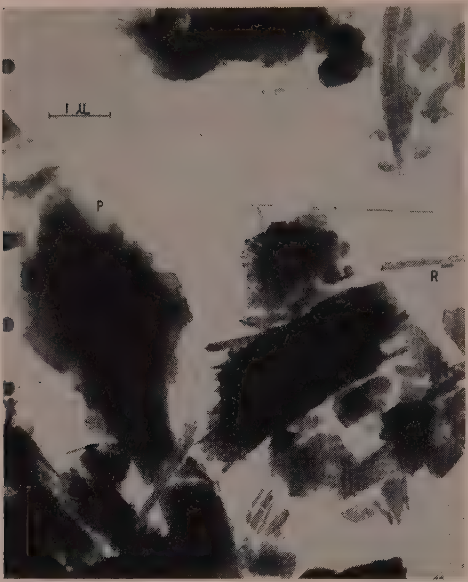

FIG. 4. Electron micrograph of finely powdered Yu Yen Stone (P=plate and R=rolled plate or lath).

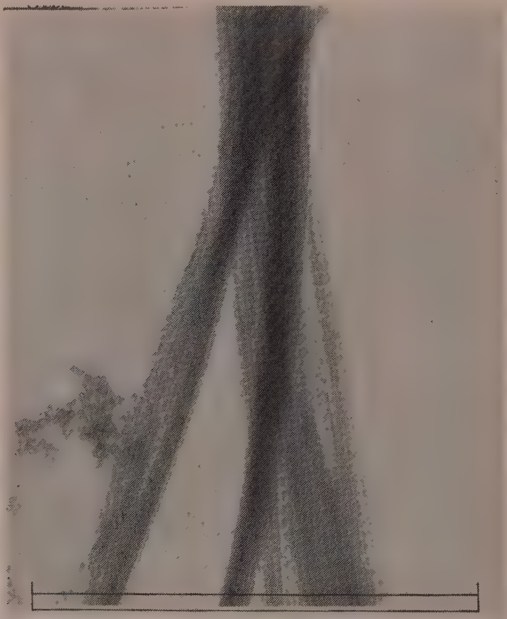

FIG. 5. Electron micrograph of tube-like fibers of Globe, Ariz., chrysotile.

of a lath but was arrested. If curling of a lath from two edges occurs the individual crystals for completely rolled crystal should consist of two tubes. Figure 7 includes some of the assumed double tube fibers which had been twisted. The immediate area of the twisted fiber is reduced in size and the photographic image is darker. The observed effect could be due to the presence of a double tube fiber rolled from the edges of a single crystal. Figure 6 also contains possibly a shred of a single fundamental layer which is apparent in the form of a twisted ribbon-like fiber in the upper part of the figure and extends from the first to the third fibers.

In the bottom of Fig. 8 are seen six fibers which further illustrate the apparent double tube morphology of the Eden Mills chrysotile. The first three fibers from the left are smaller in diameter and also of reduced photographic intensity compared to the next two. Judging by the increased size and darkness of the image, it may be that the latter two fibers consist of two elemental crystal sheets. The sixth fiber appears also to consist of two layers, one of the single layers on the left being incompletely curled.

A total of 209 measurements were made of the fiber diameters of both chrysotile and matrix using micrographs at 50,000× magnification. Statistical treatment of the data, through size distribution frequencies, indicate that two (or perhaps even three) sizes obtained for the fibers as shown in Fig. 9. The lower distribution mode of fiber diameters for both the chrysotile and matrix, centered at about 340 Å, represents the range in apparent fiber diameter. The upper mode, centered at about 650 Å, is possibly a function of "fibril" size distribution. The presence of two functions may indicate, as already deduced, that the fibers were double tubes or formed from sequential layers. The previously reported fiber diameters (3, 14) fall only somewhat below the most probable size of 340 Å shown in Fig. 9. The fiber size probably is dependent, at least in degree, on the specimen origin. The data of this study indicate an upper value of about 400 to 500 Å and a lower value of about 100 Å for diameters of single fibers.

IV. INTERPRETATIONS

Results of oxide compositions and structural formulas computed by the McConnell method suggest that small but real differences exist between chrysotile and matrix of a given serpentine. The matrix may contain a higher concentration of extraneous ions in the brucite layer and possibly also a small amount in the silica layer. The chrysotile on the other hand may contain only $(H^+)_4$ as a subsituent for the Si^{4+} ion, no other substitution occurring in the silica layer. The computations and results of experiments on water content indicate that the amount of the high-temperature

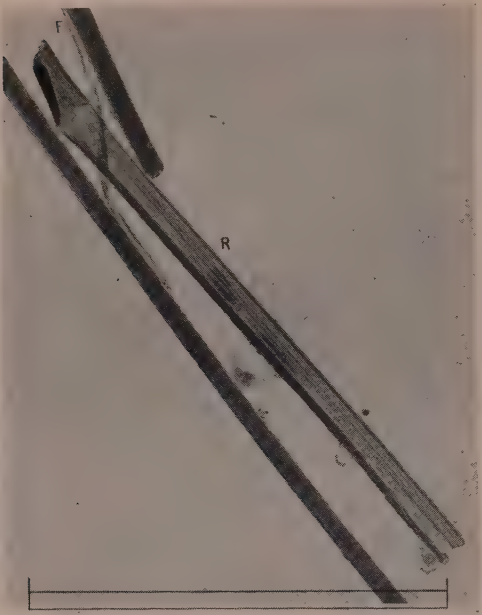

FIG. 6. Electron micrograph of Eden Mills chrysotile showing a partially rolled lath (*R*) and fragment of single layer (*F*).

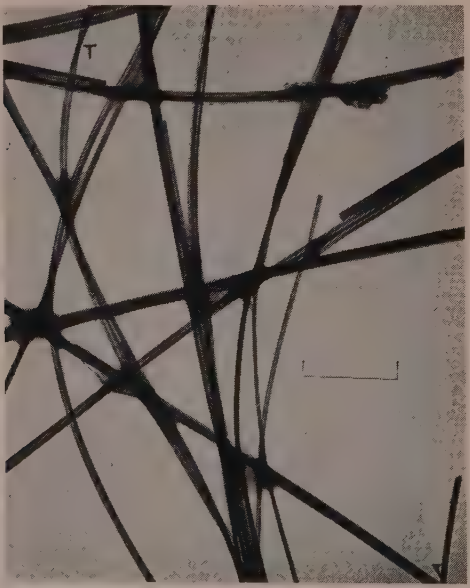

FIG. 7. Electron micrograph of Eden Mills chrysotile showing apparent double tube crystals, some being twisted (*T*).

(supposedly tetrahedral) water are about the same for both matrix and fibers of a given serpentine, and therefore would not be expected to affect the morphology.

The small differences in the amounts of Al^{3+} (and Fe^{3+}, Fe^{2+}, etc.) ions apparently correlate with crystal habit. These results substantiate at least qualitatively, the hypothesis by Bates and Mink (7) that the Al^{3+} ions stabilize the laminar structure of the matrix. Roy and Roy (9) advanced the hypothesis that the R_2O_3 content of natural antigorite (matrix) should be higher than that of the chrysotile. The present results confirm that theory. In this connection, the results on the Eden Mills chrysotile which probably contained more structurally bound Al^{3+} and other ions than the other serpentines studied, are interesting because of the general tendency of this chrysotile to occur in laminar crystals.

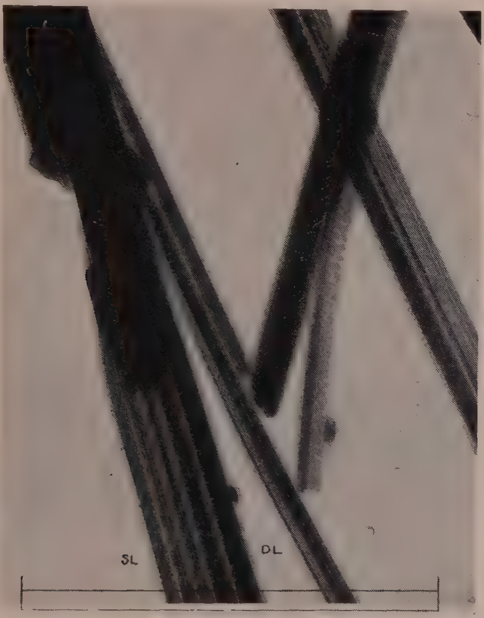

FIG. 8. Electron micrograph of six fibers, three of single layer rolls (*S.L.*), two of double layer rolls (*D.L.*) and one of double layer in which one layer is incompletely rolled.

The measurements in this study and by Pundsack (13) on the specific volume of massive chrysotile fiber revealed generally a porosity far too low compared to that required for a massive specimen consisting of tubular crystals. It would follow that chrysotile could occur largely in the form of lath or sheet crystals in native form. If such laths or sheets contain internal strains due to misfit between layers, curling of the sheets into laths or tubes should occur. The present studies suggest that such a mechanism may apply to the formation of chrysotile in tubular crystals, but the evidence does not preclude the occurrence of tubular crystals in massive chrysotile (Globe, Ariz., in present studies). It may be speculated that the "fibers" in the matrix could also originate during grinding. More detailed study, however, of the matrix in both massive and subdivided form will be required before any conclusion may be drawn.

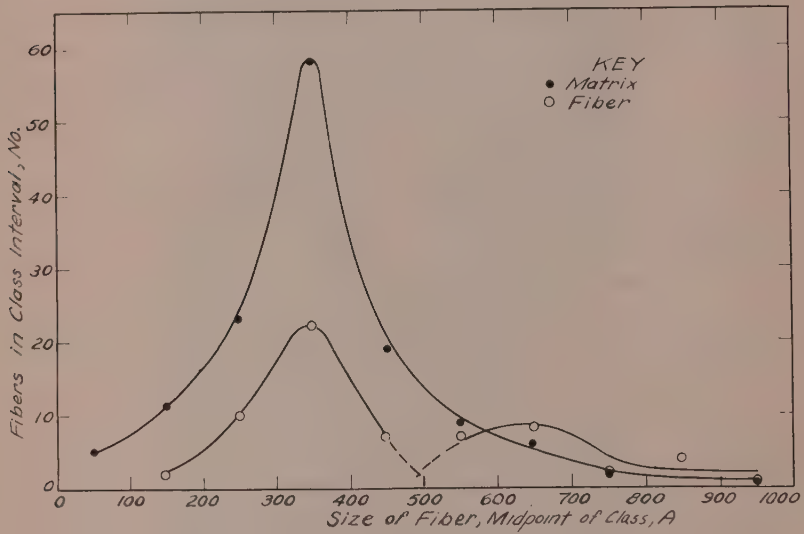

FIG. 9. Frequency distribution of sizes of fibers in seven serpentine samples.

SUMMARY

1. Results of chemical analysis showed that, for each serpentine examined, the fibers contained less Al_2O_3 and generally also less Fe_2O_3 and FeO than did the matrix.

2. Computations of structural formulas by the method of Duncan McConnell indicates that the silica layer of the fiber contains only tetrahedral water as a substitutent, but that of the matrix also contains a small amount of other ions in addition to the tetrahedral water.

3. *X*-ray patterns of the matrix were richer and sharper than those of the fiber. An outstanding feature of the *x*-ray data was the ratio of the intensities of the line at 7.3 Å to that at 3.6 Å ($I_{7.3}/I_{3.6}$ ratio), which ranged in value from about 0.8 to 1.4 for the fibers and 1.3 to 2.4 for the

matrix. In the 4.5 to 4.6 Å range of the pattern, the matrix generally showed longer spacings than did the fibers.

4. The values of the $I_{7.3}/I_{3.6}$ ratio were found to increase with increasing total contents of Al_2O_3, Fe_2O_3, and FeO, the matrix being richer in these constituents for a given serpentine composite of fibers and matrix. Although these differences appear real, no rigouous interpretation of the data could be made.

5. The specific volumes of the purest fibers and matrix specimens agreed closely with the values calculated from the published unit cell size.

6. Thermal balance and static-loss-on-heating results indicated that a small amount of the total water is liberated at temperatures higher than those required for dehydrating the brucite layer.

7. Electron microscope views showed that the matrix specimens contained varying amounts of "fibers" apparently ranging in shape from flat laths to complete tubes. Statistical analysis of 209 measurements of fiber sizes in enlarged photomicrographs indicated that the most probable fiber diameter (or cross section) for both the matrix and fiber components was 340 Å.

8. Specific volume measurements on three massive samples of chrysotile indicated porosities of 1.0, 8.5, and 12.5 per cent. The sample of low-porosities could not contain fibers in the form of capillaries, but because the sample after grinding contained tube-like crystals it may be assumed that these were formed by spontaneous rolling of the laths into tubes during the grinding.

ACKNOWLEDGMENTS

The authors are deeply grateful to Joseph G. Sayre of Owens-Corning Glass Company for electron microscope studies, to R. C. Mielenz of the Bureau of Reclamation for the thermal-balance results, and to William E. Smith for the chemical analyses. Acknowledgment is made also to W. F. Foshag of the National Museum for the serpentine specimens.

The investigation was conducted under the sponsorship of the Office of Naval Research at the University of Toledo, and acknowledgment of this aid is made.

REFERENCES

1. Turkevich, J., and Hillier, J., *Analytical Chemistry*, **21,** 475 (1949).
2. Bates, T. F., Sand, L. B., and Mink, J. F., *Science*, **111,** 512–513 (1950).
3. Noll, W., and Kircher, H., *Naturweiss*, **10,** 233–234 (1952).
4. Bates, T. F., *Denison University Bulletin*, **51,** 83–92 (1951).
5. Yoder, H. S., *Am. Jour. Sci.* (Bowen Vol.), 569–627 (1952).
6. Iler, Ralph K., Colloid Chemistry of Silica and Silicates, p. 209 (1955), Cornell University Press.

7. Bates, T. F., and Mink, J. F., *Am. Mineral.*, **36,** 310–311 (1951).
8. Pauling, Linus, *Proc. National Academy of Science*, **16,** 578–582 (1930).
9. Roy, D. M., and Roy, R., *Am. Mineral.*, **39,** 957–975 (1954).
10. Kalousek, G. L., Davis, C. W., Jr., and Schmertz, W. E., *Jour. Am. Concrete Institute, June 1949, Proc.*, **45,** 693.
11. McConnell, Duncan, *Clay Minerals Bulletin*, **1,** 178–188 (1951). See also: *Am. Mineral.* **39,** 830–831 (1954).
12. Whittaker, E. J. W., *Acta Crystallographica*, **5,** 143 (1952).
13. Pundsack, F. L., *Jour. Physical Chemistry*, **59,** 892–895 (1955), and **60,** 361–364 (1956).
14. Fankuchen, I., and Schneider, M., *Jour. Am. Chemical Society*, **66,** 500 (1944).

Manuscript received May, 21, 1956.

X-RAY DETERMINATION OF DOLOMITE-CALCITE RATIO OF A CARBONATE ROCK

C. B. TENNANT AND R. W. BERGER.*

ABSTRACT

An *x*-ray method has been developed for the determination of the percentage of dolomite in a carbonate rock. Such analyses may be useful in exploration work due to the association of highly dolomitized zones with locations favorable for mineral deposition.

INTRODUCTION

The meaning of the percentage of dolomite as used here is the per cent of the total carbonate, dolomite ($CaCO_3 \cdot MgCO_3$) plus calcite ($CaCO_3$), which is present as dolomite in a rock specimen. Mineral deposits are often found in dolomitized carbonate rock. Geologists believe that such dolomitization often precedes or accompanies the mineral emplacement. The dolomitization often extends from the center of mineralization for considerable distances.

From the association of dolomite and mineral deposits, it is obvious that a study of dolomitization of limestone might yield useful information on the location of such deposits, the more likely direction of concentration being in the direction of increasing dolomitization.

An *x*-ray method has been developed for determining the percentage of dolomitization and is here described. It should be specifically noted that the method does not give information as to whether or not the dolomite present is primary or secondary in the paragenetic sense. This information must be determined from other geological information.

EXPERIMENTAL

The procedure consists of measuring the relative intensities of the strongest powder *x*-ray diffraction line for calcite and for dolomite in a series of mixtures of known proportions, and applying these results to samples of unknown composition.

MATERIALS

The dolomite used for standardization was selected from a group of specimens purchased from Ward's Natural Science Establishment. It is the coarsely crystalline dolomite from Lee, Berkshire County, Massachusetts. Its purity was established by powder *x*-ray examination and

---

* Research Department, The New Jersey Zinc Company (of Pa.), Palmerton, Pa.

chemical analysis. The analysis expressed in terms of the carbonates is as follows:

Lee Dolomite	54.26% $CaCO_3$ 45.18% $MgCO_3$
Theoretical for Dolomite	54.27% $CaCO_3$ 45.73% $MgCO_3$

The calcium carbonate used was Baker's analyzed, calcium carbonate powder. This material gave a sharp calcite powder *x*-ray diffraction pattern. Both materials were finely ground (−325 mesh) and dried at 100° C. and stored in a desiccator.

SAMPLE PREPARATION

All samples after reduction to −325 mesh were wet ballmilled. The procedure used was an adaptation of the ideas of Ballard, Oshry, and Schrenk, 1943. The ballmills were screw top salve jars approximately $2\frac{1}{4}''$ in diameter and $1\frac{3}{4}''$ deep. The cardboard liner in the screw top was replaced with a solid rubber gasket. The mill was charged with approximately 180 grams of $\frac{1}{4}''$ diameter stainless steel balls, 2 grams of sample and 2 ml. of ethyl alcohol. Silicone stopcock grease was used on the gasket seal and the samples ground overnight (15 hours) at 24 r.p.m. Tests have shown that a grinding period of at least eight hours is essential. Klug and Alexander (1954) discuss the particle size requirements for reproducibility in *x*-ray spectrometer applications.

The arrangement of the drive mechanism allowed the mills to be tilted to approximately 45°. Following the grinding period in the horizontal position, the mills were inclined, the covers removed and the samples dried by allowing the alcohol to evaporate while the milling continued. The samples were recovered by emptying the mill contents onto a coarse (28 mesh) screen. The samples were given a brief hand mortar grind (one minute), and then back-packed through a screen into an aluminum cell against a plate glass surface (McCreery, 1949). This cell was then mounted in the *x*-ray diffractometer (North American Philips Company—high angle diffractometer).

COUNTING PROCEDURE

Nickel filtered copper *x*-radiation was used. Before counting, a strip chart was run from 26°–34° 2θ to check for interference and to select locations for background count. The background was recorded at a 2θ position slightly larger than that for the dolomite line used and also at a 2θ position just below the 2θ position for the calcite line. The exact positions of the calcite and dolomite peaks were determined by a series of counts through the appropriate 2θ range recording the time for various 2θ settings using fixed count operation.

The intensities were measured for the 3.03 Å calcite line and the 2.88 Å dolomite line at the 2θ positions determined, and corrected using the corresponding background value. Also, when the counting rate was high, corrections were made for the non-linear response of the Geiger counter. All intensity counts were made for 64 seconds. This procedure supplied data with which a calcite-dolomite intensity ratio could be calculated. Such a ratio is proportional to the ratio of concentration of these two materials in a given sample.

CALIBRATION

The procedure was calibrated by preparing known mixtures of calcite and dolomite from the materials described. These were prepared by the sample preparation procedure described and then a calcite-dolomite *x*-ray line intensity ratio was determined for each standard sample.

The following synthetic mixtures were used:

Weight per cent dolomite	Grams	
	Mass dolomite	Mass calcite
10	0.200	1.800
20	0.400	1.600
40	0.800	1.200
60	1.200	0.800
80	1.600	0.400
90	1.800	0.200

A calibration curve was then established by plotting the calcite/dolomite intensity ratio as determined against the known per cent dolomite. (See Fig. 1.)

TEST SAMPLES

Eight samples were used to check the *x*-ray method. These were field samples collected in connection with a geological study. The per cent of dolomite in each sample was determined using the *x*-ray method. Also, suitable chemical analyses of the samples were obtained so that the per cent of dolomite could be calculated. For the chemical determination Mg, Ca, and carbonate were determined on each sample. The Mg and Ca data are sufficient to calculate per cent dolomite and the equivalent amount of carbonate. The carbonate analysis serves as a check on the determination.

In Table 1 the per cent dolomite as determined by the two methods is listed for each sample.

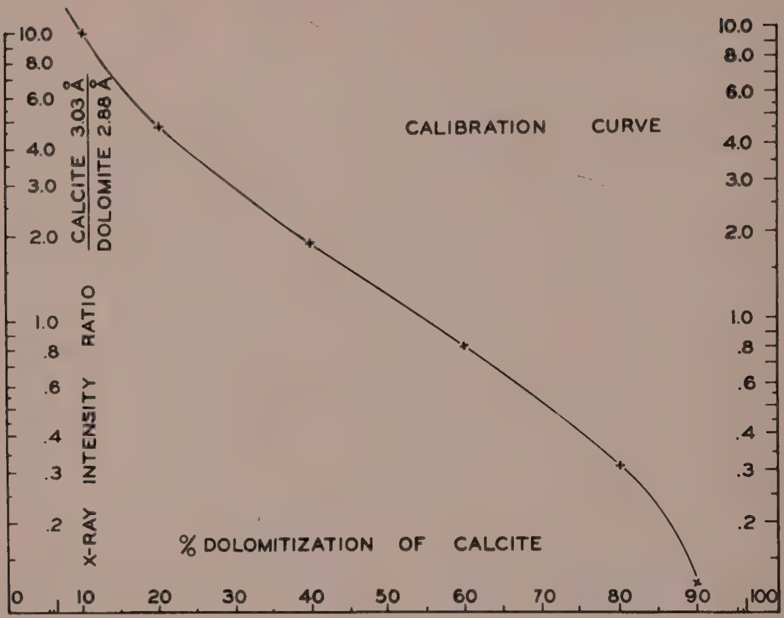

Fig. 1

Table 1

Sample No.	Chemical results per cent dolomite[1]	X-ray results per cent dolomite[1]
1	49.1	48
2	98.8	>90
3	50.2	50
4	84.0	86
5	44.8	44
6	11.5	<10
7	10.8	<10
8	34.3	35

[1] Per cent dolomite is determined from the ratio in weight of dolomite to that of dolomite plus calcite in the sample.

Table 2 lists the complete chemical data obtained on the samples.

The agreement of the x-ray and chemical analyses of per cent dolomite in Table 1 is very satisfactory for the application intended. In these particular samples (see Table 2) the carbonate analyses checked well with the carbonate results obtained from the calcium and magnesium analyses calculated to their carbonate equivalents as $CaCO_3$ and $CaCO_3 \cdot MgCO_3$. Rock specimens containing other carbonates or other calcium or magnesium-bearing minerals in addition to calcite and dolomite would not agree in this fashion. Under such conditions proper calculation of per cent dolomite from chemical analysis alone would become difficult if not impossible. In the *x*-ray method which is based on the crystal phases dolomite and calcite, the ratio of calcite-to-dolomite is determined independently of other Mg, Ca and carbonate-bearing materials.

TABLE 2

Sample No.	Weight per cent calcite[1]	Weight per cent dolomite[1]	Weight per cent CO_3[2]	Per cent CO_3 calculated from metal results[1]	Per cent dolomite[3]
1	47.20	45.5	57.7	57.91	49.1
2	1.20	97.0	63.8	63.85	98.8
3	48.87	49.3	61.8	61.38	50.2
4	15.76	82.6	63.0	63.21	84.0
5	55.09	44.7	61.2	62.12	44.8
6	87.95	11.4	59.6	60.15	11.5
7	87.63	10.6	58.6	59.44	10.8
8	64.03	33.4	59.4	60.13	34.3

[1] Values calculated from chemical determination of Mg and Ca content of samples.
[2] Values calculated from chemical determination of carbonate content of samples.
[3] (Weight per cent dolomite):(weight per cent dolomite plus weight per cent calcite).

DISCUSSION

The *x*-ray method has the advatage of giving results proportional to the total amount of material present having the calcite and dolomite structure types. A correction would be necessary in the *x*-ray calibration if samples showed major substitution of other cations for Ca^{++} and Mg^{++}. However, it seems most likely that the *x*-ray results would be affected less by small variation in chemical make up than would a method based on chemical analysis.

Harker and Tuttle (1955) and Graf and Goldsmith (1955) indicate that Mg can substitute for Ca in calcite to an appreciable per cent only at high temperature. Harker and Tuttle (1955) conclude from the ease of exsolution observed in their equilibrium studies that it is unlikely that in nature carbonate rocks would usually be quenched sufficiently rapidly from high temperatures to prevent unmixing on cooling.

We have examined the calcite samples referred to in this report by the procedure of Harker and Tuttle for lattice variations which might indicate Mg^{++} content. The lattice variations for all samples fall in a range between pure calcite and calcite with a $MgCO_3$ content of less than four weight per cent.

Goldsmith, Graf and Joensuu (1955) list measurements on a large group of natural calcites in which variations in magnesium content were measured by *x*-ray. Their results indicate that small amounts of $MgCO_3$, typically in the 4 weight per cent range, occur in solution in calcite.

Chave (1952) has noted that larger variations in magnesium content in calcite are observed in materials formed from living organisms. However, he recognizes their lack of stability and reports that the magnesium content falls to 1 or 2 per cent often within a few tens of millions of years.

The small $MgCO_3$ contents reported would not appreciably affect results of our *x*-ray analysis. Harker and Tuttle's data on solution of $CaCO_3$ and $MgCO_3$ in dolomite and Graf and Goldsmith's data on solution of $CaCO_3$ in dolomite indicate that there is no complication whatsoever as regards to solid solution of these phases.

Other divalent elements are known to substitute in calcite and dolomite and some to a large extent. Numerous examples of such substitutions can be obtained in most descriptive mineralogy texts. However, the general consensus of opinion is that such substitutions occur rarely in natural occurring calcite and dolomite.

The above considerations indicate that complications from solid solution of the phases involved and from substitution should be minor but nevertheless kept in mind and checked for in given applications of this method.

Faust and Callaghan (1948) report studies of calcite deposits which have reacted with Mg^{++}-bearing solutions. In a later paper, Faust (1949) treated the subject in more detail. The products of such reaction are calcite plus dolomite or magnesite ($MgCO_3$) plus dolomite. The combination of calcite plus magnesite does not occur in nature. These observations are in agreement with equilibrium laboratory studies of the system $CaO\text{-}MgO\text{-}CO_2$. The studies show that the combination magnesite-calcite does not occur but either one of these minerals can exist in equilibrium with dolomite.

The diffraction peaks we are using in this work are calcite 3.03 Å and dolomite 2.88 Å. The corresponding magnesite peak is at 2.73 Å, thus illustrating the continuing decrease in lattice dimension as the smaller Mg^{++} replaces Ca^{++}. As the above figures indicate, the magnesite peak falls on the opposite side of the dolomite peak from the calcite peak. The separation of the calcite and dolomite peaks is of the same order as the separation of the magnesite and dolomite peaks. With these conditions there would be no line interference due to magnestite and its occurrence could readily be detected. In our work we checked for the presence of magnesite whenever a per cent dolomite determination occurs in the 90–100% range.

If magnesite does occur in samples and information on its concentration is desired, it appears that a further application of the experimental techniques described above would readily permit determinations of magnesite-dolomite ratios by a procedure identical to that described here for the calcite-dolomite ratios.

ACKNOWLEDGMENT

We wish to acknowledge the direction and assistance we received from Mr. M. L. Fuller of the Research Department and Messrs. R. B. Hoy and R. W. Metsger of the Exploration Department of The New Jersey Zinc Company during the progress of this work.

REFERENCES

BALLARD, J. W., OSHRY, H. I., AND SCHRENK, H. H. (1943), Sampling mixing, and grinding techniques in the preparation of samples for quantitative analysis by x-ray diffraction and spectrographic methods: *J. Opt. Soc. Am.*, **33**, 667.

CHAVE, K. E. (1952), A solid solution between calcite and dolomite: *J. Geol.*, **60**, 190.

FAUST, G. T., AND CALLAGHAN, E. (1948), Mineralogy and petrology of the Current Creek magnesite deposits and associated rocks of Nevada: *Bull. Geol. Soc. Am.*, **59**, 11–74.

FAUST, G. T. (1949), Dedolomitization and its relation to a possible derivation of a magnesium-rich hydrothermal solution: *Am. Mineral.* **34**, 789–823.

GOLDSMITH, J. R., GRAF, D. L., AND JOENSUU, O. I. (1955), The occurrence of magnesian calcites in nature: *Geochimica et Cosmochimica Acta*, **7**, No. 5, 212–230.

GRAF, D. L., AND GOLDSMITH, J. R., (1955), Dolomite-magnesian calcite relations at elevated temperatures and CO_2 pressures: *Geochimica et Cosmochimica Acta*, **7**, 109–128.

HARKER, R. I., AND TUTTLE, O. F. (1955), Studies in the system CaO-MgO-CO_2, Part 2: *Am. J. Sci.*, **253**, 274–282.

KLUG, H. P., AND ALEXANDER, L. E. (1954), *X*-ray Diffraction Procedures: N. Y., John Wiley and Sons, Inc., p. 291.

MCCREERY, G. L. (1949), Improved mount for powdered specimens used on the Geiger counter x-ray spectrometer: *J. Am. Ceram. Soc.*, **32**, No. 4, 141–146.

WYCKOFF, R. W. G. (1951), Crystal Structures, N. Y., Interscience Publishers, Inc., Chap. VII, Text p. 2.

Manuscript recieved May 17, 1956.

BRANNERITE FROM SAN BERNARDINO COUNTY, CALIFORNIA*

D. F. Hewett, Jerome Stone, and Harry Levine,
U. S. Geological Survey, Washington, D.C.

Abstract

Brannerite has been found in the San Bernardino Mountains, San Bernardino County, California. It occurs typically as lenticular or roughly spherical nodules in a probable Pre-cambrian light-gray granite gneiss. The nodules have been found in two distinct modes of occurrence. Some lie along the foliation of the gneiss and in several places, for short distances, they are concentrated along a definite lamina; others lie in thin, tabular shear zones. In general, the smaller nodules (from 1 to 20 grams) are found along the foliation and seem to consist entirely of brannerite surrounded by a thin layer of biotite; the larger nodules (up to 200 grams) are found in the tabular shear zones and contain brannerite and grains of rutile. The larger nodules not only are surrounded by biotite but contain small plates and sheaves of that mineral. In the larger nodules it appears that the brannerite has replaced the biotite.

Introduction

In January 1955, B. W. Blankenship of Reseda, California, and W. P. Sykes of North Hollywood, California, brought to D. F. Hewett specimens of a highly radioactive mineral that they had found in prospecting for uranium in the low hills along the north slope of the San Bernardino Mountains, San Bernardino County, Calif. Blowpipe tests followed by a spectroscopic analysis by the Smith-Emery Company of Los Angeles, indicated that the principal mineral was brannerite. This determination was subsequently confirmed by work in the laboratories of the U. S. Geological Survey.

As the occurrence has many interesting features, Blankenship and Sykes have continued to explore the area and it has been visited four times by D. F. Hewett. The interpretation of the local geology, nature of the rocks, and relations of the minerals to geologic features are based upon work by D. F. Hewett. Laboratory work on the minerals has been done by Jerome Stone (preparation of materials and microscopic work), by George Ashby, Evelyn Cisney, Daphne D. Riska (x-ray analyses), by Katherine E. Valentine (spectroscopic analyses), and by Harry Levine (chemical analyses), all of the U.S. Geological Survey.

Location and Accessibility

Brannerite and several other uncommon minerals have been found on the steep eastward slope of a ridge that extends generally north from the San Bernardino Mountains, the largest and highest range in southern

---

* Publication authorized by the Director, U. S. Geological Survey.

California. Even though the higher parts of the range, culminating in San Gorgonio Peak, 11,485 feet above sea level, are relatively smooth surfaces, the northern and southern slopes are trenched by rugged steep canyons. The brannerite locality is in one of these canyons, at an altitude of about 4,000 feet, where it merges into one of the broad basins north of the mountains. Projecting the land net into the canyon area, the brannerite locality lies near the center of sec. 22, T. 3 N., R. 3 E., San Bernardino Meridian. The area lies within the Old Woman quadrangle which is the northeast quarter of the San Gorgonio quadrangle. (See Fig. 1.)

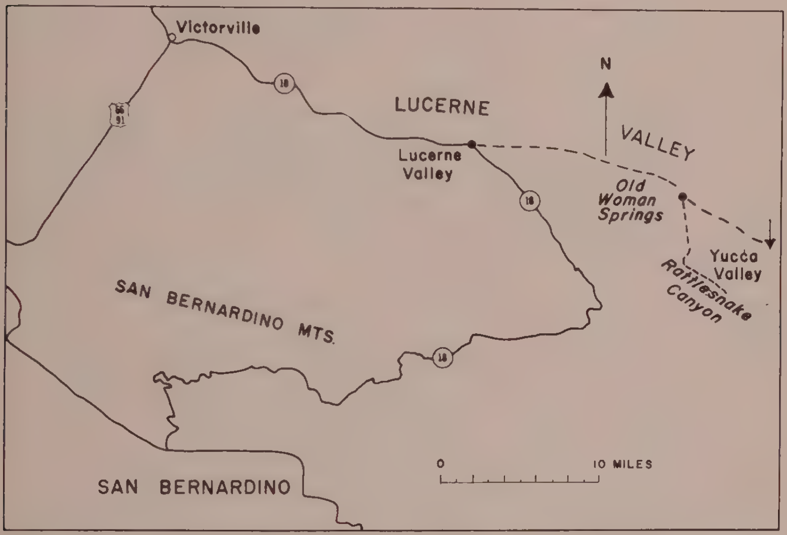

Fig. 1. Index map of Old Woman Springs area, San Bernardino County, California.

The area is most readily accessible by a road that extends eastward from Victorville to Lucerne Valley Post Office, 22.7 miles east of Victorville, and to the Old Woman spring and ranch which are 15.1 miles east of Lucerne Valley. A few hundred feet east of the ranch, the road divides; the right fork leads south to Rattlesnake Canyon and the left fork eastward to Yucca Valley. At a point on the left fork or main road, 4.0 miles east of Old Woman Ranch, a new dirt road extends southwest 1.3 miles to several low hills, beyond which is it impossible for cars with two-wheel drive to travel. Cars with four-wheel drive can divert eastward to a wash and ascend it southward about 1.45 miles. From there, a rugged trail extends eastward about one mile to another wash; the brannerite area is about 1,500 feet up the wash. Thus far, all of the brannerite specimens have been found in an area about 100 feet in diameter along the steep west slope of the valley.

Local Geology

The brannerite area lies within the San Gorgonio quadrangle, the geologic features of which were studied during 1915–1917 by Vaughan (1922). A part of the San Gorgonio quadrangle, near Blackhawk Canyon, was later studied by Woodford and Harris (1928), but the brannerite area lies just east of its eastern border. All the rocks of the area here under review are included in the "undifferentiated schists" of Vaughan, and Woodford and Harris. They are regarded as the oldest rocks of the region and are probably Precambrian. These "undifferentiated schists" are intruded by the Cactus granite of Vaughan (1922) and other "plutonic rocks," probably Mesozoic in age.

Field work by D. F. Hewett during recent years indicates that large plates and small blocks of foliated schists and gneisses form a belt that extends along the north slope of the San Bernardino Mountains from Blackhawk Canyon eastward about 20 miles to the Rock Corral area. These plates and blocks either abut against or rest upon relatively unfoliated intrusive rocks of granitic or monzonitic type. As Woodford and Harris (1928) have shown, Vaughan's (1922) Cactus granite of the type locality, Cactus Flat, south of Lucerne Valley, is quartz monzonite.

The most widespread foliated rock of the area, and the host of all of the brannerite that has been found thus far, is a light-gray granite gneiss with persistent fine texture; it underlies at least 20 acres on the north end of the ridge that extends north from the San Bernardino Mountains. A fresh specimen collected 50 feet distant from any known brannerite shows 50 per cent quartz, 20 per cent orthoclase, 20 per cent microcline, 5 per cent sodic plagioclase, 2 per cent biotite, with traces of sericite, chlorite, magnetite, zircon, monazite, and xenotime. Most of the grains range from 1 mm. to 2 mm. in diameter. Probably most of the gneiss of the area contains much more feldspar and less quartz than the examined section. The foliation of the gneiss is indicated by thin layers of biotite. In detail, the rock shows widespread plication, but in larger aspect the trend of the major foliation is northwest and the dip steeply northeast. From place to place, there is jointing that also trends northwest and dips northeast.

Most exposures of the gray gneiss exhibit large and small angular blocks of an older dark schist, persistently thinly laminated owing to the presence of considerable biotite. The areal source of this dark schist is not known.

Several hundred feet south of the brannerite locality, the gray gneiss is intruded by a pale reddish granite gneiss that shows slight but persistent foliation. A similar rock forms small lenticular sills in the gray gneiss north of the brannerite area. Boulders of a coarse quartz monzonite occur in the wash, but this rock does not crop out within half a mile south of the brannerite area.

The presence of persistent foliation in each of the three rock units described above, the biotite schist, gray granite gneiss, and reddish granite gneiss, and the general absence of foliation in the Vaughan's Cactus granite of this region, indicate that the local rocks are much older than the so-called Cactus granite and probably Precambrian.

As a result of recent work in the Rock Corral area, about 10 miles east of the brannerite area, Moxham, Walker, and Baumgardner (1955) recognize two varieties of quartz monzonite. The older variety contains abundant coarse tabular crystals of orthoclase in a finer matrix made up of oligoclase and calcic andesine, quartz, and biotite with small amounts of magnetite, allanite, apatite, muscovite, zircon, and fluorite. The younger monzonite is uniformly coarse grained and contains orthoclase, andesine, quartz, and minor amounts of biotite, magnetite, chlorite, muscovite, zircon, apatite, sphene, and allanite; it is considered the equivalent of the Cactus granite of Vaughan (1922).

An analysis of euxenite from the Pomona Tile pegmatite body in the so-called Cactus granite near Rock Corral, indicates that the age is 150 million years, or middle Jurassic (Hewett and Glass, 1953).

No bodies of rock that would commonly be called "pegmatite" have been seen in the brannerite area. At several places in the gray granite gneiss, however, there are thin lenses made up of white orthoclase which show terminated crystals in open cavities. The largest of these lenses is an inch wide and 15 inches long.

At the brannerite locality there are sparse poorly defined patches within which the normal feldspathic gray granite gneiss is wholly altered to sericite with sufficient chlorite to give it a pale-greenish color. Within the altered rock, there are small irregularly shaped masses of granular cordierite surrounded by muscovite and phlogopite. The cordierite is highly fractured and sericitized; it has not been found in the unaltered granite gneiss. Some quartz and traces of sillimanite, biotite, magnetite, zircon, and feldspar are present. One thin section of sericitized granite gneiss shows a few needles of sillimanite embedded in cordierite. During the early months of exploration, brannerite was found only in the sericitized gneiss, but as work progressed the mineral was found in unaltered gneiss. There seems to be no relation between the occurrence of brannerite and the sericitic alteration of the gneiss.

A little euxenite occurs both as small granular masses within the brannerite nodules and as small grains dispersed in the biotite-rich parts of the granite gneiss. These masses range from 1 to 4 mm. in greatest dimension, are wax-brown, and are made up of many very small grains; no crystals have been found. Thus far, the quantity of euxenite seems to be no more than several per cent of that of brannerite. Also, at several places within the brannerite locality, small masses of granular rutile have been found in biotite-rich lenses in the granite gneiss; the color is reddish brown, about that of much almandite garnet.

Brannerite

Occurrence. Thus far, all the brannerite recovered forms lenticular or roughly spherical nodules in the gray granite gneiss. The largest nodule is nearly 2 by 2 inches and weighs about 200 grams; most of the nodules range from one-half to 1 inch in largest diameter and weigh from 5 to 50 grams. The owners estimate that after six months of intermittent exploration about 25 pounds of nodules have been recovered.

Nodules have been found in two distinct modes of occurrence. Some lie along the foliation of the gneiss and in several places, for short distances, they are concentrated along a definite lamina; others lie in thin tabular shear zones filled with biotite or chlorite that definitely cut across the foliation. Most of the nodules found along the foliation planes are embedded in the feldspathic gneiss and are surrounded by a thin layer of biotite; most of these nodules range in weight from 1 to 20 grams. The nodules found in the discordant shear zones are embedded in larger nodules of fresh or altered biotite; most of these range in weight from 20 to 50 grams, but a few weigh from 100 to 200 grams.

In general, the smaller nodules seem to be wholly brannerite; the larger nodules found in the shear zones contain grains of rutile as large as grains of rice. The larger nodules not only are surrounded by biotite but contain small plates and sheaves of that mineral; in these, it appears that the brannerite has replaced the biotite. A polished section (Fig. 2) of a large nodule of brannerite reveals that the brannerite is surrounded and transected by biotite. Sodic plagioclase and rutile are present in some of the nodules of brannerite. The sodic plagioclase is present as (1) large anhedral crystals which are transected by biotite and (2) as small crystals intimately associated with biotite, which fills the numerous fractures in brannerite and rutile. The rutile is present as roughly ellipsoidal crystalline masses and as very small crystals within the brannerite. A thin section reveals that the partings of the large crystals of plagioclase are filled with sericite. The smaller crystals of plagioclase are in places almost completely sericitized.

Physical Properties. Examined by reflected light, polished sections of the nodules show that the brannerite ranges in color from black nearly metallic to dark yellowish brown; examined by transmitted light, finely crushed brannerite is transparent and ranges from pale brown to pale green. All specimens have a conchoidal fracture and a hardness of 5. The physical properties and chemical analysis recorded below are those of one of the largest nodules thus far found. It weighs about 125 grams and is nearly black by reflected light. Figure 2 shows a photograph of a highly polished section of this nodule. In order to determine any appreciable differences in composition of brown and black nodules, spectrographic analyses were made as follows:

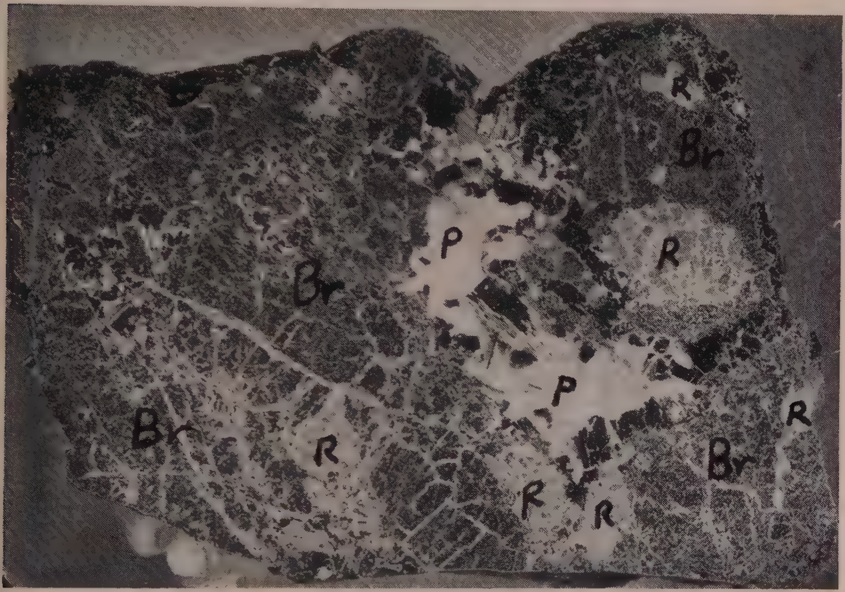

FIG. 2. Polished section of brannerite nodule. Rutile (*R*) and sodic plagioclase (*P*) are present as inclusions in the brannerite (*Br*). Biotite (*B*) surrounds and transects brannerite. The numerous fractures are filled with biotite and plagioclase. Photograph by U. S. Geological Survey.

Per cent	*Nodule, black by reflected light*	*Nodule, brown by reflected light*
Over 10	—Ti	—Ti
5–10	—U	—U, Th
1–5	—Th, Y	—Si, Fe
0.5–1.0	—Fe, Si, Mg	—Ca, Y, Nb
0.1–0.5	—Ca, Yb, Lu	—Gd, Al, Mn, Mg

The brannerite is isotropic, metamict, and has an index of refraction that ranges from 2.2 to 2.3. After heating the material for one hour at 900° C. in air, a pattern which matched that of brannerite was produced. By using a Frantz isodynamic separator at vertical and horizontal setting at 11°, brannerite is concentrated in the magnetic fraction at 0.5 ampere.

Chemical analysis. A chemical analysis of brannerite is shown in Table 1. A small part of the iron oxide, magnesia, alumina and silica in this analysis may be due to contamination by biotite. Although an *x*-ray diffraction pattern did not reveal any biotite in the brannerite, an electron micrograph of a grain of brannerite did reveal the presence of biotite.

TABLE 1. CHEMICAL ANALYSES, IN PER CENT, OF BRANNERITE FROM CALIFORNIA AND IDAHO

	San Bernardino County, Calif.[1]	Custer County, Idaho[2]	Mono County, Calif.[3]	
TiO_2	39.60	39.	32.9	=87.0 R_2O_3
UO_3	26.74	33.5	32.0	
UO_2	Trace	10.3	8.2	
ThO_2	9.15	4.1	5.0	
RE_2O_3[4]	9.75	3.9	6.5	
FeO	1.28	Trace	2.4	
Fe_2O_3	2.73	—	—	
CaO	2.70	2.9	2.8	
MgO	0.82	—	— (Mn, Mg)=0.X	
PbO	1.75	—	—	
SiO_2	2.25	0.6	0.5	
Al_2O_3	1.24	—	—	
H_2O^-	0.05	2.0	2.6	
H_2O^+	2.35			
Total	100.41	96.3		
Specific gravity	4.76	5.42	5.43	

[1] Analysis by Harry Levine, U. S. Geological Survey.

[2] Hess and Wells (1920), analysis by R. C. Wells.

[3] Analysis by J. J. Rowe (Pabst, 1954). The total R_2O_3 was determined as 92.3 per cent. The difference between 87.0 and 92.3 in R_2O_3 is stated as being probably due to Pb, Nb, Ni, Bi, Zr, Ta which were found by spectrographic analysis.

[4] RE_2O_3 is the total of the rare-earth oxides.

Rutile probably consituted about 1–2 per cent of the brannerite in the analysis, as estimated by *x*-ray diffractometer studies made by George Ashby of the U. S. Geological Survey. The estimate was made by adding a weighed amount of rutile to the metamict brannerite and measuring the change in intensity of a rutile line. UO_2 is not present in the sample. It seems that any UO_2 that may have been present has been oxidized by Fe_2O_3 to UO_3. Also in Table 1 are two previous analyses of brannerite reported by Hess and Wells (1920) and Pabst (1954) that show the presence of $UO_2 = 10.3$ per cent, FeO = Trace; and $UO_2 = 8.2$ per cent, FeO = 2.4 per cent, respectively.

In addition, a semiquantitative spectrographic analysis by Katherine E. Valentine of the U. S. Geological Survey shows the following constituents not determined in the chemical analysis:

Per cent	
0.01–0.05	Mn B Nb
0.005–0.01	Ba Zr
0.0005–0.001	Cr
0.0001–0.0005	Ag Be

The individual rare-earth metals are as follows:

Per cent	
1–5	Y
0.05–0.1	Yb Gd Er Dy
0.01–0.05	Lu Tm Ce
0.005–0.01	Ho La

PARAGENESIS

Brannerite and biotite are in very close association. Biotite commonly surrounds the brannerite in nodules, transects the brannerite, and is found within brannerite as macroscopic, microscopic, and submicroscopic crystals Electron micrographs made by Malcolm Ross of the U. S. Geological Survey show that even an apparently homogeneous fragment of brannerite contains crystals of biotite.

This suggests that the biotite crystallized first and brannerite followed, possibly as a replacement.

However, since biotite also cuts across the brannerite and fills many of the fractures in brannerite, a second generation of biotite is indicated. Rutile is present as submicroscopic and macroscopic crystals in the brannerite and probably represents an excess of titania in the brannerite solutions.

MODES OF OCCURRENCE OF BRANNERITE

Where it was first discovered in Kelly Gulch, Custer County, Idaho, brannerite formed grains in alluvial sands and the source has not been determined (Hess and Wells, 1920). Brannerite from the Deans mine, along Walker River, Mono County, Calif., formed "lustrous, black crystals firmly embedded in quartz" from a quartz vein (Pabst, 1954). According to Bateman (1955), brannerite and pitchblende "form discrete mineral particles . . . rarely seen by the naked eye" in the matrix between the quartz pebbles that form a bed of conglomerate near the base of the Huronian in the Blind River area, Ontario.

In contrast with these occurrences, the brannerite from the north slope of the San Bernardino Mountains, San Bernardino County, Calif., forms lenticular nodules from one-half to 2 inches in largest dimension that are (1) dispersed along the foliation of a Precambrian(?) granite gneiss and (2) lie along thin zones of biotite that cut across the foliation. It would seem that the brannerite from San Bernardino County has formed at great depth under conditions of high pressure and temperature.

REFERENCES

Bateman, J. D. (1955), Recent uranium developments in Ontario: *Econ. Geol.*, **50,** 361–372.

Hess, F. L., and Wells, R. C. (1920), Brannerite, a new mineral: *Jour. Franklin Institute*, **189,** 225–237.

Hewett, D. F., and Glass, Jewell (1953), Two uranium-bearing pegmatite bodies in San Bernardino County, California: *Am. Mineral.*, **38,** 1040–1050.

Moxham, R. M., Walker, G. W., and Baumgardner, L. H. (1955), Geologic and airborne radioactivity studies in the Rock Corral Area, San Bernardino County, California: *U. S. Geol. Survey Bull.* **1021-C.**

Pabst, A. (1954), Brannerite in California: *Am. Mineral.* **39,** 109–117.

Vaughan, F. W. (1922), Geology of the San Bernardino Mountains north of San Gorgonio Pass: *Univ. Calif., Dept. Geol. Sci.*, **13,** 319–341.

Woodford, A. O., and Harris, T. F. (1928), Geology of Black Hawk Canyon, San Bernardino Mountains, California: *Univ. Calif., Dept. Geol. Sci.*, **17,** 265–304.

Manuscript received May 11, 1956.

THE THERMAL EXPANSIONS OF THORIA, PERICLASE AND DIAMOND*

Brian J. Skinner, *Harvard University, Cambridge, Massachusetts.*†

Abstract

A central mount, back reflection, *x*-ray powder camera was designed for measuring thermal expansions. The camera is 16 cms. in diameter, has a temperature range from 0° to 1000° C., is inexpensive to construct and is simple to operate.

The linear (α_a) and volume (α_v) thermal expansion coefficients of ThO_2 are $\alpha_a=0.6216\times10^{-5}+3.541\times10^{-9}T-0.1125T^{-2}$ and $\alpha_v=1.865\times10^{-5}+10.96\times10^{-9}T-0.3375T^{-2}$ where T is the temperature in degrees Kelvin from 298° to 1073° K. For periclase, the coefficients are $\alpha_v=1.411\times10^{-5}+1.210\times10^{-9}T-0.5854T^{-2}$ and $\alpha_v=4.232\times10^{-5}+3.630\times10^{-9}T-1.756T^{-2}$, from 298° to 973° K. For commercial diamond dust the coefficients are $\alpha_v=0.07667\times10^{-5}+3.672\times10^{-9}T-0.0903T^{-2}$ and $\alpha_v=0.2301\times10^{-5}+11.01\times10^{-9}T-0.2708T^{-2}$, and for a single crystal of South West African diamond, $\alpha_a=0.09613\times10^{-5}+3.522\times10^{-9}T-0.0888T^{-2}$ and $\alpha_v=0.2884\times10^{-5}+10.57\times10^{-9}T-0.2665T^{-2}$ from 298° to 973° K.

The measured expansions of periclase and diamond are slightly lower than previous measurements made on macroscopic single crystals. The thermal expansion of thoria has not been measured previously.

The unit cell size (a_0) and molar volume (V_m) at 298.16° K. and 1 atmosphere are, for thoria, $a_0=5.59525\pm0.0001$ Å and $V_m=26.378\pm0.005$ cc./mole; for periclase, $a_0=4.2117\pm0.0002$ Å and $V_m=11.250\pm0.007$ cc./mole; for diamond, $a_0=3.56688\pm0.00009$ Å and $V_m=3.4168\pm0.0001$ cc./mole.

Instrumentation

A new high-temperature *x*-ray powder camera has been designed specifically to measure the thermal expansions of minerals from 20° to 1000° C. The camera is a central-mount camera, but only those reflections with Bragg angles greater than 45° are recorded. Diagrams of the camera and its component parts (Figs. 1, 2, 3), are largely self-explanatory.

Essentially the camera consists of a heavy brass plate 20 cms. in diameter with machined recesses to seat the removable film cartridge and the film housing. The brass film cartidge (*a*) has an internal diameter of 16 cms. (film diameter). The cartridge has a $\frac{3}{4}$ inch slot (*f*) machined in the front surface to allow the passage of the diffracted *x*-ray beams. When in operation the slot is covered with masking paper to make the cartridge light-tight. The top of the film cartridge is sealed by a removable light-tight lid (*d*). Vertical knife edges (*b*), 0.001 inch wide, are attached to the bottom of the film cartridge at approximately $\theta=51.141°$, where θ is the effective Bragg angle of the knife edges.

---

* Contribution from the Department of Mineralogy and Petrography, Harvard University, No. 370.

† Present Address: Department of Geology, University of Adelaide, South Australia.

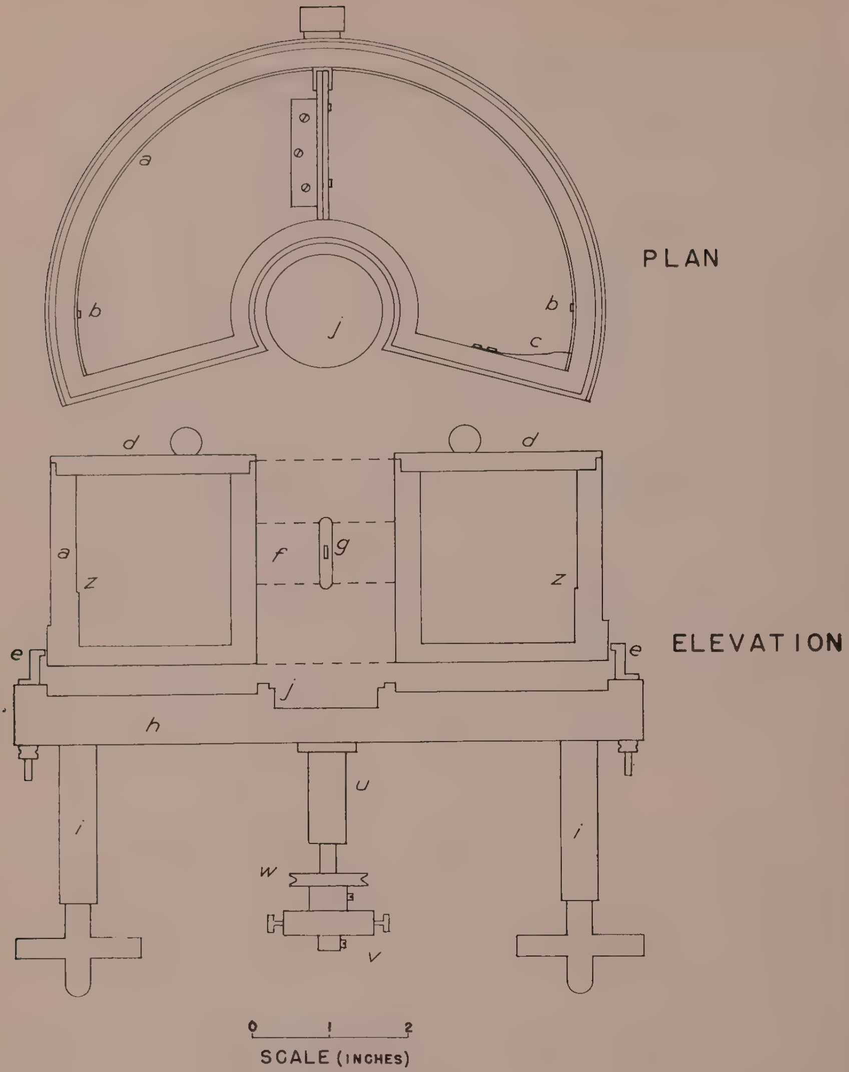

Fig. 1

Key to Camera Parts

(*a*) Brass film housing.
(*b*) Knife edges.
(*c*) Spring to hold film tight against seating.
(*d*) Removable, light-tight lid.
(*e*) Clamps to hold film cartridge steady.
(*f*) Slot in cartridge wall covered with black paper.
(*g*) Positioning bar for slit system.
(*h*) Base plate.
(*i*) Adjustable legs.
(*j*) Recess for furnace.

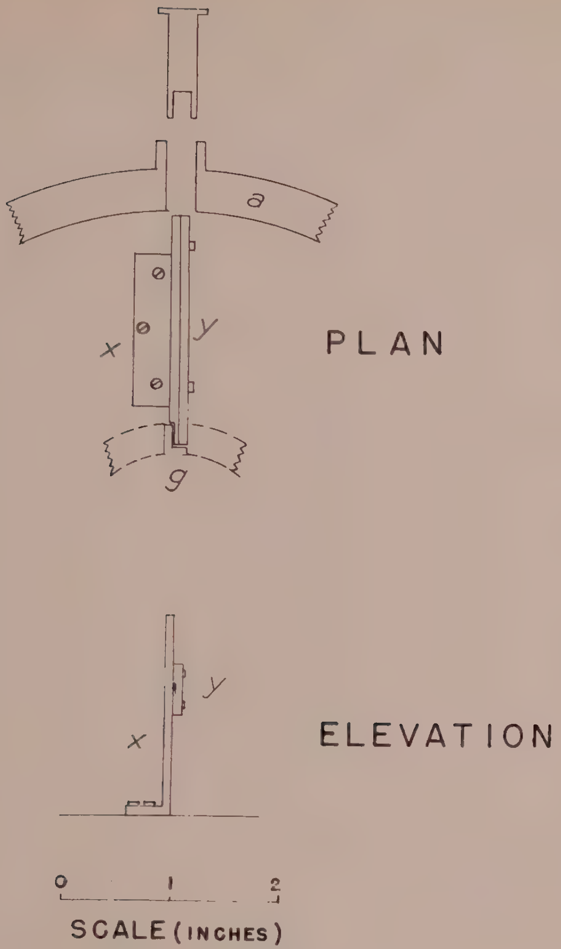

FIG. 2

(*k*) Vanes for circulating cooling water.
(*l*) Water inlet.
(*m*) Water outlet.
(*n*) Thermocouple and mechanism for rotating thermocouple around specimen.
(*o*) Specimen support and specimen.
(*p*) *X*-ray inlet, and exit for diffracted rays.
(*q*) Exit for undiffracted *x*-ray beam.
(*r*) Furnace windings, supported on alundum core.
(*s*) Furnace leads.
(*t*) Jacket soldered over water-circulating vanes.
(*u*) Support for centering system.
(*v*) Centering system.
(*w*) Drive wheel for rotating specimen in furnace.
(*x*) Main support plate for collimating slit, with three positioning screws.
(*y*) Plate with slit of desired size machined in it.
(*z*) Film seat.

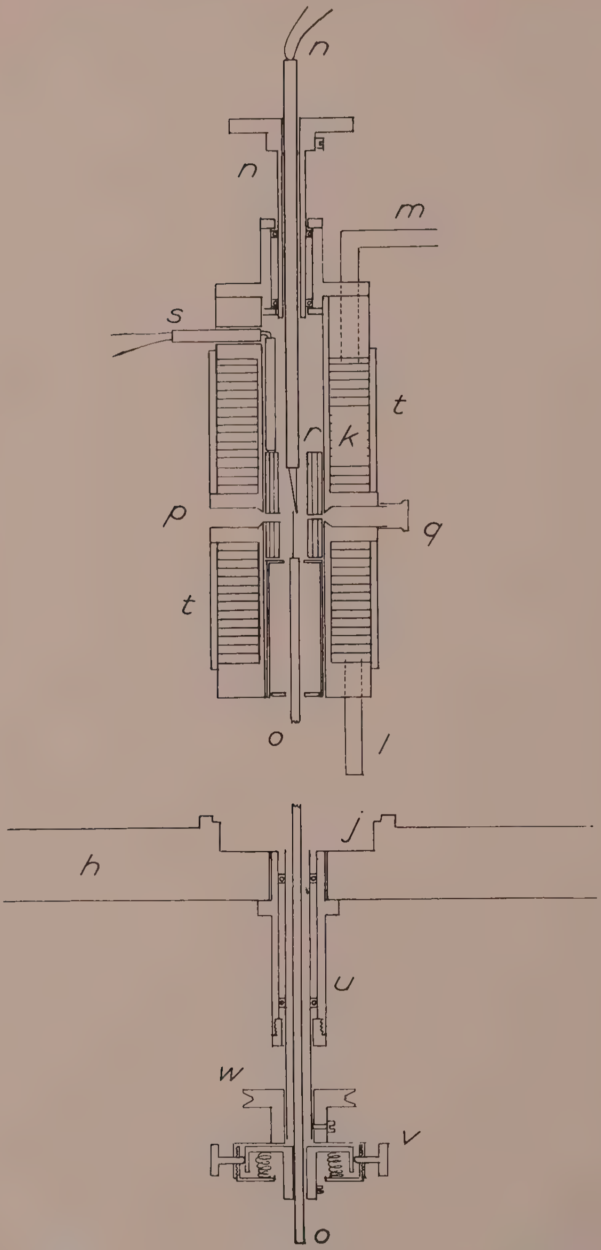

FIG. 3

The specimen under study is mounted in a silica glass capillary tube, approximately 0.2 mm. in diameter, and is then cemented in a 0.25 mm. hole in the top of a $\frac{1}{8}$ inch stainless steel rod (*o*), Fig. 3. The steel specimen support is clamped into the centering system (*v*).

The collimating slit is milled in a brass strip (*y*), screwed to the supporting plate (*x*). The dimensions of the collimating slit can be adjusted for each substance studied, until suitable line quality with minimal exposure time is obtained.

The furnace has an internal diameter of 0.25 inch and a length of 1 inch. The furnace windings (*r*) are nichrome ribbon 0.0156×0.005 inch, supported on an alundum core, and held in place with ceramic cement. Over the furnace core and windings another alundum tube has been fitted, providing some thermal insulation for the furnace. The outer alundum tube fits snugly into the furnace housing and rests directly against the inner wall of the cooling jacket. Since the region $90° < 2\theta < 180°$* is recorded on the film, it is not necessary to have an opening all the way around the furnace for the escape of the diffracted beams. A slot, 185° around the circumference from 2θ equals 87.5° to 180° on either side of the primary beam, allows the entrance of the primary *x*-ray beam and the exit of the diffracted beams. A small circular hole opposite the collimating slit allows the exit of the undiffracted *x*-ray beam.

The housing is machined from a single piece of stainless steel stock. Like the furnace, the housing has a 185° slot (*p*) cut in it, with a small exit port (*q*). In operation the slot is covered with masking paper, so that there is no contact with the circulating air outside. The water circulating vanes (*k*) are sealed externally by a stainless steel jacket (*t*). Water is circulated under a pressure of 5 lbs./sq. inch though higher or lower pressures may be used if desired.

The temperature is measured by reading the emf developed in a platinum, platinum-10% rhodium thermocouple (*n*), contained in a $\frac{1}{8}$ inch silica glass tube. The thermocouple can be raised or lowered and rotated around the specimen, allowing the detection of any temperature inhomogeneities in the furnace. In operation the thermocouple is placed $\frac{1}{32}$ inch from the specimen in the plane of the incident *x*-ray beam. Readings are taken at 60° intervals around the specimen.

The temperature of the furnace is controlled with a variable transformer on the output of a constant voltage transformer. With the furnace insulated from external air currents and the cooling water maintaining a constant flow, the temperature is held constant to ±1° C. at 400° C. for 48 hour test periods.

The knife edges can be located by using any isometric or uniaxial substance whose lattice parameters are accurately known. In the present case, the knife edges were located with an accurately measured quartz sample, after the method of Bradley and Jay (1933).

---

* θ is the Bragg angle.

METHOD OF MEASUREMENT AND COMPUTATION

In determining thermal expansion the precision of measurement is more important than the absolute accuracy. A constant error in the accuracy of each point, expressed as a percentage, will tend to cancel out in the computation of the thermal expansion coefficient.

All fims were measured on a Hilger and Watts Film Measuring Rule #185, ruled to 1.000 ± 0.001 mm., and fitted with a sliding vernier ruled to 0.050 ± 0.001 mm. Individual measurements could be estimated to 0.02 mm. by interpolation. The x-ray wavelengths used in all calculations were those recommended by Bragg (1947). The stated precisions of measurements in this paper are the standard deviations.

Measurements of the cell size were made at different temperatures, and from these values both the linear and volume expansions determined. The molar volumes at different temperatures were computed directly from the measured values of a_0 using the formula,

$$V_m = \frac{(a_0)^3 N}{x}$$

where

a_0 is the unit cell edge length in cms.
N is Avogadro's number (equal to $(6.02338 \pm 0.00043) \times 10^{23}$ mole^{-1})
x is the number of formula units in the unit cell
V_m is the molar volume

Standard values of the unit cell size and the molar volumes at 298.16° K (25° C.) and 1 atmosphere pressure were determined by making several measurements at this temperature. These values have been called a_s and V_{ms} respectively. The variation in the coefficients of thermal expansion with temperature have been expressed by functions of the form

$$\alpha_a = \frac{1}{a_s}\left(\frac{\partial a_0}{\partial T}\right)_P = b + cT + dT^{-2}$$

and

$$v = \frac{1}{V_{ms}}\left(\frac{\partial V_m}{\partial T}\right)_P = b_1 + c_1 T + d_1 T^{-2}$$

where

α_a and α_v are the linear and volume coefficients of thermal expansion respectively,
a_s and V_{ms} are the unit cell size and molar volume at 298.16° K and 1 atmosphere respectively,
T is the temperature in degrees Kelvin,
b, c, d, and b_1, c_1, d_1, are constants of the equations.

If the equations above are integrated, we get functions of the form

$$\frac{a_0 - a_s}{a_s} = bT + \tfrac{1}{2}cT^2 - dT^{-1} + I$$

where

a_0 is the unit cell size at temperature T° K
I is the constant of integration.

Since the integrated form is sometimes more useful than the differential form, all the constants b, c, d, and I have been given in Table 8.

EXPERIMENTAL DATA

THORIA

The sample used in the present study was the one used by Frondel (1955) in his accurate determination of the cell size. A spectrographic analysis by the United States Geological Survey showed Si and Mg to be the major impurities (Table 1). The Si and Mg may or may not be dissolved in the ThO_2. If all the impurities present were dissolved in the ThO_2 it is doubtful if they would alter the physical properties significantly.

TABLE 1. SPECTROGRAPHIC ANALYSIS OF ThO_2 SAMPLE

over 10%	Th
5 -10%	—
1 - 5%	—
0.5 - 1%	—
0.1 -0.5%	Si, Mg
0.05 -0.1%	—
0.01 -0.05%	Fe, B, Al
0.005 -0.01%	—
0.001 -0.005%	Sc, Cu
0.0005-0.0001%	—
0.0001-0.0005%	Be

Previous accurate measurements of the lattice parameter of thoria are limited to Frondel (1955) and Hund and Niessen (1952). Frondel's value of 5.58415±0.00005 kX at 31.6° reduces to 5.59520±0.00005 Å at 25° C. Hund and Niessen's value of 5.59530 Å was determined at an unknown 'room temperature.' The value obtained in the present study is 5.59525±0.0001 Å, and this was selected as the standard value of a_0 at 298.16° K. Table 2 shows the unit cell size and molar volume at the various temperatures of measurement. The parameters of the various functions derived from the data in Table 2 are shown in Table 8.

TABLE 2. THORIA

Unit cell edge (a_0) and molar volume (V_m) at different temperatures

Temp. °C.	a_0 Å	V_m cc./mole
8.5	5.59475	26.3707
25.0	5.59525	26.3780
33.0	5.59557	26.3823
34.1	5.59561	26.3830
103.1	5.59812	26.4184
162.0	5.60040	26.4507
256.2	5.60424	26.5052
343.1	5.60802	26.5588
398.2	5.61069	26.5968
403.0	5.61069	26.5968
404.2	5.61090	26.5998
421.3	5.61189	26.6139
446.0	5.61288	26.6279
495.9	5.61542	26.6641
593.9	5.62044	26.7357
700.0	5.62589	26.8136
787.2	5.63050	26.8795

Best values

a_0 at 298.16° K. $=5.59525\pm0.0001$ Å
V_m at 298.16° K. $=26.378\pm0.005$ cc./mole
ρ at 298.16° K. $=10.013\pm0.001$ gm./cc.
α_a at 298.16° K. $=6.00\times10^{-6}$
α_v at 298.16° K. $=18.1\times10^{-6}$

PERICLASE

The sample of periclase was a colorless single crystal prepared synthetically by the Norton Company. Similar material from the Norton Company was studied by Austin (1931) using the interferometer method and by White (1938) using a mechanical dilatometer. In a recent series of measurements Sharma (1950) measured the linear expansion of periclase by the interferometer method. The measurements of Austin and White show a reasonable agreement, though Austin's measurements are more refined than White's. Sharma's results are in distinct variance with both Austin and White and to the present study.

Previous accurate measurements of the lattice parameter of periclase are limited to Wyckoff (1925) and Jay and Andrews (1945). Wyckoff determined the lattice parameter at an unspecified room temperature as 4.203 kX (4.211_5 Å). Jay and Andrews also made their measurements at an unspecified room temperature. Their value of 4.200 kX (4.209 Å) is somewhat lower than Wyckoff's value and the present measurement. The best value of a_0 at 298.16° K. has been selected from the present measurements as 4.2117 ± 0.0002 Å. The measured values of the lattice parameter and calculated values of the molar volume at various temperatures are shown in Table 3. The parameters of the various functions derived from the data in Table 3 are given in Table 8.

TABLE 3. PERICLASE

Unit cell edge (a_0) and molar volume (V_m) at different temperatures

Temp. °C.	a_0 Å	V_m cc./mole
10.5	4.21130	11.2466
21.0	4.21160	11.2492
25.0	4.21168	11.2498
46.5	4.21243	11.2558
76.5	4.21360	11.2652
131.0	4.21595	11.2841
229.5	4.22090	11.3239
320.6	4.22576	11.3630
404.2	4.23047	11.4011
512.0	4.23679	11.4523
601.8	4.24195	11.4942
703.1	4.24812	11.5444

Best values

a_0 at 298.16° K. = 4.2117 ± 0.0002 Å
V_m at 298.16° K. = 11.250 ± 0.007 cc./mole
ρ at 298.16° K. = 3.593 ± 0.002 gm./cc.
α_a at 298.16° K. = 7.88×10^{-6}
α_v at 298.16° K. = 23.6×10^{-6}

Austin's measurements are the most accurate of the previous data. The present work gives slightly lower values than Austin's over most of the temperature range studied (Fig. 4). The curves are sensibly parallel above 423° K. (150° C.) with Austin's values about 3% higher than those of the present work. From 273° to 423° K. the two curves do not have any correspondence. Austin's curve falls away very sharply compared to the more regular decrease found in the present study. The reason for the sudden decrease in Austin's values is not known, but it is believed to be incorrect. The measurements by White have a larger scatter than Austin's, but a curve computed from the data falls between Austin's data and the curve determined in this study (Fig. 4).

Sharma's measurements are at variance with all the other measurements. Except for the region below 373° K. his values are not in serious numerical disagreement. The questionable feature of Sharma's work is the shape of his curve. Sharma found that a positive parabolic function was the one best fitting his data. The other three studies all indicate a curve which tends to flatten out at high temperatures and decrease rapidly at low temperatures. Theory predicts a curve of this general shape. It is felt that Sharma's work must contain some unexplained instrumental errors.

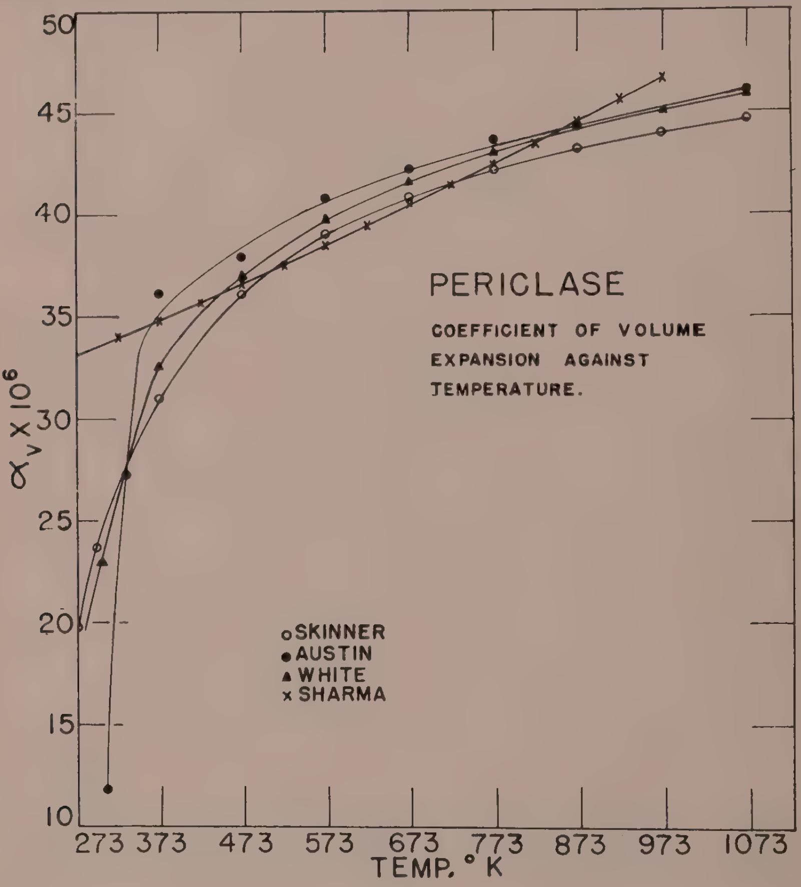

FIG. 4

DIAMOND

A number of investigators have previously determined the unit cell size of diamond. Though a considerable range in values exists, it is doubtful if the range is due as much to compositional variation, as suggested by Lonsdale (1947), as to experimental errors in the different methods of measurement. In general, the diamonds studied have not been analyzed, and where analyses have been made they must be taken with caution, since investigators generally do not state whether the impurities are present as inclusions or in solid solution. Present knowledge does not support the thesis of compositional variation sufficiently well to explain all variations in the cell size.

In Table 4 all known determinations of the cell size have been gathered.

TABLE 4. THE LATTICE PARAMETER OF DIAMOND AT 25° C. AS DETERMINED BY DIFFERENT INVESTIGATORS USING X-RAY METHODS

Cell size a_0 Å	Method used	Investigator
3.56693±0.001*	Single crystal	Ehrenberg (1926)
3.56698±0.00005	Single crystal	Tu (1932)
3.56688±0.00005	Single crystal	Tu (1932)
3.56673±0.0001	Single crystal	Renninger (1937)
3.56676±0.0001	Single crystal	Trzewatowski (1937)
3.56687±0.0001	Powder method on commercial diamond dust	Riley (1944)
3.56726±0.00005	Single crystal divergent beam	Lonsdale (1947)
3.56710±0.00005	Single crystal divergent beam	Lonsdale (1947)
3.56684±0.00005	Single crystal divergent beam	Lonsdale (1947)
3.56668±0.0001	Single crystal divergent beam	Lonsdale (1947)
3.56689±0.00003	Powder, gray bort.	Straumanis and Aka (1951)
3.56681±0.00002	Powder, average of three samples	Straumanis and Aka (1951)
3.56680±0.0001	Powder, commercial diamond dust	Skinner (1954)
3.56685±0.0001	Powder, from a single crystal	Skinner (1954)

* Precision stated by each investigator.

The measurements have all been reduced to 25° C., and where the work was stated in the old kX units the figures have been changed to Ångstrom units by applying the conversion factor of 1.00202 recommended by Bragg (1947). The average of all determinations, excluding those of the present work, is 3.56688 Å. This value is obtained by giving Straumanis and Aka's value of 3.56681 a weighting of three, since it is the average of numerous measurements on each of three samples. If the two values of the present determinations are included, the average is unchanged. It is felt that the best value for the unit cell size of diamond at 298.16° K. is 3.56688±0.00009 Å. Using this value, the molar volume of diamond at 298.16° K. is 3.41677±0.0001 cc./mole, and the density is 3.5150±0.001 gm./cc., using Wichers' (1952) value of 12.010 for the atomic weight of carbon. It is felt that the measurements of Lonsdale are given to a greater precision than her method warrants. Her values show the largest spread and include the two highest and the lowest values. It is probable that instrumental errors can account for the large variation in cell size observed by Lonsdale.

The sample of diamond dust used in the present study was a commercial grade with a grain size less than 1.0 micron. It was comprised of chips from a great many diamonds and is the finest fraction obtained from the crushing of many thousands of diamonds from many localities. If the cell size varies with composition, a sample of such a dust containing grains of many different compositions should show a range of cell sizes and the measured cell size should be the average of all the diamonds in the sample. In fact, the measured cell size of diamond dust agrees very closely with the average cell size obtained from all the values reported for single crystal measurements. The only previous measurement of the cell size of commercial diamond dust was that of Riley (1944) and his value of 3.56687 ± 0.0001 Å agrees very well with the combined average of all the single crystal measurements.

The second diamond studied in the present work was a single colorless fragment from South West Africa. Five independent spectographic analyses of a portion of the sample (Table 5), by Dr. W. H. Dennen of the Massachusetts Institute of Technology showed it to be exceptionally pure. The only comment by the analyst on the results was that the spotty distribution of impurity content was probably due in part to variations in arcing contents but is in part inherent in the sample. While the major impurity is silicon it is probable that it is present partly as inclusions in the diamond, perhaps in olivine or pyroxene, which might account for the spotty distribution.

The thermal expansions of the two samples studied differ by as much as 10% (Fig. 6). The commercial diamond dust has the lower thermal

Table 5. Spectrographic Analysis of South West African Diamond Sample
Range scanned 2,500–10,000 Å

Plate No.	Impurities in ppm.					
	Mg	Si	Fe	Al	Cu	Ca
1	2	20	1	10	<1	2
2	1	10	1	<10	<1	4
3	15	40	2	<10	<1	<0.5
4	4	<10	<0.5	<10	<1	<0.5
5	2	150	5	<10	<1	<0.5

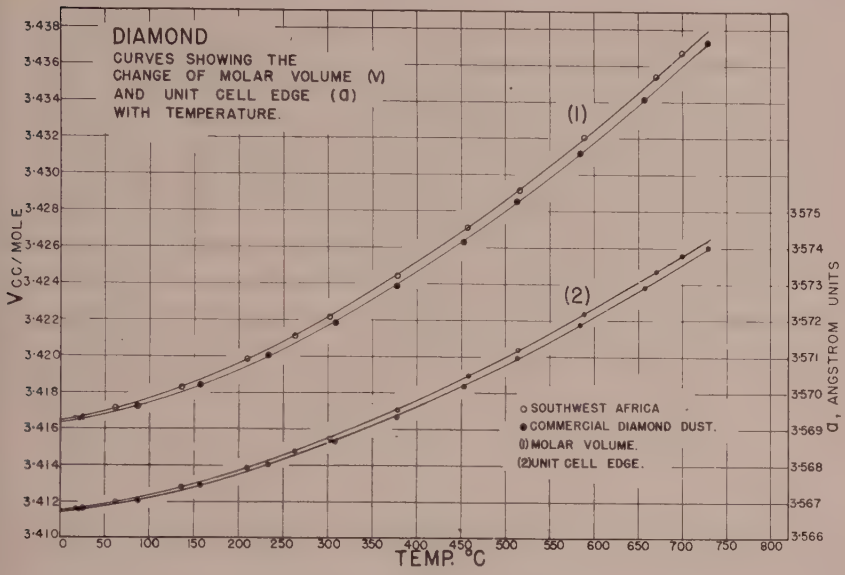

FIG. 5

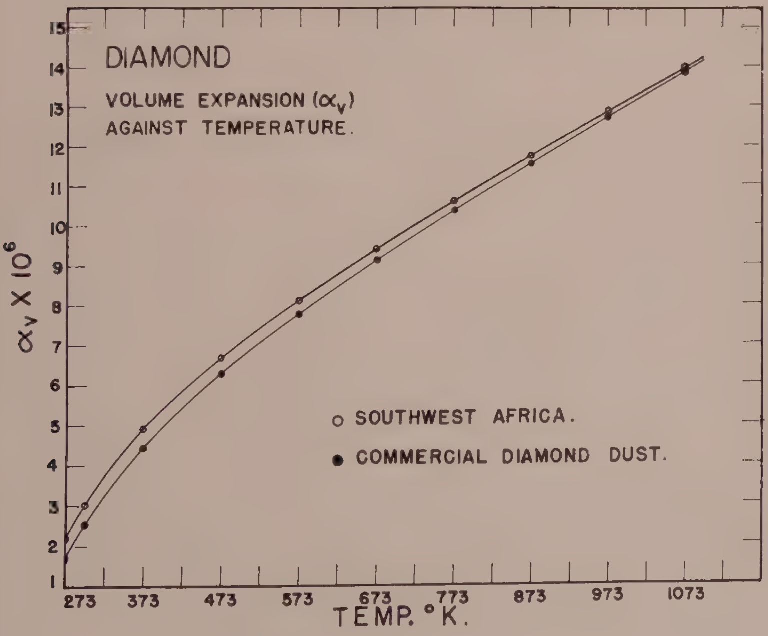

FIG. 6

U. OF I.
LIBRARY

expansion. At 298.16° K. the molar volumes of the two samples are practically the same and differ by only 0.005%. At 937° K. the molar volume of the South West African diamond is 0.02% larger than the molar volume of the commercial diamond dust (Fig. 5). To assure that experimental errors were not causing the variation in the observed thermal expansions, each sample was separately studied twice. In each case, new specimen mounts were prepared and the thermocouple system rechecked. The curves were completely reversible and reproducible.

The measured values of the unit cell size and the computed values of the molar volumes at different temperatures for the two diamond samples are recorded in Tables 6 and 7. The parameters of the various functions derived from the data in Tables 6 and 7 are given in Table 8.

TABLE 6. COMMERCIAL DIAMOND DUST
Unit cell edge a_0, and molar volume V_m at different temperatures

Temperature °C.	a_0 Å	V_m cc./mole
21.5	3.56679	3.41651
25.0	3.56680	3.41654
87.2	3.56704	3.41723
157.2	3.56745	3.41841
233.1	3.56802	3.42005
308.5	3.56844	3.42183
377.7	3.56934	3.42384
453.0	3.57019	3.42629
513.3	3.57096	3.42851
584.5	3.57187	3.43113
657.7	3.57291	3.34413
729.2	3.57401	3.43730

Several investigators have previously determined the thermal expansion of diamond. The only study comparable to the present one was that of Krishnan (1946). Krishnan used a single-crystal *x*-ray method, and measured the expansion of the crystal lattice rather than the expansion of the macroscopic crystal, which is the usual objection to single-crystal measurements. Fizeau (1869) studied the expansion from 0° to 100° C. by the interferometer method. Straumanis and Aka (1951) report an "average" coefficient of linear expansion for the temperature range 10° to 50° C. Their method of handling their data is open to some question, but it gives an estimate of the coefficient at 30° C., as $\alpha_a = (1.38 \pm 0.12) \times 10^{-6}$.

The coefficient of linear expansion at 25° C. computed from the data of Fizeau is 0.96×10^{-6}. The values obtained in the present work are

TABLE 7. DIAMOND FROM SOUTH WEST AFRICA

Unit cell edge a_0 and molar volume V_m at different temperatures

Temperature °C.	a_0 Å	V_m cc./mole
16.7	3.56683	3.41662
25.0	3.56685	3.41668
62.0	3.56700	3.41712
136.8	3.56741	3.41829
209.0	3.56793	3.41979
263.0	3.56839	3.42111
302.1	3.56874	3.42220
378.3	3.56954	3.42442
457.8	3.57047	3.42709
514.3	3.57118	3.42914
589.1	3.57219	3.43205
670.8	3.57335	3.43539

Best values

a_0 at 298.16° K.$=3.56688\pm0.00009$ Å
V_m at 298.16° K$=3.4168\pm0.0001$ cc./mole
ρ at 298.16° K.$=3.5150\pm0.001$ gm./cc.
α_a at 298.16° K.$=1.06\times10^{-6}$
α_v at 298.16° K$=2.97\times10^{-6}$

TABLE 8. PARAMETERS OF FUNCTIONS GIVING THE LINEAR AND VOLUME COEFFICIENTS OF THERMAL EXPANSION

Substance	Function	Parameters				Accuracy	Temp. range 298° K to
		b	c	d	I		
		$\times10^{-5}$	$\times10^{-9}$		$\times10^{-3}$		
Thoria	α_v	1.865	10.96	−0.3375	− 7.176	0.5%	1073° K.
	α_a	0.6216	3.541	−0.1125	− 2.387	0.2%	1073° K.
Periclase	α_v	4.232	3.630	−1.756	−18.66	0.5%	973° K.
	α_a	1.411	1.210	−0.5854	− 6.222	0.5%	973° K.
Commercial diamond dust	α_v	0.2301	11.01	−0.2708	− 2.083	0.3%	973° K.
	α_a	0.07667	3.672	−0.0903	− 0.6947	0.3%	973° K.
South West African diamond	α_v	0.2884	10.57	−0.2665	− 2.223	0.3%	973° K.
	α_a	0.09613	3.522	−0.0888	− 0.7409	0.3%	973° K.

1.011×10^{-6} for the South West African diamond and 0.844×10^{-6} for the commercial diamond dust. The coefficient at 25° C. computed from Krishnan's data is 1.13×10^{-6}. It is desirable to decide on an average value of the coefficient of linear thermal expansion for use in reducing accurate measurements of the lattice parameter of diamond to a common temperature for comparison. If all the values quoted above are averaged a figure of 1.06×10^{-6} is obtained, and it is felt that this is the best estimate of the linear coefficient at 25° C. The thermal expansion of the commercial diamond dust may conceivably be more nearly the "average" expansion of diamond than the value given above, but this suggestion must await further work.

Acknowledgments

Thanks are due to Professors Clifford Frondel and Francis Birch of Harvard University for much material assistance and guidance during the course of the work. E-an Zen has contributed many pertinent discussions and criticisms.

References

1. Austin, J. B. (1931), Thermal expansion of some refractory oxides: *Jour. Am. Ceram. Soc.*, **14**, 795–810.
2. Bradley, A. J., and Jay, A. H. (1933), Quartz as a standard for accurate lattice-spacing measurements: *Proc. Phys. Soc.* (London), **44**, 507–522.
3. Bragg, W. L. (1947), Letter to the editor: *Am. Mineral.*, **32**, 592.
4. Ehrenberg, W. (1926), Die Grösse des Diamantgitters: *Zeits. Krist.*, **63**, 320.
5. Fizeau, M. H. (1869), Tableau des dilations par le chaleur de divers corps simples metalliques ou non metalliques et de quelques composes hydrogenes du carbone: *Comp. Rend.*, **68**, 1125.
6. Frondel, C. (1955), A precision *x*-ray powder camera: *Am. Mineral.*, **40**, 876–884.
7. Hund, F., and Niessen, G. (1952), Anomalous mixed crystals in the system thorium oxide-uranium oxide: *Zeits. Elektrochem.*, **56**, 972.
8. Jay, A. H., and Andrews, K. W. (1945), Note on oxide systems pertaining to steel-making furnace slags: *Jour. Iron and Steel Inst.* (*London*), **152**, 15–18.
9. Krishnan, R. S. (1946), Thermal expansion of diamond: *Proc. Indian Acad. Sci.*, **24A**, 33–44.
10. Lonsdale, K. (1947), Divergent beam *x*-ray photography of crystals: *Phil. Trans. Roy. Soc. London, Ser. A*, **240**, 219–250.
11. Renninger, M. (1937), Unweganregung eine bisher unbeachtet Wechselwirkung-erscheinung bei Raumgitterinterferenzen: *Zeit. Phys.*, **106**, 141–176.
12. Riley, D. P. (1944), Lattice constant of diamond and the C—C single bond: *Nature*, **153**, 587–588.
13. Sharma, S. S. (1950), Thermal expansions of crystals. IV. Silver chloride, lithium fluoride and magnesium oxide: *Proc. Indian Acad. Sci.*, **32**, 268–274.
14. Straumanis, M. E., and Aka, E. Z. (1951), Precision determination of lattice parameter, coefficient of thermal expansion and atomic weight of carbon in diamond: *Jour. Am. Chem. Soc.*, **73**, 5643–5646.

15. Trzewatowski, (1937), *Roczniki Chem.*, **17,** 73. Quoted by Rossini and Jessup, *Bureau Std. Jour. Research* **21,** 491–513.
16. Tu, Y. C. (1932), A precision comparison of calculated and observed grating constants of crystals: *Phys. Rev.*, **40,** 662–675.
17. White, H. E. (1938), Electrically fused magnesia: *Jour. Am. Ceram. Soc.*, **21,** 216–229.
18. Wichers, E. (1952), Report of the Committee on Atomic Weights of the American Chemical Society: *Jour. Am. Chem. Soc.*, **74,** 2447–2450.
19. Wyckoff, R. W. G. (1925), Crystal structure of silver phosphate and silver arsenate (Ag_3XO_4): *Am. Jour. Sci.*, **10,** 107–118.

Manuscript received May 4, 1956.

GINORITE AND SASSOLITE FROM DEATH VALLEY, CALIFORNIA*

Robert D. Allen,† *U. S. Geological Survey, Claremont, California*
and Henry Kramer,‡ *U. S. Geological Survey, Washington, D.C.*

Abstract

Ginorite, $2CaO \cdot 7B_2O_3 \cdot 8H_2O$, and sassolite, $B_2O_3 \cdot 3H_2O$, have been found closely associated in efflorescent masses in colemanite-veined basalt near the head of Twenty Mule Team Canyon, Death Valley.

The ginorite is in rhomb-shaped plates, less than 0.02 mm. in diameter, with acute angle about 79° and the following indices of refraction: α_{Na} 1.520 (parallel to short diagonal) γ_{Na} 1.580 (parallel to long diagonal). Pycnometric specific gravity is 2.07. Chemical analysis, ginorite, B_2O_3 65.21 (per cent), CaO 14.56, SrO 1.10, H_2O 19.13; sassolite, B_2O_3 57.19, H_2O 42.81. The strongest lines of an *x*-ray diffractometer pattern of ginorite are as follows: 7.10 Å 10; 5.36 Å 3; 3.27 Å 2; 3.18 Å 2; 2.08 Å 2.

Sassolate is in pearly plates, usually less than 1 mm. in diameter, with the following optical properties: α_{Na} 1.340; β_{Na} 1.457; γ_{Na} 1.459; $2V_{calc}$ 14°; wavy extinction. The strongest lines of an *x*-ray diffractometer pattern are as follows: 3.18 Å 10; 6.03 Å 1; 1.590 Å 1.

Introduction

Ginorite, $2CaO \cdot 7B_2O_3 \cdot 8H_2O$, and sassolite, $B_2O_3 \cdot 3H_2O$, occur together in the Death Valley area, California. This is the third reported occurrence of ginorite in the world and the first reported occurrence of sassolite in the Death Valley area.

Occurrence

These two boron minerals were collected by James F. McAllister of the U. S. Geological Survey in October 1954 at the Mott open-cut colemanite prospect in a minor tributary to Furnace Creek Wash near the head of Twenty Mule Team Canyon, northwest of and downstream from the Corkscrew diversion channel in SW$\frac{1}{4}$ sec. 9, T. 26 N., R. 2 E., San Bernardino base and meridian, Inyo County, California. The ginorite and sassolite are closely associated, both minerals occurring in soft, white to pale yellowish brown efflorescent masses in weathered basalt within 50 cm. of the surface; the underlying altered basalt contains veins of colemanite and is associated with colemanite-bearing limestone.

The ginorite occurs in white pellets which average about 1 to 2 mm. in diameter and are embedded in a pale yellowish brown matrix of sassolite and clay. In this matrix pearly sassolite plates as much as 1 mm. in diameter are present. An unidentified mineral, present in very minor

---

* Publication authorized by the Director, U. S. Geological Survey.

† Present address: Jet Propulsion Laboratory, California Institute of Technology, Pasadena, California.

‡ Present address: Pyrotechnics Laboratory, Samuel Feltman Ammunition Laboratories, Picatinny Arsenal, Dover, New Jersey.

amount, was observed under the microscope by W. T. Schaller, U. S. Geological Survey; it has the following optical characteristics: α about 1.465; γ about 1.505; uniaxial (or biaxial with very small 2V) negative; six-sided plates with parallel (or nearly parallel) extinction. Minute grains of celestite and of quartz are sporadically distributed in the efflorescence.

Ginorite was first found in the Clinton Quarry (inaccessible in 1948—private communication from W. T. Schaller), Windsor, Nova Scotia, Canada, associated with mirabilite along the gypsum-anhydrite contact and described by How (1861) under the name cryptomorphite. Its identity with the better described hydrous calcium borate named ginorite, occurring with calcite in veins in sandstone at Sasso Pisano, Tuscany, Italy (D'Achiardi, 1934), was determined by Hey and Bannister (1952) who suggested that the name ginorite be used.

No American occurrence of sassolite is listed in the seventh edition of Dana's System of Mineralogy (Palache, Berman, and Frondel, 1944).

GINORITE

Optical Properties

At all three occurrences the ginorite is in minute rhomb-shaped plates. Those from the Death Valley area are nearly equilateral and range in diameter between 0.001 and 0.020 mm. The acute angle of the rhombs is about 79°, the average of 30 measurements, ranging from 75° to 83°. The rhombs, whose extinction directions are approximately parallel to their diagonals, show positive elongation. The indices of refraction for sodium light are: α(parallel to short diagonal) $= 1.520 \pm 0.003$; γ(parallel to long diagonal) $= 1.580 \pm 0.003$. Similar indices of refraction are reported for ginorite from the other two localities.

D'Achiardi (1934) gives for Tuscany ginorite: $\alpha = 1.517$; $\beta = 1.524$ (calc.); $\gamma = 1.577$; $2V = 42°$; positive; extinction angle, α to elongation of the "lozenges," 51°; acute angle of lozenges, 78° to 80°. The lozenges are thought to be monoclinic plates parallel to $\{010\}$. Hey and Bannister (1952) report similar optical properties for ginorite from Nova Scotia and Tuscany: $n_1 =$ about 1.526; $n_2 =$ about 1.579; rhombic plates with acute angle 77° (Tuscany) to 79° (Nova Scotia); positive elongation; extinction directions parallel to rhomb diagonals. Hey and Bannister suggest that the symmetry of ginorite may be orthorhombic rather than monoclinic as proposed by D'Achiardi.

Chemical Composition

The water insoluble ginorite from the Death Valley area was purified by solution of the sassolite in warm water and drying the residual ginorite in an oven at 105° C. Microscopic examination after the treatment showed no measurable change in the mineral.

In Table 1 the analysis of ginorite from the Death Valley area is compared with three analyses of ginorite from Sasso Pisano, Tuscany (D'Achiardi, 1934; Hey and Bannister, 1952). The formula derived from our analysis is $2(CaO,SrO)\cdot 7B_2O_3\cdot 8H_2O$. Except for the presence of strontium, this formula agrees with D'Achiardi's formula, $2CaO\cdot 7B_2O_3\cdot 8H_2O$. It should be noted that neither the analyses published by D'Achiardi nor the analysis of Hey are in close agreement with this formula. According to W. T. Schaller strontium is present in more than trace amount in

Table 1. Ginorite—Chemical Analyses and Calculation of Formula

	Death Valley area, California Ginorite		Tuscany Ginorite 1		Tuscany Ginorite 2		Tuscany Ginorite 3	
	(per cent)		(per cent)		(per cent)		(per cent)	
	Orig.	Recalc.	Orig.	Recalc.	Orig.	Recalc.	Orig.	Recalc.
B_2O_3	64.47	65.21	63.00	64.42	64.06	64.49	58.54	63.64
CaO	14.39	14.56	15.40	15.75	16.00	16.11	14.75	16.03
SrO	1.09	1.10	—	—	—	—	—	—
Na_2O	—	—	—	—	—	—	0.16	0.17
H_2O (+)	18.91	19.13	19.40	19.83	19.27	19.40	18.54	20.16
Rem.	1.48		2.20		1.22		8.34	
Total	100.34		100.00		100.55		100.33	
Less rem.	1.48		2.20		1.22		8.34	
Total	98.86	100.00	97.80	100.00	99.33	100.00	91.99	100.00
Analyst:	Henry Kramer		Gallori		Rossoni		Hey	

	Molecular proportions (Death Valley area)	Oxygen atoms	Atomic ratios	Atomic ratios on basis of 31 O's	
B_2O_3	0.9364	2.8092	B 1.8728	14.019	
CaO	0.2596	0.2596	Ca 0.2596	1.943	2.022
SrO	0.0106	0.0106	Sr 0.0106	0.079	
H_2O	1.0616	1.0616	H 2.1232	15.897	

Formula: $(Ca,Sr)_2B_{14}O_{23}\cdot 8H_2O$ or $2(CaO,SrO)\cdot 7B_2O_3\cdot 8H_2O$

typical Italian ginorite, and, if the assumption is made that 1 per cent SrO is present (as it is in the Death Valley area material), the molecular proportions calculated from the three analyses of Italian ginorite are closer to the formula $2(CaO,SrO)\cdot 7B_2O_3\cdot 8H_2O$ than they are without this assumption.

Spectrographic analysis by Hal W. Johnson, Pacific Spectrochemical Laboratory, Los Angeles, Calif., gave the following additional determinations, in per cent: 0.X = Mg, Si, Na, Fe; 0.0X = Al; 0.000X = Cu.

A pycnometric specific gravity determination at 25° C. gave 2.07, close to the value of 2.09 given by D'Achiardi (1934) for ginorite from Tuscany.

SASSOLITE

Optical Properties

The optical properties of California sassolite are compared with those published for Italian and synthetic sassolites in Table 2.

TABLE 2. OPTICAL PROPERTIES OF SASSOLITE

	California	Italy (Larsen, 1921)	Synthetic (Kracek, Morey and Merwin, 1938)
α_{Na}	1.340±0.005	1.340±0.005	1.337
β_{Na}	1.457±0.003	1.456±0.003	1.461
γ_{Na}	1.459±0.003	1.459±0.003	1.462
Optic sign	Negative	Negative	Negative
$2V_{calc.}$	14.0°	17.0°	9.6°
Orientation	X angle base is very large	X angle base is nearly 90°	X angle base is 88°
Other	Plates lack regular outlines and show wavy extinction		

Chemical Composition

Sassolite, contaminated with ginorite and clay, was analyzed for water-soluble B_2O_3 and water-insoluble material. The recalculated analysis is compared with the theoretical combining proportions for boric acid in Table 3.

X-RAY DIFFRACTION PATTERNS

X-ray powder patterns were prepared for ginorite and sassolite with nickel-filtered copper radiation over the range $2\theta = 5°$ to $90°$, being scanned with a Geiger counter spectrometer at 1° per minute. In Table 4 the pat-

TABLE 3. SASSOLITE—CHEMICAL ANALYSIS

	Death Valley Sassolite	Boric acid (theoretical)
	(per cent)	(per cent)
B_2O_3	57.19	56.39
H_2O	42.81 (by difference)	43.61
Total	100.00	100.00

TABLE 4. *X*-RAY PATTERNS: INTERPLANER SPACINGS AND RELATIVE INTENSITIES
Nickel-filtered copper radiation

Ginorite California		Ginorite, Italy (Hey and Bannister, 1952)		Sassolite, California		Boric acid, C.P.	
d(Å)	*I*	*d*(Å)	*I*	*d*(Å)	*I*	*d*(Å)	*I*
7.14	10	7.18	vs	6.02	1	6.04	2
5.36	3	5.36	s	5.89	<1	5.91	<1
4.89	<1	4.92	vw	4.59	<1	4.60	<1
4.66	1	4.68	w	4.20	<1	4.21	<1
—		4.29	vvw	4.04	<1	4.06	<1
4.06	1	4.08	w	3.52	<1	3.52	<1
3.90	1	3.90	mw	3.18	10	3.18	10
3.58	1	3.57	mb	—		3.03	1
3.43	<1	3.42	vvw	2.95	<1	2.95	<1
3.27	2	3.28	m	2.92	<1	2.92	1
3.18	2	3.18	vvw	—		2.84	<1
3.12	1	3.12	mw	2.71	<1	2.72	<1
2.98	1	2.98	w	2.64	<1	2.64	1
2.87	1	2.88	w	2.56	<1	2.56	<1
2.80	1	2.81	vw	—		2.53	<1
2.72	<1	2.73	vw	—		2.50	<1
2.65	<1	—		—		2.30	<1
2.61	<1	2.62	vw	2.23	<1	2.23	<1
2.58	<1	2.58	vvw	—		2.10	<1
2.54	<1	2.53	vvw	—		2.04	<1
2.46	<1	2.47	vw	1.949	<1	1.949	<1
—		2.36	vwb	—		1.905	<1
2.29	<1	2.28	vw	—		1.888	<1
2.23	<1	2.24	w	—		1.692	<1
2.15	<1	2.16	w	—		1.670	<1
2.11	<1	—		—		1.642	<1
2.08	2	2.09	s	1.590	1	1.591	2
2.02	<1	2.03	vw				
1.965	<1	1.96	wb				
—		1.92	vvw				
—		1.821	vvw				

terns for ginorites from California and Italy (Hey and Bannister, 1952) are in essential agreement. The pattern for analytical reagent boric acid, which is more completely developed than the pattern for sassolite from California, confirms the identity of this mineral.

Fred A. Hildebrand, U. S. Geological Survey, verified ginorite and identified sassolite in an earlier *x*-ray pattern of the first sample of efflorescence collected.

REFERENCES

D'ACHIARDI, G. (1934), Ginorite, nuovo borato di calcio di Sasso Pisano: *Periodico Mineralogia, Rome*, **5**, 22–32. (*Mineralog. Abs.*, **5**, 484.)

HEY, M. H., AND BANNISTER, F. A. (1952), The identity of cryptomorphite and ginorite: *Mineralog. Mag.*, **29**, 955–959.

HOW, H. (1861), Natro-boro-calcite and another borate occurring in the gypsum of Nova Scotia: *Am. Jour. Sci.*, **32**, 9–13.

KRACEK, F. C., MOREY, G. W., AND MERWIN, H. E. (1938), The system, water-boron oxide: *Am. Jour. Sci.*, **35A**, 166–167.

LARSEN, E. S. (1921), The microscopic determination of the nonopaque minerals: *U. S. Geol. Survey, Bull.* **679**, 130.

PALACHE, C., BERMAN, H., AND FRONDEL, C. (1944), Dana's System of Mineralogy, 7th ed., vol. 1, pp. 662–663, John Wiley & Sons, New York.

Manuscript received May 7, 1956.

EPIDOTE FROM HAWLEYVILLE, CONNECTICUT*

DAVIS M. LAPHAM, *Department of Geology, Columbia University, New York, N.Y.*

ABSTRACT

The Hawleyville, Conn. epidote occurs in a prochlorite-apatite-orthoclase pegmatite along nearly horizontal fracture planes of a medium- to coarse-grained diorite. The occurrence is unusual since the epidote is colorless to yellow brown with a radiating prismatic habit. Optical and x-ray data are presented and the material is compared with the structurally and chemically similar zoisite and clinozoisite. The distinguishing features of the members of the epidote group are reviewed. It is suggested that the mineral name "epidote" be restricted to material which is optically negative. Indices of refraction are presented for stilbite which appear to represent a high Ca variety.

INTRODUCTION

This locality was first brought to the writer's attention in an article by Wm. Agar and Earl H. Emendorfer on the manganiferous prochlorite at Hawleyville, Conn. (Agar and Emendorfer, 1937). After visiting the locality in connection with research on the chlorite minerals, a colorless to yellow brown radiating mineral was found closely associated with the prochlorite. Upon investigation, this mineral has been identified as epidote, although it lacks the characteristic pistachio green color normally associated with epidote.

I express my sincere appreciation to Professors Paul F. Kerr and Ralph J. Holmes of Columbia University for their helpful criticism of this paper.

LOCATION

Hawleyville, Conn., is east of Danbury, Conn., on route 25 a few miles north of the junction of routes 6 and 25 (Fig. 1). The samples were taken from an east-west trending railroad cut one third of a mile west of Hawleyville near the northwest border of the township of Newton, Conn. The railroad cut may be reached by taking the dirt road marked Sky Ridge which runs in a westerly direction from route 25 south of Hawleyville. The Sky Ridge road is shown as a dotted line in Fig. 1.

GEOLOGY

The Brookfield Diorite

The prominent outcrop through which the New York and New England Railroad (a branch track also used by the New York, New Haven and Hartford R.R.) has made a deep cut along Sky Ridge near Hawley-

---

* Awarded the George Frederick Kunz Prize by the New York Mineralogical Club, 1956.

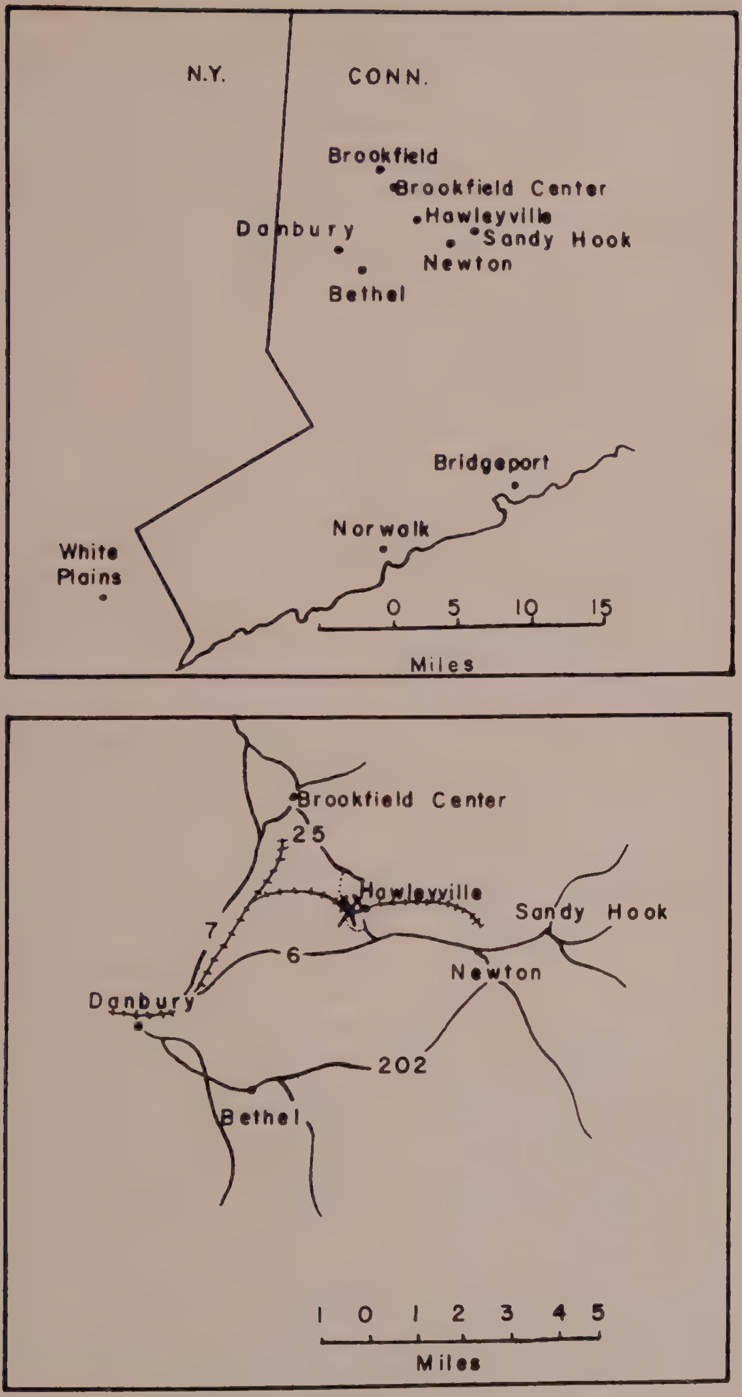

FIG. 1. Location of Hawleyville epidote.

ville is composed of medium- to coarse-grained diorite. Megascopically it is even textured and composed of equant grains of plagioclase, white orthoclase, and biotite. The white orthoclase grades into pink orthoclase near the epidote-chlorite veins to be described later. In thin section it may be seen that this pink color is the result of clouding by small flakes of hematite.

A thin section study of the Brookfield diorite revealed the following approximate composition:

- 25% to 30% biotite
- 25% microcline
- 25% plagioclase
    - 5% Ab_9An_1
    - 15% Ab_8An_2
    - 5% Ab_7An_3
- 17% orthoclase
- 8% to 13% quartz, ilmenite, zircon, and apatite.

The quartz does not exceed 5%. The ratio of alkali feldspar to plagioclase is about 5:3 and the ratio of microcline to orthoclase is about 3:2. The absence of hornblende is very striking both in hand specimen and thin section, emphasizing the similarity between the Brookfield diorite and a typical monzonite.

There are at least three prominent fracture systems which have been important in localizing various types of pegmatites. Although their occurrences are somewhat irregular, there is a dominant system which dips approximately 15 degrees to the west and strikes northwest. Another conspicuous series of fractures dips about 15 degrees to the east and strikes southeast. A third nearly vertical system strikes north-south, transecting the two nearly horizontal sets of fractures. It is these three systems which appear to have localized the later pegmatitic intrusions (Fig. 2).

On the south wall of the cut about 200 feet from the overpass and four feet above the railroad tracks, there is a narrow band of schistose rock which has a bulk composition similar to the composition of the Brookfield diorite. This band, four to six inches wide, parallels the dominant westward dipping fracture system, but pinches out into normal diorite eastward at its upper end (Fig. 2). The mica in the schistose band appears to be a light brown phlogopite or muscovite. The loosely layered character of this band has made it more susceptible to both replacement and weathering.

The Pegmatites

Although there are three distinct types of pegmatites intrusive into the diorite, two of these contain only feldspar crystals and massive quartz with muscovite crystals along the pegmatite border. The third type is a complex feldspar-quartz pegmatite paralleling the two nearly horizontal fracture systems.

The pink feldspar-epidote-chlorite bearing solutions evidently followed vertical fractures until they intersected the westward dipping schistose band. This band then offered an easy path for the solutions so that they replaced the band laterally and down the dip. In addition to this schistose band, the normal diorite has been altered in the immediate vicinity of the pegmatite. This alteration consists primarily of hematite-clouded pink orthoclase feldspar with minor amounts of plagioclase and biotite and forms a gradational transition zone between the pink orthoclase crystals bordering the pegmatite and the normal diorite. The extent of this replacement halo does not exceed two feet beyond the epidote-chlorite pegmatite center.

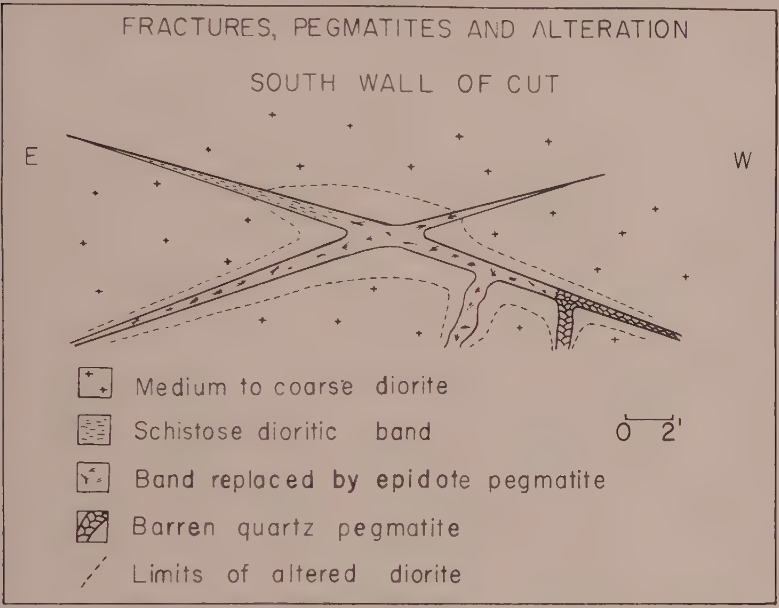
FRACTURES, PEGMATITES AND ALTERATION
SOUTH WALL OF CUT
E
W
Medium to coarse diorite
Schistose dioritic band
Band replaced by epidote pegmatite
Barren quartz pegmatite
Limits of altered diorite
0 2'

FIG. 2

A few feet to the east there is another feldspar-epidote-chlorite pegmatite following an eastward dipping fracture system so that these two oppositely dipping pegmatites intersect about five feet above the base of the rock cut. There is no visible feeder for this second pegmatite (Fig. 2).

Geologic Sequence

The following is a probable recapitulation of the sequence of events:

1. Intrusion of a diorite body which cooled rather slowly yielding a medium to coarse texture.
2. Fracturing and some slippage creating faults and a weak zone of schistose structure; —not necessarily contemporaneously.
3. Influx of feldspar-epidote-chlorite solutions following vertical frctures but crystallizing preferably along the nearly horizontal fracture systems with notable replacement of the orthoclase and microcline by clouded pink orthoclase.
4. Intrusion of nearly barren quartz pegmatites in one or more stages.
5. Deposition of stilbite along vertical fractures.

MINERALOGY

The Pegmatites

The center of the feldspar-epidote-chlorite pegmatites contains straw yellow to nearly colorless radiating crystals of epidote, yellow to colorless crystals of apatite, and a few elongated milky quartz crystals in a matrix of deep green, nearly cryptocrystalline prochlorite. According to Agar and Emendorfer (1937) the prochlorite contains a small amount of manganese.

The borders of these pegmatites usually consist of brown to greenish muscovite crystals, often in very compact books. They form along the margin of the pegmatite between the epidote-chlorite center and the pink orthoclase alteration rim. The pink orthoclase crystals are untwinned both megascopically and microscopically.

As a final phase of the mineralization, unrelated to the diorite intrusive and subsequent pegmatite formation, thin coatings of radiating white stilbite crystals formed along many of the vertical fractures.

The indices of refraction usually given for stilbite (Larsen and Berman, 1934) are $\alpha=1.494$, $\beta=1.498$, and $\gamma=1.500$. However, the indices determined for the Hawleyville material are $\alpha=1.485\pm.002$, $\beta=1.490\pm.002$, and $\gamma=1.493\pm.002$.* The index liquids used were checked on an Abbe refractometer using a sodium light source. All the other optical properties coincide with the optical properties for stilbite (Larsen and Berman, 1934). As supporting identification, an x-ray powder photograph was made with a Debye-Scherrer camera using filtered Cu radiation. The pattern of the Hawleyville stilbite matches the values given in the *A.S.T.M.* Index for stilbite from Palm Grove, Victoria Falls, Zambesi River, N. Rhodesia and it also matches the pattern of stilbite from Poonach, India, in the mineralogy laboratory reference files at Columbia University. Consequently the Hawleyville material may be identified as stilbite. From this data it seems probable that stilbite may have a range of indices of refraction greater than previously reported.

---

* Similar to the low indices of the high Ca-variety, stellarite; Neuman, *Norges Geol. Undersokelse*, No. **166**, 108–113 (1944); Pabst, *Min. Mag.*, **25**, 271 (1939).

The Hawleyville Epidote

Ordinarily epidote is pistachio green and occurs in single crystals or parallel groups. This epidote, however, varies from nearly colorless to straw yellow to light green and commonly forms large radiating groups of crystals. Such a deviation marks this as an unusual occurrence and worth investigation. A colorless epidote from Garda in northern Italy may be a similar variety (Lacroix, 1887). No specimen was available for comparison.

Although on first glance these crystals resemble vesuvianite, the two minerals most likely to be confused with this epidote are zoisite and clinozoisite. Indeed all belong to the same family, which also includes piedmontite, withamite, allanite, manganepidote, thulite, and hancockite. Of these only epidote, allanite, manganepidote, withamite, and hancockite are optically negative. Thus a distinction between epidote on the one hand and zoisite and clinozoisite on the other rests on the difference in optic sign.

In its own optic group epidote may be distinguished from withamite by an absence of strong red pleochroism and a negligible manganese content; from hancockite by lower indices of refraction; from manganepidote by lower birefringence, lower indices of refraction, and the absence of significant amounts of manganese, and from allanite by lower birefringence, an absence of rare earth elements, its greenish color, and by its lack of radioactivity.

The properties of the Hawleyville epidote are as follows:

Color: colorless, straw yellow, brownish yellow, and yellowish green.
Habit: radiating prismatic with occasional bent crystals.
Specific gravity: 3.321 ± .006.
Refractive indices: $\alpha = 1.726$.
$\beta = 1.735$.
$\gamma = 1.741$.
Optic sign: negative.
Pleochroism: X—colorless.
Y—occasionally faint pale pink.
Z—colorless to neutral.
Interference colors: regular, not anomalous.
Twinning: rarely polysynthetic on (100) 2V greater than 50°.

The pistachio green color of epidote is usually considered to be due to its high iron content while the lighter color of clinozoisite is believed to be the result of less than ten per cent iron. Zoisite, which is usually still lighter in color, contains little or no iron (Dana-Ford, 1932). In addition, the optic sign changes from positive to negative, distinguishing clinozoisite from epidote in this iron replacement series. Both the indices of refraction and birefringence increase with increasing iron content. A comparison of iron content with color and indices of refraction for minerals of this group from several localities is shown in Table 1. The Hawleyville, Conn., material is included based on an analysis by W. H.

TABLE 1. RELATION OF IRON CONTENT TO COLOR AND INDICES OF REFRACTION

%Fe_2O_3	%FeO	%Fe	Color	Indices	Biref.	Ref.
3.52	.35	2.73	golden green	1.724 1.729 1.734	.010	10.
7.62		5.33	green	1.706 1.708 1.712	.006	8.
	7.83	6.08	colorless			11.
9.67		6.77	olive green	1.722 1.742 1.750	.028	4.
8.88	.97	6.97	straw yell.-green	1.726 1.735 1.741	.015	1.
		12.0	colorless or green*	1.716 1.719 1.723	.007	7.
		13.0	dark green to gray brown	1.714 1.719 1.725	.011	9.
15.53		10.85	pistachio green			5.
17.25		12.06	pistachio green	1.729 1.763 1.779	.050	4.
		22.0	pistachio green	1.722 1.742 1.750	.028	7.
		23.0	dark green		.033	2.

* Both colors are given by Larsen and Berman (1934) in different tables apparently for the same mineral.

Note: %Fe was calculated from given oxide per cent.

Herdsman given below in Table 2. It can be seen from the standpoint of color alone, the Hawleyville epidote would probably have less than 15% iron. That it might have less than the 10% stipulated as the boundary per cent between clinozoisite and epidote (Dana-Ford, 1932) may be seen by the colorless Garda epidote with a 7.83% FeO content. As regards the indices of refraction, the high α index of the Hawleyville epidote suggests a relatively high iron content, while the low birefringence (.015) suggests a moderate iron content. The chemical analysis given in Table 2 confirms these conclusions regarding iron content based on the color and optical properties of the epidote. It should be noted that both total iron per cent and total iron oxide per cent are less than the stipulated 10% often regarded as the minimum iron content for epidote. On the other hand, if one were to define epidote on the basis of a negative optic sign, the Hawleyville material would have to be regarded as epidote and not as clinozoisite.

TABLE 2

Oxide	%
SiO_2	37.96
Al_2O_3	27.34
FeO	.97
Fe_2O_3	8.88
MnO	.16
CaO	22.07
MgO	.34
$H_2O-105°$	.08
$H_2O+105°$	2.14
	99.94

Analysis by W. H. Herdsman, Glasgow, Scotland.

It is interesting to note that, as might be expected from the associated manganese-bearing chlorite, the epidote also contains a small percentage of manganese. Evidently this quantity is insufficient to affect the optical properties appreciably. It is certainly insufficient for this mineral to be regarded as one of the manganese epidote minerals mentioned previously.

In an effort to distinguish the Hawleyville epidote from the structurally similar clinozoisite and zoisite, several x-ray powder photographs were taken. A Debye-Scherrer camera was used with Cu radiation and a Ni filter. Each pattern was measured independently several times to decrease the margin of error of two-theta measurement. The intensities shown in Table 3 are the averages of at least three independent visual estimates for each powder pattern.

The zoisite from Ducktown, Tenn., is greenish and optically positive. The Bourg d'Oisans epidote from France, is pistachio green, contains 14.88% iron, and is optically negative. The "clinozoisite" from Nightingale Range, Nev., is gray, but optically negative, and therefore probably an epidote. The clinozoisite from Timmins, Ont. (Fouqueite) is gray-brown, radiating prismatic, and optically positive. This Timmins clinozoisite is here taken to be representative of clinozoisites as a whole. Although it can be seen from Table 3 that these are all similar minerals, the following distinctions may be made:

1. The Hawleyville epidote exhibits a 7.02 Å and a 1.590 Å line, neither of which are present in the Timmins clinozoisite.
2. The Timmins clinozoisite has 6.60 Å, 3.325 Å, and 2.631 Å lines not found in any of the epidote patterns.
3. There do not seem to be any significant intensity variations between the epidotes and the clinozoisite, but the zoisite is significantly different.
4. The 3.325 Å and 2.631 Å lines of the Timmins clinozoisite are common to the zoisite, but are not found in the three epidotes.
5. The Nevada "clinozoisite" (actually epidote) and the Hawleyville epidote have consistently greater "*d*" spacing values for the same reflections than the Timmins clinozoisite and the Bourg d'Oisans epidote. The former pair correspond to lighter colored hand specimens and the latter to darker hand specimens, suggesting that the coloring agent or agents is shifting the "*d*" reflections to smaller values. In the light of the optical properties and chemical analysis, it seems probable that iron content is the major factor involved in this shift.

CONCLUSIONS

There is no prominent structural difference among the five samples which were examined by *x*-rays. However, the zoisite "*d*" value shifts, as well as the significant intensity variations indicate that there is some structural dissimilarity. Ito (1947) has proposed that zoisite is twinned clinozoisite. Such intimate twinning resulting from a change in position of Al(Fe) octahedra with respect to Al tetrahedra might explain the differences observed in the powder patterns of these two minerals. In addition, as the composition changes from the light gray zoisite to the dark pistachio green of the Bourg d'Oisans epidote, the 6 Å, 7 Å, and 8 Å lines gradually disappear, the 8 Å line being the last to disappear. This represents a structural change which may be a reflection of increasing iron content.

If the Timmins clinozoisite is accepted as a typical clinozoisite, then a consideration of the *x*-ray data leads to the conclusion that the structural similarity between epidote and clinozoisite is greater than the similarity between either epidote and zoisite or clinozoisite and zoisite. This is in sharp contrast to the optical properties. Optically, clinozoisite and zoisite are similar, both being positive, while epidote is optically negative. Since the optical properties of a mineral are also a direct consequence of its

TABLE 3. COMPARISON OF X-RAY VALUES FOR MEMBERS OF THE EPIDOTE GROUP

Zoisite Ducktown, Tenn.		Epidote Bourg d'Oisans		"Clinozoisite" Nightingale R. Nev.		Epidote Hawleyville		Clinozoisite Timmins, Ont.	
Int.	d(Å)	Int.	d(Å)	Int.	d(Å)	Int.	d(Å)	Int.	d(Å)
30	8.13			3	8.08	4	7.98	8	7.93
						3	7.02		
								6	6.60
50	5.027	40	4.950	50	5.038	40	5.018	35	4.992
15	4.675								
		½?	4.543	½?	4.631	½?	4.621		
8	4.245								
40	4.048								
		50	3.969	50	4.006	40	3.997	45	3.997
		1	3.732	2	3.749	½?	3.762	3	3.751
60	3.615								
		45	3.450	45	3.487	40	3.492	30	3.468
		20	3.370	3	3.394	6	3.372	8	3.390
2	3.328							6	3.325
		30	3.176	12	3.207	15	3.197	20	3.184
35	3.106			½?	3.060	½?	3.060	2	3.044
100	2.869	100	2.872	100	2.893	100	2.900	100	2.884
35	2.783	60	2.795	65	2.805	50	2.809	55	2.790
100	2.703								
		70	2.667	65	2.676	60	2.677	60	2.666
20	2.626							12	2.631
		65	2.588	60	2.593	55	2.593	60	2.584
30	2.531	30	2.514	15	2.529	10	2.525	15	2.511
½?	2.459	10	2.439	2	2.449	6	2.449	12	2.437
40	2.407	80	2.393	75	2.397	70	2.396	65	2.385
60	2.335	45	2.290	25	2.296	25	2.289	25	2.285
10	2.238								
		50	2.152	25	2.162	25	2.161	25	2.153
10	2.111	60	2.103	40	2.110	40	2.111	35	2.099
65	2.064	20	2.064	3	2.067	10	2.065	6	2.060
		5	2.038	½?	2.044	½?	2.043	½?	2.043
5	2.020					1	2.020		
15	1.982			½?	1.997	1	2.003	½?	1.994
20	1.903	2	1.915			½?	1.914		
		70	1.867	70	1.871	60	1.869	60	1.865
30	1.844								
		1	1.767			1	1.773	1	1.765
		½?	1.741			1	1.742	½?	1.740
½?	1.715	½?	1.700			1	1.705	½?	1.699
8	1.685	½?	1.682			1	1.687	½?	1.684
4	1.666	½?	1.666			1	1.669		
		85	1.635	75	1.633	65	1.635	65	1.631
75	1.615	20	1.622	12	1.622	10	1.622	20	1.618
25	1.591			20	1.585	10	1.590		
		25	1.575	20	1.575	12	1.574	15	1.571
20	1.544	20	1.541	6	1.539	6	1.539	6	1.536
				2	1.530			½?	1.524
35	1.453	40	1.456	20	1.457	15	1.458	25	1.451
10	1.429	2	1.437	4	1.435	6	1.435	6	1.433
½?	1.406	55	1.406	30	1.404	30	1.404	35	1.398
45	1.388	50	1.392	15	1.393	25	1.389	15	1.388
2	1.369	1	1.363						
30	1.347	8	1.344	2	1.342	4	1.346	1	1.339
20	1.291	8	1.295	4	1.296	6	1.297	4	1.2934
8	1.268	12	1.267	20	1.265	8	1.265	10	1.262

structural arrangement, this seems to present a paradox. Epidote has been regarded as an iron-rich zoisite and presumably the change in optic sign could be attributed to the increase in iron content. A similar feature occurs in the forsterite-fayalite series in which there is a continuous transition from the optically negative iron-rich member, fayalite, to the optically positive forsterite. Olivine of intermediate composition, may be either positive or negative.

Tempel (1938) found that the presence of rare earths, in addition to the water and ferrous-ferric content, influences both the physical and optical properties of epidote. Thus even a chemical classification becomes a complex problem. Since ferric iron is able to substitute diadochically for aluminum in the epidote structure, it seems that the distinction between epidote and clinozoisite, at least for the present, should be based on the difference in optic sign which reflects both the chemical and the slight structural dissimilarities of the two minerals.

The Hawleyville material may be considered to be an epidote as long as the definition of epidote rests upon the optic sign determination. However, should clinozoisite eventually take the analogous position of olivine as either optically positive or negative, then the Hawleyville material will have to be reclassified on another basis. Additional x-ray analyses on the effect and position of iron substitution in the members of the epidote group might reveal a better basis for differentiating the minerals of this group.

REFERENCES

1. AGAR, WM. M., AND EMENDORFER, EARL H. (1937), Manganiferous prochlorite from Hawleyville, Conn.: *Am. Jour. Sci.*, **34,** 77–80.
2. ANDERSON, O. (1911), On epidote and other minerals: *Archiv. for Math. og Naturvidensk*, **31,** Nr. 15.
3. DANA, E. S., AND FORD WM. E. (1932), A Textbook of Mineralogy, 4th edition, pub. John Wiley and Sons, N.Y.C., pp. 620–625.
4. GOLDSCHLAG, M. (1917), Über die optischen Eigenschaften der Epidote: *Tsch. Min. Pet. Mit.*, **34,** 23–60.
5. ITO, T. (1947), The structure of epidote: *Am. Mineral.*, **32,** 309–321.
6. LACROIX, M. A. (1887), Études critiques de minéralogie: *Lex. Bull. Soc. Min.*, **10,** 150.
7. LARSEN, E. S., AND BERMAN, H. (1934), The microscopic determination of the nonopaque minerals: *U. S. Geol. Surv., Bull.*, **848.**
8. TEMPEL, VON H-G. (1938), Der Einfluss der Seltenen Erden . . . der Epidotgruppe: *Chemie der Erde*, **11,** 525–551.
9. THOMAS, H. H. (1905), On an epidote from Invernesshire: *Mineral. Mag.*, **14,** 109–114.
10. WEINSCHENK, E. (1896), Ueber Epidot und Zoisit: *Zeit. Krist.*, **26,** 161, 433.
11. WINCHELL, A. N. (1927), Elements of Optical Mineralogy, Part II, Description of minerals, pp. 445–452.

Manuscript received May 31, 1956.

FASSAITE FROM NEAR HELENA, MONTANA

Adolph Knopf and Donald E. Lee, *Stanford University, California.*

Abstract

The aluminous pyroxene fassaite, along with spinel, garnet, and the brittle mica clintonite, forms a lode 400 feet long and 8 feet thick, 12 miles southeast of Helena, Montana. The fassaite contains more Al_2O_3 (15.75 per cent) and Fe_2O_3 (6.10 per cent) than any natural fassaite recorded. It strikingly illustrates Tilley's thesis that monoclinic pyroxene associated with spinel in metamorphosed limestone can be expected to contain a notable amount of alumina.

Introduction

Fassaite is the name applied to diopsidic pyroxene relatively high in alumina and ferric oxide, practically devoid of alkalis, and having a content of CaO essentially that of the ideal diopside (Tilley, 1938, p. 87).The balancing of the electric charge in fassaite is accomplished by substitution of aluminum for silicon and of aluminum and ferric iron for magnesium.

Fassaite is found only in environments poor in silica, being usually associated with spinel in contact-metamorphosed limestones. It is probably more widespread than the few descriptions available in the literature would indicate (Tilley, 1938, p. 81). The senior author, who has previously reported fassaite from the contact zone of the Boulder bathylith (Knopf, 1953, p. 1114, 1117), recognized the present occurrence and turned the material over to the junior author for detailed study.

The chemical analysis of the fassaite here given was made possible by the Shell Oil Company through the Shell Grant for Fundamental Research. The writers are indebted also to Dr. C. O. Hutton for helpful advice offered during this study.

Geologic Occurrence

A vertical tabular mass of spinel and silicates occurs on the Knapp ranch, in Lewis and Clark County, Montana. It is several hundred yards southwest of the old Economy mine, 12 miles by road southeast of Helena.

The spinel mass is 8 feet thick; it trends N. 60° W. and dips steeply, probably vertically. It extends 400 feet or more southeastward from the creek bottom to the summit of the ridge, where it ends in a mass composed mainly of vesuvianite, with calcite, diopside, and chondrodite. The spinel mass separates a body of olivine gabbro on the northeast from a body of granogabbro on the southeast occurring along the northern boundary of the Boulder bathylith. It is interpreted to be a limestone septum that has been pyrometasomatically altered.

The spinel lode, as it can be called, consists of black spinel and pale green silicates in roughly equal amounts by volume. The minerals appear to be fairly uniformly distributed and a representative specimen of the rock has a density of 3.45. The spinel is in subhedral crystals which are a millimeter or two in size and are more or less clustered together. The silicates were not identifiable megascopically, except that a micaceous mineral is recognizable, subsequently determined to be the brittle mica clintonite.

Under the microscope the spinel is seen to be associated with pyroxene, garnet, and clintonite, with traces of phlogopite and muscovite, and a secondary mineral resembling jarosite. The mineral that immediately attracts attention is the pyroxene fassaite. It is of most un-pyroxenic appearance, chiefly because of the poor development of its cleavage. It was seen to have a powerful dispersion comparable to that of sphene. The optic axis *B* emerging on sections with rectangular cleavage shows strong dispersion, but the optic axis *A*, emerging perpendicularly on (100), shows no dispersion. Because of its striking properties it was thought desirable to have the fassaite chemically analyzed. Purification of the sample and the quantitative determination of the physical properties of the fassaite and associated minerals is largely the work of the junior author.

MINERALOGY

Techniques.—All optical properties listed were measured in sodium light, and specific gravity values were determined in Clerici solution by means of the suspension method. (In the case of clintonite, methylene iodide was used as the heavy liquid.) Amperage readings for the Frantz Isodynamic Separator are quoted as a measure of paramagnetic susceptibility of the various minerals; in every case the readings apply to a track setting of slope 15° and tilt 12°.

Fassaite.—About three grams of fassaite were purified for analysis and a powder diffraction pattern was obtained for a split from the pure material; this pattern proved to correspond to that of an analyzed diopside, with slight differences in spacing resulting from compositional differences. Other determinations, all made on the material prepared for analysis, are: specific gravity 3.325–3.355 ± .01, average 3.34; $\alpha = 1.712 \pm .003$, $\beta = 1.719 \pm .003$, $\gamma = 1.736 \pm .003$; $\gamma - \alpha = .024$; and dispersion $r > v$, strong. Optic axial angles were measured on the universal stage for five crystals and both axes were observed in every case. The results, all (+), are: 51, 56, 56, 57, and 58°. $Z \wedge c$, the mean of 10 readings made on a section showing a centered flash figure, is 46°; in white light it was determined to be 47°. Only a few of the grains (100-mesh size) were attracted at 0.45 ampere, but all were attracted at 0.60 ampere.

The analysis is given in Table *A*; earlier fassaite analyses have been brought together by Tilley (1938, p. 84). The present example is appreciably higher both in Al_2O_3 (15.75%) and $Al_2O_3+Fe_2O_3$ (21.85%) than any natural fassaite previously recorded. Several studies of synthetic pyroxenes have been made in order to determine the amount of Al_2O_3 that diopside can contain (see for example Schumoff-Deleano, 1917; Zvetkov, 1945; and Segnit, 1953). The results of these studies are not in complete accord, but all indicate that the present occurrence represents at least an approach to the limit of alumina that can be accommodated by the diopside structure. Aside from its low content of SiO_2 and high Al_2O_3 and Fe_2O_3, the Montana fassaite is notable for its extremely high ratio of Fe_2O_3: FeO.

Table A. Fassaite, Lewis and Clark County, Montana
Analyst: Eileen H. Oslund

	Weight per cent	Metal atoms			
SiO_2	41.36	1.537			2.00
Al_2O_3	15.75	.689	.463		
			.226		
TiO_2	.76	.021			
Fe_2O_3	6.10	.170			1.00
MgO	10.34	.576			
FeO	.24	.007			
MnO	.03	.001			
CaO	25.27	1.006		1.01	
Na_2O	.06	.004			
K_2O	.03				
H_2O^+	.10				
H_2O^-	.00				
Total	100.04				

The refractive indices, $Z \wedge c$, and specific gravity of the Montana specimen are all higher than any values previously reported for fassaite. However, several compositional variables are involved, and analytical data are still too few for graphs to be constructed of physical properties against composition.

Spinel.—Spinel comprises about 50 per cent of the rock by volume. The spinel composition appears to average about 30 molecular per cent hercynite and 60 molecular per cent spinel proper, but the compositions suggested by specific gravity, refractive index, and unit cell edge are not mutually consistent. Thus it is apparent that here these properties do not all vary directly with composition in the $FeAl_2O_4$–$MgAl_2O_4$ series. A probable reason is the partial substitution of ferric iron for aluminum and a small amount of other elements for magnesium and divalent iron. A semi-quantitative spectrographic analysis shows about 0.5 per cent Mn. 0.4 per cent Ca, and traces of Cr, Ni, V, Ti, and Ba. Lines for both Mg and Fe are strong, but those for Mg are the more intense.

The mineral is black in grains of 100-mesh size and grass green in thin section; most of the grains are attracted at 0.45 ampere and all are attracted at 0.53 ampere. The following data were recorded: Specific gravity = 3.67–3.77; R.I. = 1.750 ± .004, and the unit cell edge = 8.111 Å ± .002.

Garnet.—On the basis of physical properties and a semi-quantitative spectrographic analysis, the following composition of the garnet is deduced: grossularite, 76–80; andradite (including a possible minor amount of almandite), 15–18, and pyrope, 3–7. Zoning in a few individual grains was noted, but this is rare.

Practically all of the garnet has a specific gravity of 3.60–3.66; further, over 90 per cent is included in the more narrow range of 3.62–3.64. Therefore the latter material was selected for study, and the following properties and values refer to that garnet with a specific gravity of 3.63 ± .01: R.I. = 1.755 ± .005, and unit cell edge = 11.87 Å ± .01. In grains of 100-mesh size the mineral is off-color white, with a slight suggestion of a yellowish hue; as powder, it is chalk-white. The first grains are drawn off at 0.45 ampere, and all are attracted at 0.55 ampere. Thus the paramagnetic susceptibility of the garnet is very like that of the fassaite. Spectrographic analysis shows that the mineral contains about 5 per cent iron, less than 0.05 per cent manganese, and perhaps as much as 2 per cent magnesium.

Clintonite.—The portion of the sample crushed for fractionation work contained about 5 per cent micaceous materials, but some thin sections suggest that this figure is low as an average for the whole rock. Most of this mica has a specfic gravity of 3.08–3.15; a small portion is between 3.00 and 3.08, and practically none has a gravity of less than 3.00 or more than 3.15. The crushed material is leek green in color. In thin section the mineral shows very faint pleochroism, with X = light orange, Y and Z = pale green. Refractive indices are $\alpha = 1.646 \pm .004$ and $\gamma = 1.659 \pm .004$. Cleavage flakes give centered interference figures with $2V = 5\text{–}10°(-)$. The mica is identified as clintonite. This species has previously been reported in contact rocks from the Boulder bathylith: xanthophyllite near Butte by Felts (1947) and clintonite, probably near seybertite, from many localities by Knopf (1953).

CONCLUSION

The notable features of this rock, in addition to the unusual composition of the fassaite, are the complete absence of carbonate and overall simplicity of the mineralogy. Practically the entire rock is composed of four minerals, and so by way of summary the main components of these minerals, as they are known or can be approximated, are listed in Table *B*. Since spinel makes up about half the rock, and none of the silicates present contains as much SiO_2 as anorthite, the overall silica content of the rock must be less than 20 per cent.

TABLE B. COMPOSITIONS OF MINERALS IN FASSAITE-SPINEL LODE, HELENA, MONTANA (Stanford Mineralogy Research Collection Number 7960)

	Weight per cent			
	1	2	3	4
SiO_2	41.36	39–41	—	17–20
Al_2O_3	15.75	18.5–19.5	66–70	39–43
TiO_2	.76	—	Tr	—
Total iron as Fe_2O_3	6.37	4.5– 5.5	9–15	1–4
MgO	10.34	1–3	17–22	20–21
MnO	.03	$>.05$	.3–.7	—
CaO	25.27	33–35	.4(?)	10–14

1. Analyzed fassaite.
2. Garnet, composition deduced from physical properties and semi-quantitative spectrographic analysis.
3. Spinel, composition estimated from physical properties and semi-quantitative spectrographic analysis, but somewhat problematical.
4. Clintonite, composition as suggested by five clintonite analyses listed by Koch (1935, p. 460).

REFERENCES

1. FELTS, W. M. (1947), Xanthophyllite near Butte, Montana: *Geol. Soc. Am., Bull.* **58,** 1179 (abstract)
2. KNOPF, ADOLPH (1953), Clintonite as a contact-metasomatic product of the Boulder bathylith, Montana: *Am. Mineral.*, **38,** 1113–1117.
3. KOCH, G. (1935), Chemische und physikalisch-optische Zusammenhänge innerhalb der Sprödglimmergruppe: *Chemie der Erde*, **9,** 458–461, esp. p. 460.
4. SCHUMOFF-DELEANO, V. (1917), Synthetische Versuche zur Pyroxengruppe: *Zentralbl. f. Min., Geol. u. Pal.*, 290–304, esp. pp. 295–299.
5. SEGNIT, E. R. (1953), Some data on synthetic aluminous and other pyroxenes: *Mineral. Mag.*, **30,** 218–226.
6. TILLEY, C. E. (1938), Aluminous pyroxenes in metamorphosed limestones, with chemical analyses by H. C. G. Vincent: *Geol. Mag.*, **75,** 81–86.
7. ZVETKOV, A. I. (1945), Synthesis of alumina pyroxenes and dependence of their optics on composition: *Mem. Soc. Russe Min.*, Ser. 2, **74,** 215–222. (With English summary, p. 222.) *Mineral. Abstracts*, **XI,** 92 (1952).

Manuscript received June 11, 1956.

A NEW METHOD OF DIFFERENTIAL THERMAL ANALYSIS EMPLOYING MULTIPLE THERMOCOUPLES

William Lodding and Edward Sturm, *Bureau of Mineral Research, Rutgers University, New Brunswick, N.J.*

Abstract

A method is described which permits the investigation of thermal reactions too small in magnitude to be detected by ordinary methods of Differential Thermal Analysis. The *e.m.f.* generated by thermal reactions can be multiplied by placing a number of thermocouples in series. Peak amplitudes in thermograms are increased by a factor directly related to the number of differential couples employed.

Introduction

Differential Thermal Analysis is employed in the analysis and study of minerals which upon heating undergo endothermic or exothermic reactions at characteristic temperatures. In this technique, a differential thermocouple is used (see Fig. 1*a*). One junction is inserted into the test material, while the other junction is placed in a substance which is thermally inert within a given temperature range. The inert and sample materials are heated simultaneously at a constant rate. Endothermic or exothermic reactions taking place in the sample material produce a temperature difference between sample and inert substance, causing an *e.m.f.* in the differential thermocouple. By means of a recorder, these temperature differences can be plotted against the temperature. Endothermic and exothermic reactions register as deviations from the base line.

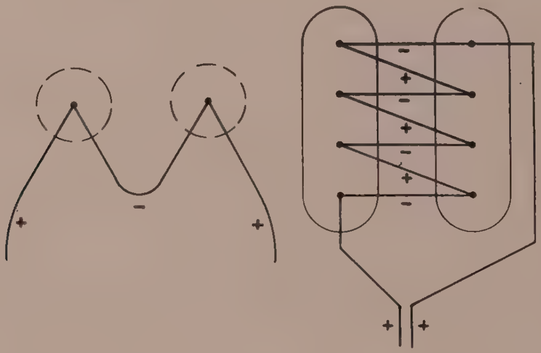

(*a*) (*b*)

Fig. 1. Schematic diagrams of a dual differential thermocouple (*a*) and a multiple differential thermocouple (*b*).

Reactions accompanied by the liberation or absorption of energy, such as decomposition, loss of structural or absorbed water, or phase changes, are recorded as peaks above or below the base line. In order to detect thermal reactions of small magnitude, a *D-C* voltage amplifier is frequently placed in series between the differential thermocouple and the recorder (Kerr, *et al.*, 1949).

Electronic amplification of the weak signal generated by a differential thermocouple has been carried to a practical limit (Rowland, 1955). A full-scale sensitivity range of 50 microvolts has been used by some workers. However, because unavoidable noise is amplified along with the signal generated by the heat of the reaction, investigators rarely attempt to work in high sensitivity ranges.

The method described here results in an increase of the primary *e.m.f.* generated by the temperature difference accompanying the diagnostic chemical reactions. This is achieved by employing several thermocouples connected in series (see Fig. 1*b*). The total *e.m.f.* generated by the multiple thermocouple is directly related to the number of differential thermocouples used.

Multiplication of the original *e.m.f.* within the first stage of the system, rather than amplification in the second stage is proposed here. The stronger signal thus obtained can then be amplified by means of a *D-C* voltage amplifier. The advantage of increasing the primary (frequently small) *e.m.f.* over amplifying a weak signal lies in the reduction of the influence of noise and drift. An amplifier increases the *e.m.f.* due to the latter as well as the signal.

METHOD

The *e.m.f.* developed by a single differential thermocouple can be multiplied a number of times by employing several series-connected thermocouples (Fig. 1*b*). The amplitude of the peaks recorded is directly related to the number of couples making up the assembly. Fig. 3 (*a*) shows a thermogram of quartz obtained with a single couple. Fig. 3 (*b*) shows a thermogram of the same sample of quartz tested with a multiple thermocouple of four units. The peak amplitude of the latter is four times larger than the former. A greater factor of multiplication of peak amplitude may be obtained by using a multiple thermocouple consisting of more units. The principle of multiple thermocouples has been used in calorimetry (Roth and Becker, 1935), in radiation thermopiles (Gier and Boelter, 1941) and others.

One of the difficulties encountered in the standard dual-differential thermocouple assembly is the necessity of accurately centering the couple terminals and equalizing the sizes of the beads. This has to be done in

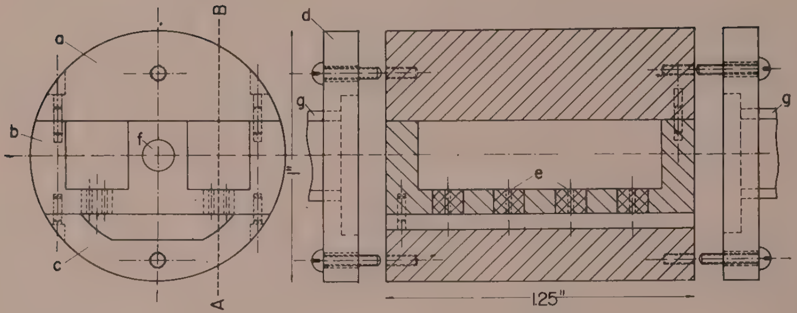

FIG. 2. Specimen-holder for a four-unit multiple differential thermocouple. The line *A-B* refers to the cross-section shown on the right.

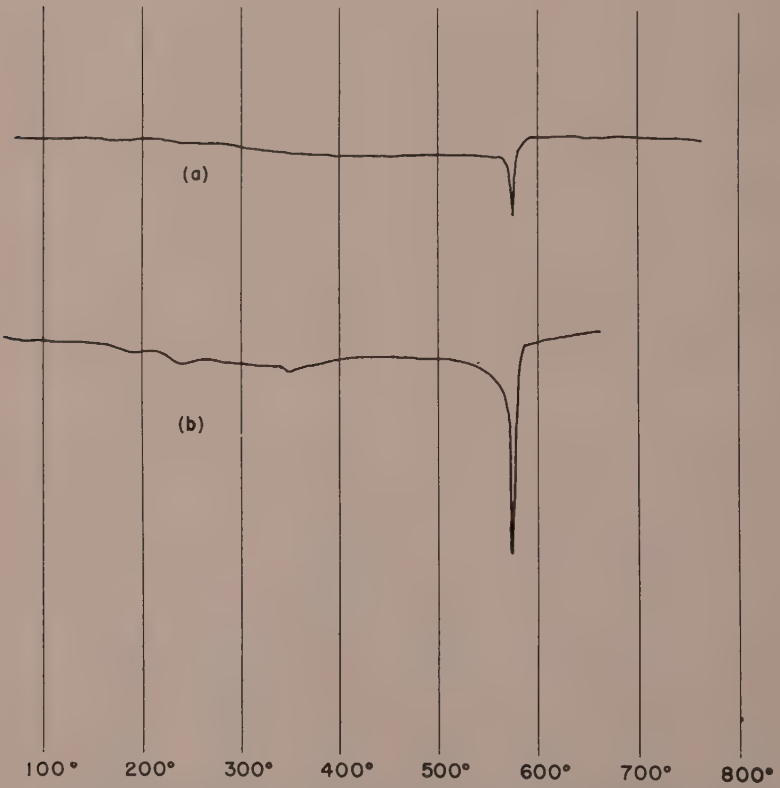

FIG. 3. Thermograms of quartz, (*a*) with conventional unit, (*b*) with multiple differential thermocouple.

order to obtain a straight base line. In the multiple couple assembly, centering of terminals and equalizing of bead sizes is not as critical. Asymmetrical tendencies caused by differences in bead sizes or unequal positioning of the terminals have the tendency to cancel each other out when several units are employed. Further, the larger size of the sample (the cavities hold 1 mm. of sample each or about 1.3 grams) tends to minimize the effects of non-homogeneity and stratification in the sample proper.

The increase in peak amplitude resulting from the increased *e.m.f.* causes the peak slopes to be steeper and thus facilitates the determination of the temperature of reaction. Quantitative work, involving the measurement of areas under peaks (Bramao, *et al.*, 1952), is also facilitated because of the greater ease of determining areas under large peaks.

It is believed that multiplication of the primary *e.m.f.*, as proposed here, will permit investigation of thermal reactions which, because of the difficulties mentioned above, could not be measured heretofore. If the four-unit multiple thermocouple shown in Fig. 1*b* is used in conjunction with a *D-C* voltage amplifier, the full range of sensitivity of 50 microvolts could be extended to 12.5 microvolts. Because, as mentioned above, drift of the base line and unwanted signals due to asymmetry of the dual-thermocouple are almost eliminated in a multiple assembly, the increased *e.m.f.* fed into the amplifier is due to the signal generated by the thermal reaction.

APPARATUS

Figure 2 shows a specimen holder which was designed for use with a four-unit multiple thermocouple. The holder consists of five parts machined from scale-resistant stainless steel.

The central segment (*b*) contains the wells for the sample and the inert substance. The hole (*f*) in the center of the segment (*b*) serves as cavity for the single thermocouple which controls the furnace temperature recorder. Four holes in the bottom of the wells serve to hold short pieces of two-hole porcelain insulator tubes (*e*). The latter support the individual thermocouples. The thermocouples were welded after the wires had been inserted in the insulator tubes. Segment (*c*) is hollowed out to permit space for the wires leading to and connecting the thermocouple terminals. The space also permits the adjustment of the terminals by manipulating the wires leading to them. Segment (*a*) serves as cover to the wells and completes the circular cross-section of the assembled specimen-holder. Small, tapered pins help to align the three segments. The disk-shaped end-plates (*d*) which are of the same diameter as the specimen-holder, complete the assembly. Two quarter-inch diameter tubes (*g*) support and position the specimen-holder in the furnace. The tubes contain two-hole porcelain insulators for the lead wires of the thermocouples. One of the stainless steel tubes can also be connected to a gas supply line if an analysis is to be made in controlled atmosphere (Stone, 1951). The tube on the opposite end then serves as an exit tube for the gas.

References

Bramao, L., Cady, J. G., Hendricks, S. B., and Swerdlow, M. (1952), Criteria for the characterization of kaolinite, halloysite, and a related mineral in clays and soils: *Soil Sc.*, **73**, 273–287.

Gier, J. T., and Boelter, L. M. K. (1941), The silver-constantan plated thermopile: *Temperature* (*Am. Inst. Phys.*) 1284–1292.

Kerr, P. F., Kulp, J. L. and Hamilton, P. K. (1949), Differential thermal analysis of reference clay mineral specimens: *API Proj.* **49**, *Prelim. Rep. 3*, Columbia University.

Roth, W. A., and Becker G. (1935), *Zeits. physik. Chem.*, **174,** 104–114.

Rowland, R. A. (1955), Differential thermal analysis of clays and carbonates: *Bull.* **169,** *Div. of Mines, Cal.* (*Proc. First Nat. Conf. on Clays and Clay Technology*).

Stone, R. L. (1951), Differential thermal analysis of clay minerals under controlled thermodynamic conditions. *Bull.* **146,** *Eng. Exp. Sta., Ohio State University.*

Manuscript received May 19, 1956.

NEW DATA ON FERRITUNGSTITE FROM NEVADA*

D. H. Richter, Laura E. Reichen, and D. M. Lemmon, *U. S. Geological Survey, Washington 25, D. C.*

Abstract

A yellow ocherous mineral from cavities in a limonitic gossan from the Nevada Scheelite mine, Mineral County, Nevada, is shown by *x*-ray diffraction studies to be identical with ferritungstite from the type locality, the Germania tungsten mine, Deertrail mining district, Stevens County, Washington. New data obtained on the ferritungstite from Nevada show that it is tetragonal, commonly dipyramidal; indices of refraction between 2.09–2.15; specific gravity 5.2; three strongest diffraction lines are 5.94, 2.966, and 3.10 Å; probable unit cell dimensions: $a=10.28$ Å, $c=7.28$ Å, and $c/a=0.708$. The new formula is $Ca_2Fe_2^{++}Fe_2^{+++}(WO_4)_7 \cdot 9H_2O$. In the original material from the Germania mine, jarosite was intimately mixed with the ferritungstite, both minerals being very fine grained.

Introduction

In a recent study of tungsten-bearing gossan collected by D. M. Lemmon and Earl Pampeyan from the Nevada Scheelite mine, near Rawhide, Mineral County, Nevada, a yellow ocherous mineral was observed which at first could not be identified by *x*-ray diffraction data or other means. Spectrochemical analysis showed the presence of Ca, Fe, and W, the latter being the most abundant, and it was suggested by W. T. Schaller that the mineral might be ferritungstite, a mineral described by him many years ago (Schaller, 1911).

Kerr (1946) later reexamined the ferritungstite from the same cavity in the type specimen (U. S. National Museum 86985) from which Schaller obtained his analyzed material. In his report on tungsten mineralization, with reference to his *x*-ray studies of the type material Kerr states on p. 78: "*x*-ray data are inconclusive. Five different *x*-ray diffraction patterns have been taken, all of which show minor variations. One pattern agrees closely with jarosite from several localities and also with synthetic jarosite prepared in the laboratory. Others fail to agree exactly either with normal jarosite or natrojarosite, either natural or artificial. All patterns, on the other hand, bear a resemblance to examples of the jarosite group."

Comparisons and measurements of the *x*-ray powder patterns of our mineral from Nevada and of those taken by Kerr on the Germania material showed complete identity of the pattern of the mineral from Nevada with one of the five films (Graf no. 4) taken by Kerr, which film therefore must have been taken of essentially pure ferritungstite. The

---

* Publication authorized by the Director, U. S. Geological Survey.

other four films must have been taken of mixtures of ferritungstite and jarosite.

The hexagonal plates, described by Shaller (1911) and thought by him at that time to be ferritungstite, are now known to have been jarosite, which explains in part Kerr's statement that "All patterns, on the other hand, bear a resemblance to examples of the jarosite group." Most of the samples *x*-rayed by him probably were mixtures of ferritungstite and jarosite. The relatively large hexagonal crystals shown in his Plate 23, facing page 77 (Kerr, 1946), are probably jarosite and not ferritungstite.

That the hexagonal plates of Schaller were jarosite is shown by the following comparison of their determined optical properties.

"Ferritungstite," Larsen (1921), p. 74: $\omega=1.80$, $\epsilon=1.72$. Probably uniaxial
"Ferritungstite," Kerr (1946), p. 77: $\omega=1.815$, $\epsilon=1.716$
Jarosite, Larsen and Berman (1934), p. 90: $\omega=1.820$, $\epsilon=1.715$. Uniaxial
Ferritungstite, this paper. Incides between 2.09–2.15.

Further evidence that much of the original Germania material was a mixture of ferritungstite and jarosite is shown by the results of the partial analysis made by Ledoux and Company on material furnished them by Kerr and given by him (Kerr, 1946, p. 78), namely, $WO_3=20.0$ per cent and $SO_3=17.4$ per cent. These values can be interpreted as representing a mixture of 28 per cent of ferritungstite (new formula) and 55 per cent of jarosite, and if to these figures be added the average value of Schaller's "insoluble," namely 15 per cent, the summation comes to 98 per cent. The sample analyzed by Ledoux and Company then was about $\frac{1}{3}$ ferritungstite and $\frac{2}{3}$ jarosite, after deducting insoluble. This sample probably represents the kind of material on which Schaller observed his hexagonal plates and explains Kerr's statement (p. 78): "One pattern agrees closely with jarosite . . . ," but probably does not represent the kind of material originally analyzed.

Similar conclusions were reached by Graf (1947), who, in an attempt to clarify the problem extended the investigations by Kerr, concentrating chiefly on the synthesis of ferritungstite. His lack of success in this attempt may have been due to the incorrect formula proposed by Schaller. Graf states, after studying the *x*-ray powder pattern of type material (presumably patterns taken by Kerr), that jarosite was more abundant than Kerr had indicated and that the unidentified lines were both consistent in, and common to, all patterns. From these conclusions, Graf reasoned that the SO_3 reported by Kerr (Ledoux's analysis) was due to admixed jarosite, and not, as Kerr intimated, a chemical constituent of ferritungstite. Graf also mentions the possibility that the indices of refraction reported for ferritungstite by Larsen (1921) were actually determined on the associated jarosite.

It is now apparent that the original material on which Schaller based his description of ferritungstite and now nearly all consumed (as only a thin dusty film remains in the quartz cavity) was a mixture of two minerals, both very fine grained, the better crystallized being jarosite and the other being ferritungstite, which apparently was deposited, at least in part, on previously formed jarosite.

Only two other published reports of occurrences of ferritungstite are known and one of these, from the quartz-wolframite deposits at Silvermine, Missouri (Singewald, 1929) has been shown by Graf to be jarosite. The other occurrence has been reported by Kittl (1939) from Cerro Liquinaste, Argentina. Kittl describes "ferritungstite" as a brown mineral with a greasy luster (chestnut brown streak) pseudomorphous after wolframite. The specific gravity was determined as 5.57. These properties are not in accord with those of ferritungstite from either Washington or Nevada.

Occurrence

The Nevada Scheelite mine is in Mineral County, Nevada, approximately 4 miles east of the nearly deserted town of Rawhide. Scheelite was discovered there in 1930, and development of the principal deposit was undertaken in 1936 by Nevada Scheelite, Inc. The mine has been a substantial producer since then, and is now operated as a subsidiary of Kennametal, Inc.

The ore bodies are scheelite-bearing tactite along the contact between granite and limestone of Triassic age (Geehan and Trengove, 1950). The primary ore consists dominantly of andradite garnet accompanied by variable quantities of calcite, quartz, amphibole, epidote, pyroxene, wollastonite, pyrite, chalcopyrite, magnetite, and scheelite. Above the 200-foot level the ore bodies are largely oxidized, and remnants of sulfides are found only in isolated spots. The content of tungsten in the oxidized ore is somewhat greater than in the sulfide ore, due principally to the leaching of gangue minerals during oxidation. The metallurgical recovery from oxidized ore has been unexpectedly difficult and the mill tailings contain nearly a third of the tungsten originally present. It is believed that the tungsten in these tailings occurs largely as very fine grained ferritungstite mixed with limonite.

On the fringes of the oxidized ore bodies, particularly in the footwall against limestone, there are masses of quartzose limonitic gossan that contain very little scheelite but assay several per cent of tungsten trioxide in the form of ferritungstite. The material investigated was collected from two stopes a few feet above the 200-foot level. The gossan contains other secondary minerals in addition to ferritungstite, including bismutite and jarosite, all apparently deposited later than the limonite and possibly contemporaneous with the ferritungstite. No tungstite or hydrotungstite was observed.

The two forms of ferritungstite (crystals and fibers) observed under the microscope seem to be habit modifications and not separate phases. The indices of refraction fall within the same range for the two types, and *x*-ray powder diffraction patterns do not show inconsistent or variable interplanar spacings that might be attributable to two phases.

PROPERTIES

Structural

Probable unit-cell dimensions and contents, as determined from *x*-ray powder patterns, are: $a = 10.28$ Å, $c = 7.28$ Å, $c/a = .708$, cell volume $= 769.3$ Å^3, S.G. (calc.) $= 4.75$ (with $Z = 1$). The *x*-ray powder diffraction data indexed for all interplanar spacings to 1.15 Å are shown in Table 1.

TABLE 1. OBSERVED AND CALCULATED INTERPLANAR SPACINGS FOR FERRITUNGSTITE, INDEXED ON A TETRAGONAL CELL

CuKα radiation, $\lambda = 1.5418$ Å*
Dia. of camera $= 114.59$ mm.

	d(Å)		
I	*Measured*	*Calculated*	*hkl*
10	5.94	5.92	101
9	3.10	3.10	301
10	2.966	2.968 2.970	311 202
6	2.572	2.572 2.570	222 400
3	2.361	2.362 2.359	103 411
½	2.294	2.298 2.299 2.302	420 331 113
1	2.101	2.099	402
5	1.979	1.979 1.980	501, 431 303
8	1.819	1.820 1.817	004 440
5	1.738	1.739	413
½	1.625	1.626	442
3	1.569	1.569 1.568	433 541
7	1.550	1.550 1.551	602 513
3	1.485	1.485 1.484	404 622

* CuKα_1 ($\lambda = 1.54050$ Å) radiation for interplanar spacings below 0.8739 Å.

TABLE 1—(*continued*)

I	*d*(Å) *Measured*	*d*(Å) *Calculated*	*hkl*
4	1.441	1.440	701
		1.442	105
4	1.341	1.340	305
		1.339	543
2	1.286	1.286	444
		1.285	800
½	1.257	1.257	415
		1.256	741, 811
1	1.188	1.188	435, 505
5	1.180	1.180	515
		1.180	733
		1.179	751
		1.179	822
4	1.150	1.149	662
		1.151	226
2	1.129		
2	1.079		
3	1.051		
2	1.035		
½	0.9948		
6	.9902		
1	.9602		
1	.9285		
1	.9105		
3	.8989		
1	.8739		
6	.8700		
4	.8575		
2	.8492		
2	.8270		
4	.8139		
2	.7871		
6	.7850		
6	.7758		

There are still certain features of ferritungstite that, in light of our present knowledge of the mineral, are difficult to explain. The odd number of large $WO_4^=$ groups in a tetragonal mineral and the discrepancy between measured and calculated specific gravity necessitate definition by single-crystal and other studies when suitable material is found. Still another problem is the presence of ferrous iron in a mineral supposedly deposited in an oxidizing environment.

Physical and Optical

Ferritungstite occurs as a bright-yellow ocherous powder lining and filling cavities in the limonitic gossan. Ferritungstite is tetragonal (Fig. 1); crystals dipyramidal, some exhibiting prismatic faces, and also commonly in small fibers. The crystals and fibers are translucent, have

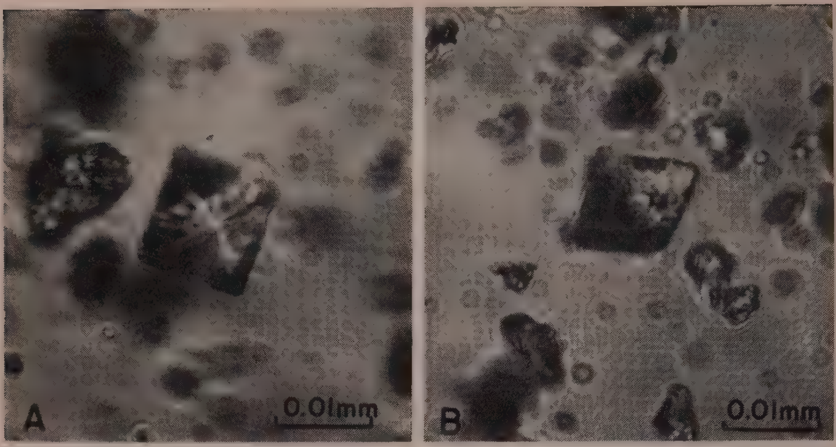

Fig. 1. Ferritungstite crystals. (*A*) Normal to *c*-axis showing four tetragonal pyramid faces. (*B*) Crystal resting on pyramid face showing dipyramidal character.

exceedingly high relief and are very small; the largest single fragment observed was approximately 0.025 mm. in diameter. The optical character and exact indices of refraction were not measurable because of the minute size of the crystals, but n is between 2.09 and 2.15. The specific gravity of the analyzed sample, determined with a fused silica Adams-Johnston pycnometer is 4.89; after correcting for approximately 6.5 per cent quartz as an impurity, the probable specific gravity of ferritungstite is 5.2.

Chemical

A 500 mg. sample was carefully hand-picked for chemical analysis (Table 2). The derived formula is $Ca_2Fe_2^{++}Fe_2^{+++}(WO_4)_7 \cdot 9H_2O$. Ferritungstite is decomposed with difficulty in hot HCl.

Briefly, the analytical procedure used was as follows: water, tungsten, total iron, and calcium were determined on one portion, and ferrous iron and insoluble material on another. Water was determined by measuring the loss of weight when the sample was ignited, with subsequent correction for oxidation of divalent iron. The sample was then fused with sodium carbonate, leached with water, and filtered to separate the tungsten from the iron and calcium. Tungsten was determined polarographically in a supporting electrolyte of 4.5 molar hydrochloric acid and 0.1 molar tartrate. The total iron and calcium were determined according to the usual gravimetric procedures for silicate rocks. The sample for the divalent iron determination was boiled gently for 3 hours in 10 ml. of

TABLE 2. CHEMICAL COMPOSITION OF FERRITUNGSTITE FROM NEVADA

	Chemical analysis	Recalculated to 100%	Moles	Mole ratios	Theoretical chemical composition
WO_3	67.70	72.61	0.3131	6.8	73.75
Fe_2O_3	6.84	7.33	0.0459	1.0	7.26
FeO	6.07	6.51	0.0906	2.0	6.52
CaO	5.62	6.03	0.1075	2.3	5.10
H_2O	7.01	7.52	0.4178	9.0	7.37
SiO_2 (quartz)	6.56				
Total	99.80	100.00			100.00

Formula: $Ca_2Fe_2^{++}Fe_2^{+++}(WO_4)_7 \cdot 9H_2O$.

concentrated hydrochloric acid under an atmosphere of carbon dioxide. After cooling, the divalent iron was titrated with permanganate in 5 per cent sulfuric acid containing about 10 per cent Zimmerman-Reinhardt solution. The solution was then filtered through a sintered glass crucible, the tungstic acid dissolved with ammonium hydroxide, and the residue weighed as insoluble material.

Trace amounts of lead, strontium, magnesium, sodium, potassium, copper, manganese, titanium, and uranium are also in the sample.

The chemical formula given in this note is at considerable variance with that originally presented by Schaller. The research reported here shows that Schaller analyzed a mixture of ferritungstite and jarosite.

ACKNOWLEDGMENTS

We wish to thank Paul F. Kerr of Columbia University for sending us his *x*-ray powder pattern of the type material, D. L. Graf for the loan of his master's thesis on ferritungstite, Janet Fletcher for the spectrographic analysis, and W. T. Schaller for his participation in our discussions of the problem and our arrival at a new formula.

REFERENCES

GEEHAN, R. W., AND TRENGOVE, R. R. (1950), Investigation of Nevada Scheelite, Inc., deposit, Mineral County, Nevada: *U. S. Bur. Mines, Rept. Inv.* **4681.**

GRAF, D. L. (1947), A study of the mineral ferritungstite: Unpubl. master's thesis, Columbia University.

KERR, P. F. (1946), Tungsten mineralization in the United States: *Geol. Soc. America, Mem.* **15.**

KITTL, E. (1939), Nuevos hallozgos de minerales en la república: *Soc. Argentina de Minería y Geología, Rev. Minera,* **10,** 78–81.

LARSEN, E. S. (1921), The microscopic determination of the non-opaque minerals: *U. S. Geol. Survey, Bull.* **679.**

——— AND BERMAN, H. (1934), The microscopic determination of the nonopaque minerals: *U. S. Geol. Survey, Bull.* **848.**

SCHALLER, W. T. (1911), Ferritungstite, a new mineral: *Am. Jour. Sci.*, 4th ser., **32,** 161–162.

SINGEWALD, J. T. (1929), Greisen and associated mineralization at Silvermine, Missouri: *Econ. Geology*, **24,** 569–591.

Manuscript received June 9, 1956.

STORAGE OF ENERGY IN METAMICT MINERALS*

SHELDON F. KURATH, *Department of Chemistry, University of Wisconsin.*

ABSTRACT

A number of radioactive minerals have been studied by means of differential thermal analysis. The amount of heat evolved in heating under nitrogen and the radioactivity of these minerals have been quantitatively determined.

Metamict minerals are capable of storing appreciable quantities of energy from radioactivity in the form of atomic displacements within the crystal. These minerals which were originally crystalline, have had their crystal structures partially destroyed by the radioactive disintegration of uranium, thorium and their radioactive decay products which are present in the mineral. The fast moving alpha particles and recoiling parent nuclei interact with the atoms present at the lattice sites, displacing them and causing the partial disordering of the crystal structure. Accompanying this rearrangement of the crystal lattice is the storage of energy together with marked changes in the physical and optical properties of the minerals.

If the disordered crystal is annealed by raising the temperature, the original crystal structure is reconstituted with the evolution of heat. Faessler, in making a calorimetric study of the mineral gadolinite, observed the evolution of heat amounting to 89.1 cal./gm. (2). Kerr and Holland (4) also noted the evolution of heat in performing thermal analysis experiments on davidite, fergusonite, priorite and other metamict minerals.

Morehead and Daniels (5), using differential thermal analysis, reported the evolution of heat amounting to 25 cal./gm. for one polycrase mineral. The experimental work described herein is an extension of this work, carried out with improved apparatus, in an attempt to find still larger quantities of stored energy.

DIFFERENTIAL THERMAL ANALYSIS

The theory underlying the use of thermal analysis to determine heats of reaction is discussed by many investigators (5, 9, 10, 13). Two samples are placed in adjacent holes within a metal sample block. One sample is thermally active, (i.e. exhibits an absorption or evolution of heat) the other is thermally inert. Both samples are then heated at a uniform rate. If heat is absorbed by the active sample, by fusion or a polymorphic transition, the temperature will fall below that of the inert material.

---

* More complete details of this investigation may be obtained from the Ph.D. thesis of Sheldon F. Kurath filed in the library of the University of Wisconsin, 1953.

Such temperature differences, measured with a differential thermocouple, appear as minima in the curve when plotted against the temperature. Similarly the evolution of heat from a chemical reaction or the release of energy stored in the displacement of crystal units will place the active sample at a temperature higher than the inert sample and give a maximum in the curve. Such maxima and minima are shown in the differential thermal analysis (*DTA*) curves of Fig. 1. The areas under the peaks are proportional to the heat evolved (10).

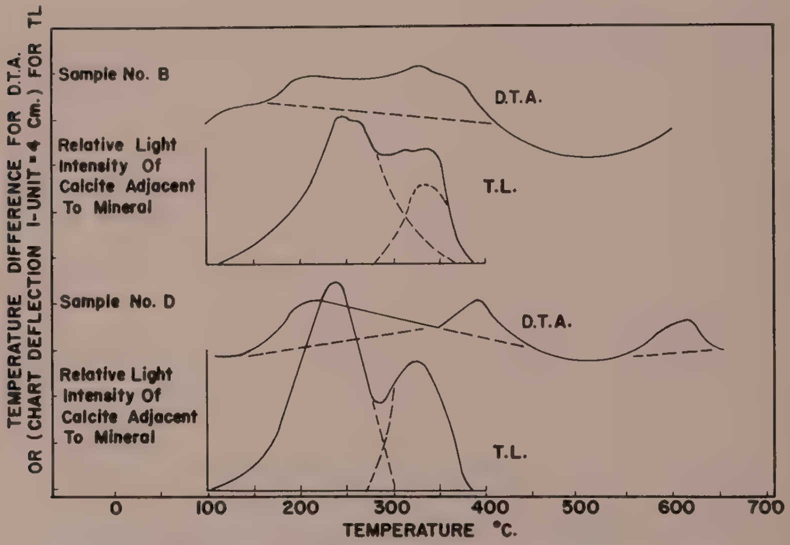

DIFFERENTIAL THERMAL ANALYSIS CURVES FOR ELLSWORTHITE AND THERMOLUMINESCENCE CURVES FOR ADJACENT CALCITE

FIG. 1

EXPERIMENTAL

The apparatus used in this investigation is similar to an improved differential thermal analysis apparatus developed by Whitehead and Breger (11). A small stainless steel cylinder 1″ by $\frac{7}{8}$″ in diameter contained two holes $\frac{1}{4}$″ in diameter which served as sample holders. One hole is the holder for the thermally active material and the other contains thermally inactive alumina. A thermocouple, placed in a small hole between the two sample holes, serves to measure the mean temperature of the sample holder. The temperature difference betweeen the inert and active samples is measured by means of a chromel—"*P*"—alumel differential thermocouple. The out put potential from the differential thermocouple is fed in to a Liston Becker Model 14 D.C. amplifier. After amplification, the potential is recorded on a Brown Model 142 two-pen continuous potentiometric recorder. The differential temperature and the temperature of the sample holder are recorded simultaneously. The sample holder is heated by means of a nichrome wound alundum tube furnace. Both sample holder and furnace were constructed to fit inside of a heavy steel cylinder. The cylinder was made so that it could be evacuated, purged with nitrogen and then operated under nitrogen at reduced pressures.

The most convenient manner in which to evaluate the area under the thermal analysis peaks, is to run heating curves on substances having known melting and inversion points. If the weight of the sample and the heat of fusion are known, the area under the curve can be evaluated in terms of cal./cm.^{2} /gm. as described by other authors (1, 5, 12). The sample weights ranged from 0.1 to 0.01 g. The following materials whose heats of fusion are well known were used for calibration in the present work; Bi, Pb, anhydrous $CdCl_2$, PbI_2, Zn and Al.

All samples were heated from room temperature up to 700° C. under nitrogen at reduced pressure, (10 mm). Mineral samples which had been annealed for reference material under nitrogen at 700° C. to remove exothermic maxima or peaks in the *DTA* curves were also analyzed thermally. The differential thermal analysis curves of both active and annealed samples were then compared before determining the area under the peaks of the active samples.

Measurements of the radioactivity exhibited by the minerals were also carried out. The apparatus used in radioactivity measurement included a scaling unit model No. 162 made by Nuclear Instruments and Chemical Corporation, and was equipped with a radiation counter type D-33 operated at 1200 volts D. C. and having a mica window with a stopping power of 3.5 mg./cm^2. Samples were placed 0.2 mm. from the mica window of the geiger tube. Checks were made with scintillation counters, sensitive only to alpha particles, to convert the readings into alpha ray activity. The alpha activity of these minerals, which are in radioactive equilibrium, was from $\frac{1}{4}$ to $\frac{1}{6}$ of the total activity determined by geiger counting. The alpha activity was estimated by multiplying the geiger count values by the appropriate factor.

RESULTS

The results of thermal analysis experiments and radioactivity measurements are presented in Table 1. The temperatures at which *DTA* peaks were observed are reported along with the heat evolved or absorbed. The radioactivity is reported in terms of alpha counts/min./cm.^{2} emitted from the surface of the sample. Typical differential thermal analysis curves are shown in Fig. 1 for several samples of ellsworthite.

TABLE 1. RADIOACTIVITY AND STORED ENERGY IN METAMICT MINERALS

Sample	Peak temperature °C.	Heat evolved cal./gm.	Radioactivity α counts/min./cm²
Ellsworthite			
A[a]	none	none	2,170
B[b]	flat 112–517° C.	18.6	2,220
C	197	1.8	2,200
	302	5.5	
	405	13.9	
	608	43.1	
		Total 64.3	
D[b]	215	5.4	2,280
	395	4.0	
	615	28.3	
		Total 37.7	
Fergusonite			
A[c]	680	49.4	1,080
	543	7.8	
		Total 57.2	
B[d,e]	210–417°	7.2	900
	440	15.2	
		Total 22.4	
C[e]	440	4.6	770
D[d,e]	none	none	700
E[f]	633	64.9	800
	360	2.2[f]	
	183	1.9[f]	
		Total 64.9	
F[g]	680	36.6	150
	619	27.3	
	347	1.0[f]	
	176	1.8[f]	
		Total 63.9	

[a] Samples from MacDonald Mine, Bancroft, Ontario, collected by Dr. D. F. Saunders.

[b] Examined by x-ray and found to yield no x-ray diffraction pattern.

[c] Sample from Dr. J. C. Rabbitt of the U. S. Geological Survey.

[d] Examined by x-ray and found to yield no x-ray diffraction pattern.

[e] From J. J. Goll Mine, Madawaska, Ontario.

[f] Heat was absorbed instead of evolved.

[g] From Baringer Hill, Texas, collected in 1902 by Marshall Hanks.

TABLE 1—(*continued*)

Sample	Peak temperature °C.	Heat evolved cal./gm.	Radioactivity α counts/min./cm.^{2}
Sammarskite			
A[c]	640	3.2[f]	1,000
	510	5.2	
	200	9.4	
		Total 14.6	
B[c]	650	44.2	1,450
Euxenite[a]			
	610	32.8	1,900
	395	15.4	
	305	0.9[f]	
	135	6.0[f]	
		Total 48.2	
Exchynite-priorite[c]	515	46.3	870

Ellsworthite: Experimental data on four samples of ellsworthite $CaO \cdot Nb_2O_5 \cdot 2H_2O$) are given in Table 1. Typical *DTA* curves for samples *B* and *D* are shown in Fig. 1. They indicate evolution of heat at several different temperatures. Although the samples were obtained from the same locality and had similar amounts of radioactivity, they failed to yield the same peak structure in the heating curve. Surprisingly, sample *A* yielded no peak structure even though highly radioactive. The failure of this sample to evolve heat is probably due to the fact that the sample was not heated to a high enough temperature. Other investigators have noted exothermic peaks as high as 980° C. (4), but it was not possible with the present equipment to go above 700° C. In the case of sample *C* the differential thermal analysis yielded four distinct peaks.

All of these samples were imbedded in salmon colored calcite which was found to exhibit a high degree of thermoluminescence. Thermoluminescence glow curves labelled *TL* are presented in Fig. 1 for the calcite adjacent to the ellsworthite for samples *B* and *D* as obtained with a photomultiplier tube.

Fergusonite: Sample *A* was kindly given to us by Dr. J. C. Rabbitt of the U. S. Geological Survey. Three samples, *B*, *C* and *D*, were obtained from the J. J. Goll Mine at Madawaska, Ontario. Samples *E* and *F* were given to us by Mr. Marshall Hanks from a collection which he had made in a pegmatite cerium mine in 1902 at the Baringer Hill of Texas.

The results are given in Table 1. As in the case of ellsworthite, samples *B*, *C* and *D* from the same location yielded different thermal analysis peaks although they all had about the same radioactivity. Sample *D* showed no evolution of heat even though it was highly radioactive and metamict in character as shown by the absence of *x*-ray diffraction patterns. Presumably this sample would have yielded an exothermic heat of reaction at temperatures above 700° C. (2). Samples *E* and *F* gave small endothermic peaks which may be due to dehydration.

Samarskite, Euxenite-Polycrase, Eschynite-Priorite: A limited number of samples of other minerals were also found to evolve heat when their temperatures were raised. Two samples *A* and *B* of samarskite were kindly given to us by Dr. J. C. Rabbitt of the U. S. Geological Survey. The euxenite sample came from the MacDonald Mine at Bancroft, Ontario. The eschynite-priorite sample was given by Dr. J. C. Rabbitt. The results are presented in Table 1. All of these minerals were highly radioactive and evolved large amounts of heat during differential thermal analysis. As in the case of fergusonite, endothermic peaks may be traced to the evolution of water of hydration.

Minerals Indicating No Energy Storage

Two samples of allanite were found to have no stored heat releasable below 700°, even though they had radioactivity counts of 103 and 81 counts/min./cm.^{2} respectively. Two samples of cyrtolite yielded radioactive counts of 525 counts/min./cm.^{2} and gadolinite and zircon had counts of approximately 50 counts/min./cm^2. These minerals are found in the metamict state and probably have energy peaks well above 700° C. (4, 6).

Several samples of purple fluorite showed no stored energy although nearly black in color. Uraninite (UO_2) and xenotime similarly exhibited no stored energy. All these minerals had high alpha ray activity. These results support the generalization that highly ionic materials are not found in the metamict state.

DISCUSSION

The majority of the minerals exhibiting energy storage showed complex peak structures in the differential thermal analysis curves. The fact that all of these experiments were carried out in nitrogen, after previous evacuation, precludes air oxidation as a factor in these exothermic peaks. The appearance of a multiple peak structure can be compared with the mineral thorium silicate in which the appearance of several phases was noted (6).

The low-temperature peaks are probably associated with the production of crystalline components of the metamict mineral while the other components remain in their amorphous state. Similarly, the peaks which appear at the higher temperature correspond to the conversion of the other materials to their crystalline form or to the reaction of crystalline components with the surrounding isotropic medium to form an entirely crystalline medium.

In some instances, no energy evolution was observed even though the mineral was highly readioactive. There are a number of explanations for this lack of heat evolution. In the case of zircon, gadolinite, and cyrtolite the energy evolution, in all probability, does not take place in the temperature range from room temperature to 700° C. It is known, for example, that gadolinite evolves energy in the neighborhood of 800° C. (4). This limitation to low temperatures probably accounts for the fact that one fergusonite sample which was known to be metamict, failed to evolve heat in these experiments. Other minerals may have been geologically too young to have sufficient radiation damage to detect and in other cases in which heat was not evolved the radioactivity may have been too low to cause appreciable structural damage (e.g. gadolinite, 50 α counts/min./cm^2).

The data presented in previous sections may be used to estimate the time necessary for a mineral to become metamict. Making the qualified assumption that all the energy from radioactive decay is spent in disrupting the crystal structure, Pabst (6) estimated that it would take a sample of gadolinite (Ytterby), at least 110,000 years to become metamict.

An alternate approach to estimating the time of metamictization is given in the following paragraph. A sample of powdered fergusonite in a deep layer in a 5.3 cm.^{2} dish gave 3,580 alpha counts per minute. Assuming that the alpha particles have an energy of 5.0 mev with a range of 3.5 cm. in air, that the "atomic number" of fergusonite is 70, that the density is 5.7 g. per cc. and that the "atomic number" and density of air are 7.2 and 1.23×10^{-3} respectively, the range of the alpha particles in fergusonite is given by the relation

$$\text{range} = \frac{3.5 \times 1.23 \times 10^{-3}}{7.2}\left(\frac{70}{7.2}\right)^{1/2} = 22.6 \times 10^{-3} \text{ cm.}$$

It can be shown that 25 per cent of the alpha particles within 2.26×10^{-3} cm. of the sample surface may escape to be counted (3). If all the alpha particles that escape the surface of the sample are counted, the alpha particles that are emitted per year per gram of sample may be estimated at

$$\text{alphas/year/gm.} = \frac{3.580 \times 60 \times 24 \times 365}{0.25 \times 2.26 \times 10^{-3} \times 5.3 \times 5.32} = 1.10 \times 10^{11}.$$

A 5 mev alpha particle will give about 10,000 electron-volts of energy in collisions and the recoil atom will transfer about 60,000 electron volts as collision energy making a total of 70,000 ev. (8). If all of the collision energy of the alpha particle and the recoil atom are stored, then every alpha count should represent an energy storage of about 70,000 ev. The rate of energy storage in the fergusonite sample is, therefore,

$$1.10 \times 10^{11} \times 7 \times 10^{4} \times \frac{(1.6 \times 10^{-12})}{(4.18 \times 10^{7})} = 2.95 \times 10^{-4} \text{ cal./gm./year}$$

where $1.6 \times 10^{-12}/4.18 \times 10^{7}$ is a factor to change electron volts per alpha particle into calories. Since the heat evolved upon thermal analysis was 57.2 cal./gram, a minimum time for this highly radioactive mineral to become metamict may be estimated at

$$\frac{57.2}{2.95 \times 10^{-4}} = 198{,}000 \text{ years.}$$

This estimate is to be regarded as a minimum value because only part of the collision energy from the disintegration process will appear as stored energy, much of it being dissipated immediately as heat. Many metamict minerals have a considerably lower content of radioactive elements and would require a much longer time than this to become metamict. Moreover, the efficiency of energy storage decreases as the mineral becomes more metamict and the crystal structure becomes more disordered.

According to other views (7, 8), a 5 mev alpha particle and its recoil atom might produce less than 890 interstitial atoms and if each interstitial atom involves the storage of approximately 10 ev, there would be an energy storage of 8,900 ev per alpha particle. This value is considerably less than the 70,000 ev used in the preceding calculation and would lead to a much longer time requirement for metamictization.

The fact that many of the highly radioactive minerals, which have reasonably simple crystal structures, do not store any energy in the crystal structures suggests that there is something about the complicated crystal lattices of the metamict minerals which holds a dislocated ion or atom of the lattice in its abnormal position so that the disorder will not be annealed out at earth temperature.

Acknowledgment

The author is glad to acknowledge the help of Professor Farrington Daniels under whose direction this research was carried out. He is indebted to the Atomic Energy Commission for financial support of the project which provided him with a research assistantship. He wishes to also thank Dr. Donald F. Saunders, and Dr. John C. Rabbitt who provided some of the metamict minerals.

REFERENCES

1. BARSHAD, I. (1952), Temperature and heat of reaction calibration of the differential thermal analysis apparatus: *Am. Mineral.*, **37**, 667–694.
2. FAESSLER, A. (1942), Untersuchungen zum Problem des metamikten Zustandes: *Zeits. Krist.*, **104**, 81–113.
3. HALLIDAY, D. (1950), Introduction to Nuclear Physics, p. 145, John Wiley and Sons.
4. KERR, PAUL F., AND HOLLAND, H. D. (1951), Differential thermal analysis of davidite: *Am. Mineral.*, **36**, 563–572.
5. MOREHEAD, F., AND DANIELS, F. (1952), Storage of radiation energy in crystalline lithium fluoride and metamict minerals: *J. Phys. Chem.*, **56**, 546–548.
6. PABST, A. (1952), The metamict state: *Am. Mineral.* **37**, 137–157.
7. PELLAS, P. (1954), *Bull. Soc. Franc. Miner. Krist*, **77**, 447–460.
8. SEITZ, F. (1949), On the disordering of solids by action of fast massive particles: *Disc. of the Faraday Society*, **5**, 271–282.
9. SMOTHER, W. (1951), Bibliography of differential thermal analysis. *University of Arkansas Institute of Science and Technology.*
10. SPEIL, S. (1944), Applications of thermal analysis to clays and aluminous materials: *U. S. Dept. of Int., Bur. of Mines, R. I.* **3764**.
11. WHITEHEAD, W. L., AND BREGER, I. A. (1950), Vacuum differential thermal analysis: *Sci.* **111,** 279–281.
12. WITTELS, M. (1951), The differential thermal analyzer as a microcalorimeter: *Am. Mineral.*, **36**, 615–621.
13. WITTELS, M. (1951), Some aspects of mineral calorimetry: *Am. Mineral.*, **36**, 760–767.

Manuscript received June 2, 1956.

NOTES AND NEWS

EFFECTS OF GAMMA IRRADIATION ON PHYSICAL PROPERTIES OF MINERALS

Manuel N. Bass,* *Princeton University, Princeton, New Jersey.*

In connection with studies of radiation damage in zircons it became of interest to know the effects of various types of radiation on crystals. The present study sought to determine the effects of intense gamma irradiation on a number of minerals.

Homogeneous-appearing mineral samples were selected and examined under the binocular and petrographic microscope in the search for pure specimens. Inclusions and bubbles could not be entirely avoided, especially in quartz, fluorite and halite. Of the materials finally selected, a portion was powdered or otherwise prepared for measurement of physical properties. Parts of both bulk samples and powders were packed with glass wool in glass vials, corked and sent to Brookhaven National Laboratory. There they received 1.5×10^8 Roentgens of Co^{60} gamma irradiation. Density of irradiated and non-irradiated portions of all minerals tested and refractive index of most of them were measured. In addition, the 2V's of the micas and the d_{001} dimension of lepidolite were measured.

Densities were measured by a flotation method. After flotation of an 80- 120-mesh powder of a mineral in a CCl_4–$C_2H_2Br_4$ mixture or Clerici solution, the density of the liquid was measured with a Christian Becker liquid-density balance which gives direct density measurements to 0.0001 gm./cc.

Refractive indices were measured in immersion liquids using a temperature-variation and a half-shadow method. Illumination was supplied by a sodium vapor lamp. The 2V's of the micas were measured on a universal stage, and the d_{001} dimension of lepidolite was measured with a North American Philips high-angle spectrometer using Fe $K\alpha$ radiation.

Experimental conditions were kept as constant as possible throughout all measurements in order to minimize systematic differences between measurements on irradiated and non-irradiated materials.

Except for difference in color, no significant differences were detected between irradiated and non-irradiated samples (see Tables 1–4).

Precision measurements by Frondel and Hurlbut (1955, p. 1216) showed that decolorization of smoky quartz by heating at 350° was attended by an increase in the indices of refraction. They (1955, p. 1217) stated that density changes attendant on decolorization of smoky quartz were unknown, but that Frondel had found earlier that the elastic constants of a particular sample had changed appreciably upon decolorization. The color of all glass specimens and all except one quartz specimen (amethyst) in the present study changed to brown or smoky (smoky quartz became smokier) as a result of gamma irradiation. These results suggest that changes in the physical properties of the samples used in the present study may have been induced by the irradiation, but that these changes were too small to detect with the techniques used.

---

* Present address: Dept. of Geology, Northwestern University, Evanston, Illinois.

For each type of fluorite the apparent change of density was within the assigned experimental uncertainty, but in each case the density decreased slightly between 0.001 and 0.003 gm./cc.

Muscovite showed an apparent increase in density and the overlap of the ranges of error of the two measurements was very small. The results on biotite and lepidolite suggest that the result on muscovite was not significant.

Lepidolite showed a significant apparent increase in density (questioned value in Table 1). However, after remeasurement of densities of irradiated and non-irradiated lepidolite, the two values on non-irradiated material and the second on irradiated material lay within a range of

TABLE 1. DENSITY AND REFRACTIVE INDEX MEASUREMENTS

Mineral	Non-irradiated		Irradiated	
	Density	Refractive index (±0.0003)	Density	Refractive index (±0.0003)
Colorless fluorite	3.187±0.005	1.4337	3.183±0.0035	1.4337
Blue fluorite	3.185±0.003	1.4336	3.184±0.002	1.4337
Blue-green fluorite	3.186±0.003	1.4339	3.183±0.0035	1.4336
Pink fluorite	3.187±0.0005	1.4336 1.4337	3.184±0.002	1.4338
Halite	2.164±0.004	1.5439	2.162±0.001	1.5440
Colorless quartz	2.655±0.0055	1.5440*	2.650±0.0035	1.5442*
Amethyst	2.651±0.0035	1.5441*	2.651±0.002	1.5441*
Rose quartz	2.650±0.002	1.5441*	2.650±0.003	1.5442*
Epidote	3.467±0.005		3.465±0.004	
Allanite	3.618±0.013		3.606±0.007	
Muscovite	2.847±0.005	ca. 1.596	2.854±0.003	
Biotite	2.884±0.0035	ca. 1.600	2.884±0.002	
Lepidolite	2.846±0.006	ca. 1.560	2.860±0.001?	ca. 1.5595
	2.844±0.004		2.845±0.004	

* Omega index.

TABLE 2. 2V MEASUREMENTS

Mineral	Non-irradiated	Irradiated
Muscovite	43.1°±0.4°	43.6°±0.4°
Biotite	ca. 5°	8.8°±0.5° 7.3°±0.6°
Lepidolite	47.2°±0.1° 44.9°±0.4° 43.4°±0.1° 32.2°±0.4°	44.3°±0.2° 44.4°±0.1° 44.5°±0.2°

0.002 gm./cc. As a further check, 2V's of several specimens of irradiated and non-irradiated lepidolite were measured (Table 2). Those of irradiated specimens were consistently about 44°; the non-irradiated lepidolite exhibited 2V's ranging generally from 43° to 47°, but one flake showed a quite different 2V of about 32° (in some portions the flake showed a 2V of more than 43°). The d_{001} spacing of three specimens each of irradiated and non-irradiated lepidolite was measured on the assumption that a change in density would likely be reflected in this lattice dimension. All values lay in the range 9.93 to 9.94 Å (see Table 3; note that, among non-irradiated specimens, that with a 2V of 32° showed the most anomalous value). It was concluded that no significant change occurred in the lepidolite.

Observed color changes in those minerals in which it was discernible are presented in Table 4. Only the micas and the initially deeply colored allanite and epidote failed to show a noticeable change.

CONCLUSION

1.5×10^8 Roentgens of Co^{60} gamma irradiation are insufficient to induce, within the limits of experimental error of the present study, significant changes in the density and refractive index of halite, fluorite,

TABLE 3. LEPIDOLITE, d_{001} (Å)

Non-irradiated	9.930 9.939 (2V ca. 32°) 9.934
Irradiated	9.936 9.936 9.941

Table 4. Color Changes upon Irradiation

Mineral	Non-irradiated	Irradiated (bulk)	Irradiated (powder)
Colorless fluorite	colorless	"pure" blue, moderate intensity	very light blue
Blue fluorite	light purplish blue	bluish purple, moderate intensity	very lightly colored
Blue-green fluorite	light blue-green	deep blue-green	deep blue-green
Pink fluorite	very light pink	purple with patches of blue like that of irradiated colorless fluorite; moderate intensity	(powder lost)
Halite	colorless	deep brown	brownish gray
Colorless quartz*	colorless	brown (between irradiation smoky and irradiated rose in intensity)	smoky (between irradiated smoky and irradiated rose in intensity)
Amethyst	purple, somewhat variegated, light intensity	purple, variegated, moderate intensity	no visible change
Rose quartz*	light pink	brown (smoky), very intense	gray-brown (smoky), intense
Smoky quartz*	light gray-brown	no change	intensification of smoky color
Epidote	moderate to dark green	no change	no change
Allanite	dark brown or black	no change	no change
Muscovite	colorless	no change	——
Biotite	dark brown to black	no change	——
Lepidolite	pink	no change	——
Vial glass	colorless	deep brown	——
Glass slide	colorless	deep brown	——
Pyrex(?) tubing	colorless	moderate brown	——
Cover glass	colorless	light brown	——

* Relative intensities of brown color or smokiness in those quartzes showing it, from most to least intense: irradiated rose, irradiated colorless, irradiated smoky, non-irradiated smoky.

quartz, epidote, allanite, muscovite, biotite and lepidolite; in the 2V's of the three micas; and in the d_{001} spacing of lepidolite. Color changes are quite striking in many colorless and light-colored minerals and glasses.

Acknowledgments

This study was supported by Office of Naval Research contract *Nonr-250 (00)*, *NR-081–149* with Princeton University. The problem was

suggested by Dr. H. D. Holland, and was carried out at Princeton University during 1951 and 1952. Dr. Holland and Dr. H. H. Hess showed a continued interest during the course of the work. The writer is indebted to them for many helpful suggestions and for critically reading the manuscript.

REFERENCE

FRONDEL, C., AND HURLBUT, C. S., JR. (1955), Determination of the atomic weight of silicon by physical measurements on quartz: *Jour. Chem. Phys.*, **23**, 1215–1219.

URANOTHORITE NEAR FOREST HOME, SAN BERNARDINO COUNTY, CALIFORNIA*

D. F. HEWETT AND JEROME STONE, *U. S. Geological Survey, Washington, D. C.*

The intensive search for uranium in southern California during recent years is yielding discoveries of some uncommon uranium and thorium minerals, some of which occur under unusual or unique geologic environments. The presence of uranium minerals near Forest Home, San Bernardino County, was brought to the attention of D. F. Hewett early in 1955 by Pierre George, an amateur collector of minerals, of San Gabriel. After some preliminary tests of the materials collected by Mr. George, the area was visited by D. F. Hewett in April. Laboratory work by Jerome Stone and others of the U. S. Geological Survey has confirmed the presence of uranothorite and several other thorium-bearing minerals at several localities near Forest Home.

Forest Home P. O. is on the south side of Mill Creek, due south of San Bernardino Mountain, in the principal valley that drains the south slopes of San Bernardino Mountain (Fig. 1). Eastward from Forest Home, the successive tributaries of Mill Creek from the north are Lost Creek, Alger Creek, and Falls Creek. The uranothorite locality is an opencut on the east slope of Alger Creek valley about 300 feet above the creek and about 3,000 feet north of the point where Alger Creek joins Mill Creek. A rough road follows Alger Creek to an ore bin, and a chute extends up the slope to the opencut. The opencut is about 30 feet long and it is limited by a vertical wall about 15 feet high. During 1954, a few tons of material, probably less than 10 tons, were sorted and shipped for its content of uranium. The names of the owners or shippers are not known.

At another locality, higher on the ridge west of Alger Creek, several

---

* Publication authorized by the Director, U. S. Geological Survey.

prospect pits have yielded similar material but no ore has been shipped; several claims have been located by Mr. Gilliam and associates of Rialto, Calif.

The eastern half of the San Bernardino Mountains is within the San Gorgonio quadrangle, the geologic features of which have been studied and described by Vaughan (1922). According to Vaughan, Mill Creek valley coincides with a large fault, one of the San Andreas fault zone.

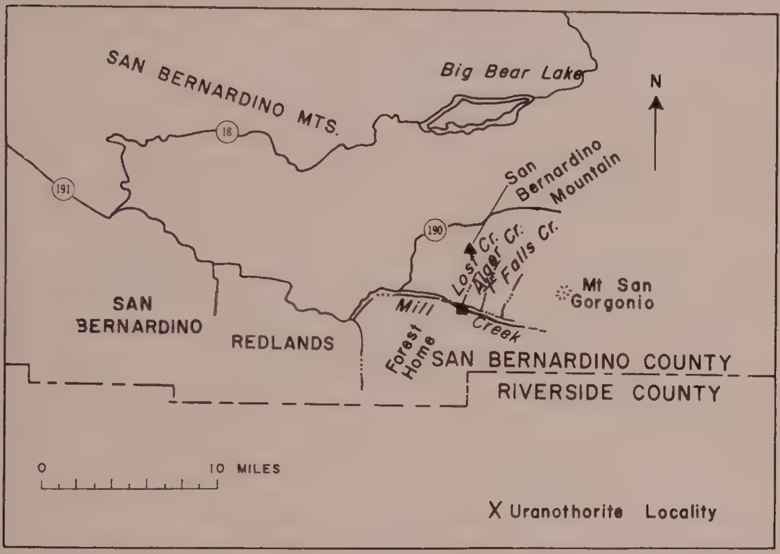

FIG. 1. Index map of Forest Home Area, San Bernardino County, California.

San Bernardino Mountain lies within an area about 4 by 7 miles, north of the fault, underlain by probable Precambrian "undifferentiated schists," which range from thinly laminated biotite schists to fine-grained gray granite gneiss. Along Alger Creek, the lamination trends west to northwest and dips southwest to steeply northeast; at the open-cut east of Alger Creek, the strike of the lamination is N. 30° to 40° W. and the dip is 35° to 40° SW.

The large body of schist and gneiss which includes San Bernardino Mountain is surrounded by and probably underlain by younger "heterogeneous plutonic rocks" of undetermined but probably Mesozoic age. These rocks have not been found along Alger Creek and Lost Creek. Cactus granite (Vaughan, 1922), probably of Jurassic age, underlies large areas on the north slopes of the San Bernardino Mountains, but is not known along Alger Creek.

On the ridges east and west of Alger Creek, the prevailing gray granite gneiss is sporadically replaced by reddish-brown feldspar in such a manner that specimens of the resulting rock resemble pegmatite. These bodies of rock, however, do not have the sharply defined boundaries commonly shown by bodies of pegmatite. In the opencut east of Alger Creek, the body of reddish-brown feldspathic rock is roughly lenticular with the larger dimensions parallel to the lamination of the gray granite gneiss; the maximum thickness is about 15 feet. The borders of this lens are not sharp but show gradual transition into the gneiss. All uranothorite thus far found is within the reddish-brown feldspathic rock; at no place nearby is the gneiss radioactive.

The explored body of reddish-brown rock is largely feldspar and quartz, but it contains sporadic poorly defined lenses of dark minerals. The most abundant feldspar is microcline, but a little orthoclase and microperthite are widespread; a little sodic plagioclase also is present. Curved laminae composed of plates of biotite are present in the feldspathic rock. The most abundant dark mineral is magnetite in lenticular aggregates of small grains; ilmenite has not been noted. Intimately associated with the magnetite are small crystals and grains of allanite, uranothorite, and zircon. The quantities of dark minerals in the feldspathic lens vary greatly from place to place. Some layers are wholly magnetite and show no radioactivity; other layers, an inch or more thick contain as much allanite and uranothorite as magnetite.

Allanite was identified by an *x*-ray diffraction pattern; a spectrographic analysis by K. E. Valentine of the U. S. Geological Survey is as follows:

Over 10 per cent—Si
5–10 per cent—Fe, Ce
1–5 per cent—La, Nd, Al, Ca
0.5–1.0 per cent—Pr, Th
0.1–0.5 per cent—Mn, Y

This mineral has a high magnetic susceptibility and was therefore easily removed from the sample. All of the allanite was concentrated in the magnetic fraction of the Frantz isodynamic separator at vertical and horizontal settings of 10 degrees and 0.3 ampere.

Uranothorite is dark brown and has a greasy to adamantine luster. It has a mean index of refraction of 1.79. The magnetic susceptibility of uranothorite and zircon were about the same, because they were concentrated in the magnetic fractions at the vertical and horizontal settings of 10 degrees and 0.7 ampere. Superficially the two minerals have a similar physical appearance, but uranothorite is dark brown and commonly occurs as anhedral grains and subhedral crystals; zircon is pale brown and occurs as small subhedral to euhedral tetragonal prisms in aggregates of magnetite, allanite, and biotite. The uranothorite was handpicked and identified by an *x*-ray pattern. A spectrographic analysis by Helen Worthing of the U. S. Geological Survey is as follows:

Over 10 per cent—Si, Th
5–10 per cent—U
1–5 per cent—Al, Fe, Pb
0.1–1.0 per cent——

Recently, Neuerberg (1954) has described the mineralogy and features of a large pegmatite dike that crops out on the south wall of the South Fork of Pacoima Canyon, Los Angeles County, Calif., about 90 miles west of the Alger Creek deposits. The pegmatite in Pacoima Canyon contains an assemblage of minerals similar to that here described, including very large euhedral crystals of allanite and zircon, and much smaller crystals and grains of uranothorite; it also contains sparse grains of beryl and apatite which are not recognized at Alger Creek. In contrast, however, the pegmatite in Pacoima Canyon presents definite, sharp boundaries to the host rock, norite, which is a border phase of a large mass of anorthosite, whereas the Alger Creek body is much smaller and shows transitional boundaries to the host rock, granite gneiss.

References

Neuerberg, G. W. (1954), Allanite pegmatite, San Gabriel Mountains, Los Angeles County, California: *Am. Mineral.*, **39,** 831–834.

Vaughan, F. W. (1922), Geology of the San Bernardino Mountains north of San Gorgonio Pass: *Univ. California Dept. Geol. Sci., Bull.* **13,** 319–341.

IDENTIFICATION OF THE 14 Å CLAY MINERAL COMPONENT

Tsuneo Tamura, *The Connecticut Agricultural Experiment Station, New Haven, Conn.*

In clay mineral identification an 00*l* spacing of 14 Å which does not expand with glycerol treatment is attributed to chlorite and/or vermiculite. Differentiation is accomplished in several ways; one is based on the collapse of the 14 Å spacing to 10 Å when vermiculite is saturated with potassium. It has been reported that vermiculite found in some soils resists collapse by this method when a salt such as KCl is used. Collapse has been achieved when hot KOH+KCl or NH_4F were used (2, 4). However, both treatments are relatively drastic. Rich (4) reports that NH_4F should be limited to five minutes to minimize clay destruction and that prolonged treatment with KOH+KCl was also found to be destructive.

Since the soils of New England contain high amounts of the 14 Å component which resists collapse with KCl treatment, studies were conducted to characterize this component as well as to develop a procedure which would be less destructive than the NH_4F or KOH+KCl treatment. The results obtained thus far are highly significant in identifying the 14 Å component found in these soils and should caution against the use of NH_4F or KOH+KCl.

Only the clays in the two lower horizons of a New Jersey Brown Podzolic soil (Table 1) exhibited an 18 Å spacing diagnostic for montmorillonite after treatment with calcium chloride and glycerol with and without free iron oxide removal. Heating the clays at 100° C. with N KCl gave the same results except that the montmorillonite clay showed a 14 Å spacing. Applying the NH_4F+KCl treatment used by Rich (4), the clays showed varying degrees of collapse. The montmorillonite sample showed complete collapse to 10 Å. With the exception of the montmorillonite-containing horizon, the mineral identification would be that the 14 Å component is a vermiculite-chlorite interstratified system. Heating the clays to 550° C. showed that spacings greater than 10 Å were still present thus confirming the chloritic component.

Evidence thus far obtained on these clay systems points to hydroxy aluminum ($Al(OH)_2^+$ type) compounds as being responsible for non-collapse of vermiculite (4. 5). On this basis the beneficial action of OH^- and F^- ions is apparent. It was further reasoned that the citrate ion should also complex the alumina; preliminary tests on these clays confirmed this reasoning (5).

Although the free oxide removal treatment used on this system contained sodium citrate as a compound, tests showed that the clays did not change in spacing but the intensity of the patterns were increased. Significantly Barshad (1) has shown that the free oxide removal treatment employing citrate improved the sensitivity of *x*-ray diffraction identification of clay minerals. These clays then were treated for three hours in N potassium citrate (pH=7.3); no changes were noticed in spacing characteristics. However, when N sodium citrate (pH=7.3) was used with calcium saturation and glycerol treatment, the clays from Connecticut and New Jersey expanded; the spacing ranged from near complete conversion to 18 Å in the New Jersey soil to 14–18 Å range in the Connecticut Brown Podzolic soil clays. This series of tests show that the 14 Å component is a montmorillonite-chlorite interstratified system.

These series of tests should caution against the use of NH_4F or KOH treatments as diagnostic for vermiculite if preliminary tests show non-expansion of the 14 Å component with glycerol. Since NH_4F and KOH

TABLE 1. EFFECT OF VARIOUS TREATMENTS ON THE EXPANSION AND CONTRACTION OF THE 14 Å COMPONENT; DATA TAKEN FROM FREE OXIDE REMOVED 50 MGM SAMPLES

The saturating salt, complexing anion and glycerol applications are listed in order

Source and depth (inches)	$CaCl_2$ 0.1 gm.	KCl	KCl 0.1 gm.	NH_4F+KCl Fluoride	K-citrate citrate 0.1 gm.	$CaCl_2$ citrate 0.1 gm.	$CaCl_2$[*] citrate 0.1 gm.
Hartford Co. Connecticut							
0–3	14 vs[†]	14 vs	14 s	—	14 s	18 m 14 m^b	14 w 10 m^b
3–8	14 vs	14 vs	14 s	14 m 10 mw^b	14 s	18 m 14 m^b	14 w 10 m^b
8–18	14 vs	14 vs	14 s	14 m 10 m^b	14 s	18 m 14 m^b	
18–28	14 vs	14 vs	14 s	—	14 s	18 ms 14 m^b	12 w 10 m^b
28–48	—	14 vs	14 s	—	14 s	18 m 14 m^b	14 w 10 m^b
Essex Co. New Jersey							
½–4	14 vs	14 vs	14 s	14 w 12 m^b	—	—	—
4–8	14 vs	14 vs	14 s	14 w 10 w^b	14 s	18 m 14 m	14 m 10 m^b
8–16	14 vs	14 vs	14 s	14 w 10 m^b	14 s	18 ms 14 w	—
16–30	18 vw 14 s	14 vs	14 s	—	14 ms 10 vw^b	18 ms 14 w	14 vw 10 m
30–40	18 s	14 vs	18 vw 14 s	10 ms	14 m 10 w^b	18 s	12 vw 10 s
40–54	18 s	14 vs	18 m 14 m	—	14 m 10 w^b	18 s	—

[*] This sample is the same sample used in the previous column except that it was heated for 2 hours at 550° C.

[†] v=very; s=strong; m=medium; w=weak; b=broad spacing; these letters refers to the intensities of the diffraction maxima and the character of the maxima.

have been used to identify dioctahedral vermiculites, identification would be tentative until the above tests with citrate or its equivalent are made. The "non-expanding" montmorillonite of these soils verifies the laboratory synthesis of this type of mineral by Caillere and Henin who used magnesium saturated montmorillonite made basic with ammonia and dried at 1000° C. (3).

The importance of this identification is exemplified by considering the New Jersey profile. With the identification of montmorillonite below 30 inches, it was difficult to consider the solum as being derived from the underlying material if the 14 Å component was concluded to be vermiculite. However, with the identification of the component as montmorillonite, the pH, base saturation, and clay content can be correlated with the existing information on the genesis of this soil. A detailed report of this investigation will be reported later; this note emphasizes the necessity of testing for expansion even though preliminary tests may show non-expansion before concluding that the 14 Å mineral is vermiculite.

References

1. Barshad, I., The use of salted pastes of soil colloids for x-ray analysis: *Proc. Second National Conference on Clays and Clay Minerals. National Academy of Sciences-National Research Council Publication*, **327,** 209–217 (1954).
2. Brown, G., The dioctahedral analogue of vermiculite: *Clay Minerals Bulletin*, **2,** 64–70 (1953).
3. Caillere, S., and Henin, S., Experimental formation of chlorite from montmorillonite. *Mineralog. Mag.*, **28,** 612–620 (1949).
4. Rich, C. I., and Obenshain, S. S., Chemical and clay mineral properties of a red-yellow podzolic soil derived from muscovite schist: *Soil Sci. Soc. Amer. Proc.*, **19,** 334–339 (1955).
5. Tamura, T., Weathering of mixed layer clays in soils: *Fourth National Clay Minerals Conf.* (In press, 1955).

USE OF THE TERM "ALTERITE"*

Dorothy Carroll, *U. S. Geological Survey, Beltsville, Md.*

Some Dutch mineralogists use the term "alterite" for those mineral grains which are difficult to identify because their optical properties have been changed or altered by weathering processes. Thus, in describing the size-frequency distribution of some heavy minerals from the Rhine near Wageningen, the following minerals are listed by Van Andel (1952, p. 22)—garnet, epidote, alterites, blue-green hornblende, and augite. In his description of the minerals in the Rhine region Van Andel (1952, p. 45) defines alterites as "very fine-grained aggregates of unknown composition. They have probably originated by the alteration of various minerals. In some cases this can be proved by the existence of transitional forms. The word must be understood as a group name that has no mineralogical significance." He goes on to give diagnostic features of alterites such as roundness, lack of extinction between crossed nicols, interference colors evenly gray or variegated, specific gravity ±3.1. In general, "if more than $\frac{3}{4}$ of the grain has been altered, it has been called alterite"; further, "coarse aggregates of epidote in which the individual crystals can still be distinguished, are also called alterites if the particles are not uniformly oriented." Van Andel (1952, p. 46) then describes a number of different kinds of alterites which have been recognized:—aggregate-alterite (with transitions to epidote alterite), epidote-alterite, hornblende-alterite, augite-alterite, saussurite.

---

* Publication authorized by the Director, U. S. Geological Survey.

Recently in North American literature the term alterite has been introduced by Groot (1955) in his study of the Cretaceous rocks of northern Delaware. In his Table IV (p. 32) "alterites" are listed with other heavy minerals in the various formations. The average content of "alterites" based on grain counts, rises to 34 per cent in the Patapsco and Raritan formations, 8 per cent in the Mt. Laurel and Navesink formations and 12 per cent in the Magothy formation. Such grains are present in all the Cretaceous formations examined. In Table III (1955, p. 30) "alterites" are given as characteristic of the mineral suites of the Patapsco and Raritan and the Patuxent. Figure 4 (1955, p. 38) shows very clearly the proportion of "alterites" in the heavy mineral suites of the Patuxent, Patapsco and Raritan formations and Pleistocene deposits at New Castle, Delaware. However, Groot gives no definition of the term "alterite."

In a paper on "Lower Cretaceous heavy mineral suites from the New Jersey and Pennsylvania subsurface" presented by McCallum at the southeastern section meeting of the Geological Society of America in March, 1956, "alterite" was listed among the heavy minerals, similarly with no definition or explanation, though such may well appear in the published paper.

It is felt that use of the term "alterite" merely obscures facts of mineralogical significance and that every effort should be made to identify such mineral grains as completely as possible.

Van Andel's list (*op. cit.*, p. 46) contains minerals that are low on all mineral stability lists (Pettijohn, 1949, p. 380–382), and are exclusively ferromagnesian in composition with the exception of saussurite, which is a feldspar mass more or less completely altered to a mixture of zoisite, new feldspar, actinolite, chlorite, etc. In any heavy residue containing ferromagnesians, grains of "alterite" are likely to be found, but it serves no useful purpose to hide their real identity under this name, even though identification may be difficult. If, for example, a heavy residue consists largely of transported epidote, such as occurs in a stream sand near its source of supply, among the fresh epidote grains there will be many which can be called alterite-epidote, and all stages between fresh epidote and very much altered epidote can be recognized. The composition of such a residue could be stated to be 25 per cent epidote and 50 per cent "alterite" but it would have much greater mineralogical accuracy to state the epidote content as 75 per cent. If "alterite" is to be used at all as a descriptive term, its parent mineral should be stated, but it is preferable to list such grains as altered epidote, or merely to include this altered epidote in the total epidote percentage and to describe the optical characters leading to the identification. Altered grains of amphibole, pyroxene, epidote, biotite, chloritoid, and andalusite observed by the writer are recognized by their variation in optical properties. In strongly weathered soils, for example, amphibole may have been changed to a chloritic or micaceous substance which has the same general appearance as the unaltered mineral but has a lower index of refraction and birefringence. Many such grains do not extinguish under crossed nicols; others have a very low interference color and may even be isotropic. In biotite the interference figure is reduced or lost completely as described by Denison *et al.* (1929), and the mineral, if colored, undergoes a loss of color.

An interesting point about the presence of "alterites" in any heavy residue is that they indicate a stage in the removal of a mineral from its environment. Mineral suites obtained from river sands which are derived from freshly eroded rocks containing ferromagnesian minerals will generally contain altered grains, and it should be recalled that the Dutch mineralogists introduced the term for heavy minerals in river sands where source areas supplied ferromagnesian minerals in some quantity.

The term "alterite" should not be used in the description of heavy minerals obtained from sedimentary formations or from unconsolidated deposits of any kind; there the name serves no useful purpose and obscures mineralogical facts. In the hands of inexperienced mineralogists it will merely be used as a "sack" term.

References

DENISON, I. A., FRY, W. H., AND GILE, P. L. (1929), The alteration of muscovite and biotite in the soil: *U. S. Dept. Agric., Tech. Bull.* **128**.

GROOT, J. J. (1955), Sedimentary petrology of the Cretaceous sediments of northern Delaware in relation to palaeographic problems: *Delaware Geol. Survey, Bull.* **5**.

PETTIJOHN, F. J. (1949), Sedimentary Rocks, New York, Harper & Bros.

VAN ANDEL, J. H. (1950), Provenance, transport and deposition of Rhine sediments. Thesis, Wageningen.

A NEW OCCURRENCE OF MILLERITE

C. D. WOODHOUSE AND R. M. NORRIS, *University of California, Santa Barbara College, Goleta, California.*

INTRODUCTION

A previously unreported occurrence of millerite and other associated nickel minerals was recently observed at the Klau quicksilver mine in the Santa Lucia Range, San Luis Obispo County, California (sec. 33, T 26 S, R 10 E). The only other occurrence of millerite in the southern part of the state is described by Eckel *et al.* (1941) from the nearby Libertad mine.

GEOLOGIC SETTING

Mineralization at Klau occurs along the Los Tables thrust zone, a major structural feature of this part of the coast ranges. At Klau the thrust zone is a mass of gouge and breccia nearly a thousand feet wide. Most of the gouge has been derived from the serpentines of the Franciscan formation which crop out on either side of the fault zone. Most of the brecciated blocks are shales and sandstones of probable lower Cretaceous age. The entire gouge and breccia zone as well as some of the adjacent rocks has been extensively altered by hydro-thermal action which has produced a silica-carbonate rock.

MINERALIZATION

The quicksilver veins at Klau exhibit several groups of minerals which are not commonly associated with cinnabar at other places in California and Nevada. Open cuts made during the past year provided much information on the deposit and the sequence of mineralization. Most of the earlier workings had caved so badly that they were not examined.

The following brief descriptions are confined to the minerals closely associated with the ore deposits and the gouge zone. The most striking mineral associations are found in the silica-carbonate masses in the main vein and in the associated gouge. The shales and sandstones which occur as breccia fragments in the mineralized zone contain little of special interest. Mineralization seems to have occurred in three waves: First, quartz, sparse pyrite and very minor amounts of linnaeite were deposited. Second, chalcedony, millerite and some calcite were deposited. Third, and last, the deposition of cinnabar, sparse metacinnabar and marcasite occurred. The latter two minerals are closely associated with one another. Subsequently, the action of meteoric waters has produced an array of hypergene minerals including morenosite, bieberite, epsomite and a series of hydrous iron sulfates.

Sheaves of slender millerite crystals occur in the chalcedony vugs and in some instances have attached euhedral cinnabar crystals. The cinnabar crystals are usually rhombic, quite clear and present a striking appearance with the brass yellow millerite and sparkling minute quartz crystals which line the vugs. In no instance are the millerite crystals more than a millimeter long, but their perfection and mode of occurrence make them ideal for micromounts. In addition, millerite occurs in quantity in the clay gouge adjacent to the vein together with the green alteration product, morenosite. In some instances, the morenosite gives the gouge a bright apple green color. The abundant millerite, surprisingly, seems to have gone unnoticed in earlier descriptions of the region and the morenosite was called "unidentified sulfates of iron" (Forstner, 1903).

Occurrence of bieberite in several specimens led to a search for the primary mineral, which proved to be linnaeite occurring as microscopic isometric crystals in the fractured vein quartz. Both nickel and cobalt are believed to have been carried by hydrothermal solutions from the serpentines during the formation of the vein system.

Earlier reports on the district referred to all iron sulfides present as pyrite. This is, without doubt, an error because bulk of the observable mineral is marcasite. The crystals have a pale yellow color, a hardness of 6+, an uneven fracture, and are commonly tabular cockscomb or spear-shaped twins. No marcasite was observed growing on the millerite filaments although millerite and cinnabar are intimately associated in this manner. It is quite likely that much of the marcasite is of supergene origin and was one of the last minerals to be deposited. Melanterite, the decomposition product of marcasite, is found as a coating on the walls of the underground drifts and the acid mine waters have the disagreeable odor of decomposing marcasite.

Acknowledgment

Appreciation is expressed to Mr. Edward Tye for this assistance in the field.

REFERENCES

ECKEL, E. B., YATES, R. G. AND GRANGER, A. E. (1941), Quicksilver deposits in San Luis Obispo County and Southwestern Monterey County, California: *U. S. Geological Survey, Bull.* **922-R,** 515–580.

FORSTNER, WILLIAM (1903), The quicksilver resources of California: *California State Mining Bureau, Bull.* **27,** 157–159.

HYDROCUPRITE DISCREDITED[1]

GEORGE SWITZER, *U. S. National Museum, Washington, D. C.*

The name hydrocuprite was proposed for a supposedly new mineral from Cornwall, Pennsylvania by Genth.[2] It was described by Genth as follows:

"Peculiar orange-colored coatings associated with cuprite and magnetite from Cornwall, were first noticed by Prof. W. Th. Roepper, of Bethlehem, who showed them to me several months ago. On a visit to the mines, a short time ago, I secured a considerable number of specimens from the 'big hill' at Cornwall, and proved them to be a new mineral."

"Amorphous; orange yellow to orange red; forms very thin, sometimes raglike coatings upon magnetite; soft."

"On heating looses water and becomes black; contains water and cuprous oxide. It is impossible to obtain from the quantity that I have noticed, enough for analysis; its composition is probably H_2O, Cu_2O."

This is the entire description of the mineral and no subsequent work has been done. In Dana's "System of Mineralogy," 7th edition, it is listed as an "ill-defined, supposedly amorphous, form of Cu_2O with an indefinite amount of water."

Specimens in the U. S. National Museum labelled hydrocuprite from Cornwall, Pennsylvania, fit Genth's description perfectly, and it seems quite certain that they are identical with his "hydrocuprite." This material, on the basis of its *x*-ray powder photograph and optical properties, has been identified as cuprite, variety chalcotrichite. Likewise, specimens in the collection labelled hydrocuprite from Somerville, New Jersey, have been found to be cuprite. The indefinite amount of water found by Genth is not essential water, but rather is surface-held, due to the fine-grained, felt-like nature of the material.

INTERNATIONAL UNION OF CRYSTALLOGRAPHY
FOURTH GENERAL ASSEMBLY AND INTERNATIONAL CONGRESS

The International Union of Crystallography has accepted the invitation of the National Research Council of Canada to hold its Fourth General Assembly and International Congress in Canada from the 10th July to the 17th July, 1957, followed by two Symposia on the 18th and 19th. At the Congress papers will be presented on all aspects of Crystallographic research; the subjects of the Symposia will be "Physical Techniques of Crystallographic Interest" and "Electron Diffraction." Through the co-operation of McGill University and the University of Montreal, the meetings are being held in the City of Montreal. Technical excursions are being arranged. These include a four-day excursion to the iron deposits of the Labrador Trough, a two-day excursion to the asbestos and copper deposits of southeastern Quebec, and a seven-day excursion to the Bancroft and Sudbury areas in Ontario.

---

[1] Published by permission of the Secretary, Smithsonian Institution, Washington, D. C.

[2] Genth, F. A., Prel. Rep. Mineral. Penn., *2nd Geol. Surv. Penn. Rept. of Progress*, **B,** p. 46 (1875).

The Canadian National Committee on Crystallography is acting as the Local Committee of the Congress and has prepared a brochure giving details of the technical programme topics, and accommodation for the Congress. Copies of this have been forwarded to the Secretaries of the National Committees of the Member Countries of the Union. Copies may be obtained from them; from the General Secretary of the Union, Dr. D. W. Smits, Laboratorium voor Anorganische en Fysische Chemie, Bloemsingel 10, Groningen, The Netherlands; or from the Secretary of the Canadian Committee, Dr. W. H. Barnes, Division of Physics, National Research Council, Ottawa 2, Ontario, Canada (envelope to be clearly marked "Personal"); or from the Chairman of the Programme Committee, Dr. W. N. Lipscomb, School of Chemistry, University of Minnesota, Minneapolis, U. S. A.

The Secretary of the U. S. National Committee on Crystallography is Dr. G. A. Jeffrey, The Chemistry Department, The University of Pittsburgh, Pittsburgh 13.

WORLD DIRECTORY OF CRYSTALLOGRAPHERS

The International Union of Crystallography is considering the possibility of preparing a World Directory of Crystallographers. This list would contain the names and addresses of all practicing crystallographers, including advanced graduate students. It is planned to compile a preliminary list in time for the Fourth General Assembly to be held in Montreal, July 10–17, 1957. The secretaries of the national committees (Acta Cryst. **8,** 857, 1955) have been asked to prepare a list of crystallographers in their countries. In many countries a Crystallographic Society does not exist and the compilation of the list becomes difficult. In certain instances a Crystallographic Society does exist, but some mineralogists, ceramists, biologists, etc., who carry on crystallographic work are not members and hence might not be listed in the directory. If there is a possibility that your name may not be included because your country does not adhere to the International Union of Crystallography, or you are not a member of your national Crystallographic Society, or the latter does not exist in your country, send your name and address to the undersigned as soon as possible. Please use English printed letters.

WILLIAM PARRISH
Philips Laboratories
Irvington-on-Hudson, New York, U. S. A.

Professor Arthur L. Parsons, President of the Mineralogical Society of America in 1929 and former head of the Department of Mineralogy at the University of Toronto, died on Jan. 6, 1957, at the age of 83 years.

ERRATUM

The mineral name *niocalite* is misspelled twice in the annual index of Vol. 41 of this journal, on page 969, and also in the "Contents of Volume 41" on page vi, in the November–December issue for 1956.

NEW MINERAL NAMES

Istisuite

M. A. Kashkai and A. I. Mamedov, The new mineral istisuite. *Doklady Akad. Nauk Azerb. S.S.R.*, **11,** No. 1, 21–25 (1955), from an abstract by C. Guillemin in *Bull. soc. franc. mineral. et crist.*, **78,** 617 (1955).

Analysis by F. I. Vekilovoi gave SiO_2 47.69, Al_2O_3 3.94, Fe_2O_3 2.28, FeO 0.14, MgO 0.41, CaO 41.38, MnO 0.09, Na_2O 1.13, H_2O^- 0.02, H_2O^+ 3.47, SO_3 0.26; sum 100.81%, corresponding to $(Na_{.32}Ca_{6.68})(Si_{7.07}Al_{0.93})O_{20.8}(OH)_{3.21}$. Dissolves in HCl on heating. The mineral is monoclinic. The characteristic *x*-ray lines are at 2.919, 3.254, and 1.666 Å. A *D.T.A.* curve shows an endothermic effect at 450°. The mineral is gray; it occurs in elongated prisms and in fibers. Occurs with wollastonite in the skarn zone near Istisu, Dalidag, Little Caucasus.

Michael Fleischer

Carobbiite

H. Strunz, Carobbiit, ein neues Mineral. *Rend. soc. mineralog. Ital.*, **12,** 212–213 (1956).

Carobbi, *Atti accad sci., lettere e arti Modena,* **14,** 1–12 (1936), described small cubic crystals, $n=1.362$, from cavities in lavas from Vesuvius, that were apparently KF. Strunz has re-examined this material and confirms the presence of colorless cubic crystals with cubic cleavage and $n=1.362$. *X*-ray powder photographs indicated a mixture, but 5 of about 30 lines were those of KF, a_0 5.40 Å. Spectrographic analysis showed K and a little Na; micro-chemical tests showed F and a little Cl.

KF	$n=1.352$, a_0 5.34 Å
Carobbiite	$n=1.362$, a_0 5.40 Å
NaCl	$n=1.544$, a_0 5.64 Å

The name is for Professor Guido Carobbi, Institute of Mineralogy and Geochemistry, University of Firenze (Florence).

M. F.

Simplotite

Mary E. Thompson, Carl H. Roach, and Robert Meyerowitz, Simplotite, new calcium tetravanadite from the Colorado Plateau. *Science* **123,** No. 3207, p. 1078 (1956).

Microchemical analysis on about 70 mg. (by R.M.) gave V_2O_4 67.7, V_2O_5 0.5, CaO 11.6, H_2O 18.4, insol. 0.5; sum 98.7%. Qualitative spectrographic analysis by K.E. Valentine indicated Mg and Al 0.1–0.5%, and Na, K, Fe 0.05 to 0.1%. The analysis gives the formula $CaV_4O_9 \cdot 5H_2O$. Simplotite is dark green, nearly black, in coarse aggregates to yellow-green in thin flakes. It is biaxial, negative, $\alpha=1.705$, $\beta=1.767$, $\gamma=1.769$ (all ± 0.002), 2V about 25°, $X=b$ (yellow), Y (green), $Z \wedge c\,58°$ (green), dispersion $r>v$, weak and crossed. $G.=2.64 \pm 0.02$. Very soft. *X*-ray study by M. E. Mrose showed simplotite to be monoclinic, pseudo-tetragonal, space group *C2/m*. The unit cell has a_0 8.39, b_0 17.02, c_0 8.37 (all ± 0.02 Å), $\beta=90°25' \pm 5'$, Z=4, G. calcd. 2.65. Cleavage (010) very easy, micaceous.

Simplotite occurs as hemispherical aggregates of platy crystals at the Peanut Mine, Montrose County, Colo., where it occurs as coatings on fractures in the ore-bearing sandstone with duttonite, melanovanadite, native Se, and an undescribed V oxide. It has also been found at the Sundown claim, San Miguel County, Colo., the Shattuck-Den lease on

Club Mesa, and the J. J. Mine in Paradox Valley, both in Montrose Co., and the Vanadium Queen Mine, San Juan County, Utah. It is found in comparatively unoxidized ore, associated with montroseite, paramontroseite, vanadiferous silicates, uraninite, and coffinite.

The name is for J. R. Simplot, former owner of the Peanut Mine.

M. F.

Kupletskite

E. I. SEMENOV, Kupletskite—a new mineral of the astrophyllite group. *Doklady Akad. Nauk S.S.S.R.*, **108**, 933–936 (1956) (in Russian).

The mineral occurs in lamellar masses up to 5×3×1 cm. in size, consisting of individual plates with perfect cleavage on [100]; it also occurs as fine plates. Monoclinic (or triclinic with small departure from monoclinic symmetry). Color dark-brown to black, streak brown. Hardness about 3.

Analyses gave:

	1	2	3
SiO_2	32.60	33.54	—
TiO_2	12.04	10.64	—
ZrO_2	1.19	none	—
Nb_2O_5	0.66	2.48	4.35
Al_2O_3	1.68	1.00	—
Fe_2O_3	5.44	7.80	—
FeO		5.35	—
MnO	27.65	23.60	20.45
MgO	2.98	1.63	—
CaO	3.60	1.45	—
BaO	—	0.32	—
K_2O	4.38	5.63	—
Na_2O	2.14	2.14	—
H_2O^+	3.83	3.90	—
H_2O^-	1.08	0.80	—
F	1.22	—	—
	100.49	100.28[a]	
$-O=2F$	0.51		
	99.98		
Sp. gr.	3.201	3.229	

Analyst T. A. Burova, V. A. Moleva.

[a] Given as 100.18 in original.

X-ray spectrographic analysis showed the presence of about 1% Sr, 0.2% Rb, 0.1% Ce, 0.1% Nd. Spectrographic analysis showed weak lines of Be, Zn, Ga, and Ta. The analyses agree well with the formula $(K, Na)_2$, $(Mn, Fe)_4(Ti, Nb)Si_4O_{14}(OH)_2$ except that they give for K+Na 1.12 and 1.31 instead of 2. Kupletskite is therefore the manganese analogue of astrophyllite; nearly the entire series from the pure Fe″ end member to analysis no. 1 is known.

X-ray powder data are given for kupletskite and astrophyllite; they are nearly identical. The strongest lines of kupletskite are in Å., 3.505 (8), 2.642 (8), 2.573 (4).

Kupletskite melts easily before the blowpipe to a weakly magnetic dark globule. The dehydration curve shows an endothermal break at 740–800°, probably due to melting. The mineral is soluble in acids. Easily alters to porous black manganese oxides.

Kupletskite is optically biaxial, negative, $2V=79°$, $\gamma=1.731$, $\beta=1.699$, $\alpha=1.656$ (calculated). Strong dispersion, $r>v$. Pleochroic with Z brown to X orange-yellow. Elongation positive.

Kupletskite occurs in four pegmatites of the Lovozero massif of alkalic rocks, Kola Peninsula. It occurs mainly in a natrolite-rich central part of the pegmatites, associated with schizolite and neptunite, also in small amount in the border zone of the pegmatite in microcline and eudialyte which are associated with nepheline and aegirine, and also in small amount in the nepheline syenites themselves.

The name is for the geologists Boris Mikhailovich Kupletsky and Elsa Maximilianovna Bohnshtedt-Kupletskaya.

M. F.

Hibonite

Hubert Curien, Claude Guillemin, Jean Orcel, and Micheline Sternberg, La hibonite, nouvelle espèce minérale. *Compt. rend.*, **242**, 2845–2847 (1956).

The mineral occurs in hexagonal prisms flattened parallel to (0001) or in steep pyramids; the crystals are up to 4 cm. in largest dimension. The face (0001) is commonly divided into 6 sectors. Cleavage (0001) easy, parting on $(10\bar{1}0)$.

Fracture sub-conchoidal. Hardness = 7½–8, G. = 3.84, color brownish-black to black, reddish-brown in thin fragments. Optically uniaxial, negative, $\omega=1.807\pm0.002$, $\epsilon=1.79\pm0.01$; pleochroic with O brownish-gray, E gray. Analysis by Patureau gave SiO_2 1.50, Al_2O_3 74.00, TiO_2 8.50, Fe_2O_3 0.45, FeO 2.30, rare earth oxides 3.50, CaO 6.50, Mg 3.20; sum 99.95%. Spectrographic analysis showed traces of Cu, Cr, Mn, and Na. The radioactivity is weak, corresponding to 1000 ppm Th or 100 ppm U. The analysis corresponds to $(Ca_{1.61}\,Ce\ etc._{0.31})(Al_{20.31}Fe_{0.53}Ti_{1.48}Si_{0.35}Mg_{1.11})O_{37.9}$ or essentially $CaAl_{12}O_{18}$. The mineral is infusible, slowly soluble in a mixture of H_2SO_4 and H_3PO_4.

Laue, rotation, and Weissenberg photographs showed the space group to be $P6/m\,mc$, the unit cell has $a=5.60\ kX$, $c=22.12\ kX$, containing $2(CaO \cdot 6\,Al_2O_3)$. The structure is similar to those of magnetoplumbite $(PbO \cdot 6\,Fe_2O_3)$, the artificial oxide $CaO \cdot 6\,Al_2O_3$, and beta-alumina.

The mineral occurs in an alluvial deposit at Esiva, Fort Dauphin region, Madagascar. Also found in a metamorphosed limestone rich in calcic plagioclase, associated with corundum, spinel, and thorianite.

The name is for P. Hibon, who discovered the mineral. Pronounced Ee′bonite; not to be confused with hibbenite.

M. F.

Karpinskyite

L. L. Shilin, Karpinskyite—a new mineral. *Doklady Akad. Nauk S.S.S.R.*, **107**, 737–739 (1956) (in Russian).

Chemical analysis by V. A. Moleva gave SiO_2 56.68, TiO_2 trace, Al_2O_3 16.40, Fe_2O_3 0.06, BeO 2.58, ZnO 3.26, MgO 0.78, Na_2O 9.18, K_2O 1.55, H_2O^- 2.50, H_2O^+ 5.00; sum 97.99%. (Given as 99.99 in the original and the molecular ratios agree with the figures given. *M. F.*) Spectrographic analysis by A. S. Dudykin showed Ga, Ca 0.X%, Pb, Cu, Zr, Sr, Mn 0.0X%, Nb 0.01%. This gives the formula $(Na_{1.79}K_{0.20})(Be_{0.62}Zn_{0.24}Mg_{0.12})Al_{1.95}Si_{5.71}O_{14.65}$-$(OH)_{3.35}$ or $Na_2(Be,Zn,Mg)Al_2Si_6O_{16}(OH)_2$. The mineral is insoluble in 1:1 HCl, HNO_3, and H_2SO_4. The *DTA* curve shows endothermic breaks at 90°, 540°, and 900°.

Karpinskyite is white with vitreous to pearly luster. Soft, H. not more than $1\frac{1}{2}$–2. Sp. gr. = 2.545, by hydrostatic suspension. Fracture uneven, easily cleavable to fine fibers. Optically uniaxial, positive, with *n*s $\epsilon = 1.518$, $\omega = 1.511$.

The crystals are prismatic, acicular. The hexagonal cell has $a = 14.24$, $c = 4.83$ Å, but the mineral is rhombohedral, with possible symmetry classes D_{3d}, C_{3v}, or D_3. *X*-ray powder data are given; the strongest lines are 3.161 (10), 3.388 (7), 2.463 (7), and 1.741 (7).

Karpinskyite occurs in rosettes of radiating crystals in a pegmatite vein cutting lujavrites on "the northern slope of one of the alkalic massifs." (Kola Peninsula? *M. F.*) Associated minerals are natrolite and albite, the latter partly replaced by karpinskyite. Also mentioned is "a yellow lamellar mineral kozhanovite (karnasurtite)," not otherwise identified (new mineral? *M. F.*).

The name is for A. P. Karpinsky, late President of the Academy of Sciences, U.S.S.R.

Discussion: Calculation of the hexagonal cell content does not give satisfactory results. Further *x*-ray study is needed. This is the first instance of isomorphous substitution of Be by Zn, often postulated previously on the basis of the relations between willemite and phenakite in spite of the large differences in ionic radii.

M. F.

Karpatite

G. L. Piotrovsky, Karpatite—a new organic mineral from Transcarpathia. *Lvovskoe geol. Obshch., Mineralog. Sbornik*, No. **9**, 120–127 (1955) (in Russian).

The mineral was found associated with curtisite (idrialine) and amorphous organic material in cavities at the contact of diorite-porphyry with Flysch argillites. It forms acicular crystals and fibrous, radiating aggregates about 0.05–0.2 mm. thick, up to 5 mm. long. Monoclinic with $\beta = 110°$; goniometric measurements on natural material agree closely with those on material prepared by recrystallization from aniline or by sublimation; cleavage excellent parallel to the length. Hardness about 1, G. = 1.40, melts about 430° with partial decomposition, sublimes if held just below the melting point. Optically biaxial, negative, $\alpha = 1.780 \pm 0.002$, $\beta = 1.977$–1.982, $\gamma = 2.05$–2.15; optic axial plane parallel to length (= X). Analyses by T. G. Sokolov, L. M. Samtsov and L. B. Lebedev gave C 92.22, 92.08; H 4.08, 4.03; O (by diff.) 3.70, 3.89%, corresponding to C:H:O approximately 33.17:17:1 (actually 32.3:16.9:1 *M. F.*). *X*-ray powder diagrams by Ya. L. Giller are different from those of curtisite and hoelite. Apparently named for the locality.

M. F.

Heidornite

Wolf v. Engelhardt and Hans Füchtbauer, with *x*-ray data by *Josef Zemann*. Heidornit, $Na_2Ca_3Cl(SO_4)_2B_5O_8(OH)_2$, ein neues Bormineral aus dem Zechsteinanhydrit. *Heidelberger Beitr. Mineralog. Petrog.* **5**, 177–186 (1956).

The mineral occurs, mixed with an equal amount of glauberite, in a cavity in a drill core at 1968 m. depth in the upper anhydrite of the Zechstein formation on the German-Dutch border northwest of Nordhorn. It is found as terminated (some doubly), transparent crystals up to 7 cm. long. The crystals are steep, spear-like, with the forms {110}, {11$\bar{1}$}, and {11$\bar{2}$} dominant. H. 4–5. G. 2.753 ± 0.002, by suspension in bromoform-methanol.

Analysis by R. Kühn gave NaCl 9.40, Na_2O 5.07, CaO 27.61, SO_3 26.55, B_2O_3 27.99, H_2O^- (105) 0.14, H_2O^+ 3.15, insol. in acid 0.07, sum 99.98 per cent, corresponding to $Na_2Ca_3Cl(SO_4)_2B_5O_8(OH)_2$. Fe was detected in the insoluble residue. The water is given off between 500° and 600° C.

Goniometric study showed heidornite to be monoclinic, $a:b:c=1.29:1:2.37$, β 93°15′. The {11$\bar{2}$} faces and the perfect cleavage on {001} were smooth, but {11$\bar{1}$} and {110} were striated and showed vicinal faces so that measurements were approximate. Weissenberg and rotation diagrams gave a 10.21, b 7.84, c 18.79 Å. (all ±0.5%), β 93°30′±15′, $a:b:c=1.30:1:2.40$. The unit cell contains 4 of the above formula weights. G. calcd. 2.70. The space group is either $C\ 2/_c-C^6_{2h}$ or $Cc-C^4_s$, probably the former, as a positive test for piezoelectricity was not obtained. X-ray powder data are given; the strongest lines in Å. are: 3.11 vs, 3.77 s, 2.74 s, 2.96 ms.

Heidornite is optically biaxial, positive, ns at 587 mμ α 1.579_5, β 1.588_5, γ 1.604_5, 2 V 74° calcd., somewhat variable 63–77° measured, $\beta=b$, $\gamma:a=23°$, dispersion $v>r$.

The name is for F. Heidorn, geologist.

M. F.

Kettnerite

Lubor Zak and Vladimir Synecek. Kettnerite, $(CaF)(BiO)CO_3$, a new mineral of the phosgenite-bismutite group: preliminary note *Časopis mineral. geol.* **1,** No. 3, 195–197 (1956) (Czech with English summary).

The mineral occurs as small brown, brownish-yellow, to lemon-yellow plates in cavities in a quartz vein cutting pegmatitic K-feldspar near Krupka (Graupen), Krušné hory (Erzgebirge), N. W. Bohemia. Associated minerals are fluorite, Bi, bismuthinite, hematite, and altered topaz. Chemical and spectrographic analysis (not given) yield the formula $CaBi(CO_3)OF$. The mineral is ditetragonal dipyramidal, space group $P_4/n\ m\ m$ (D^7 4h) with a_0 3.79, c_0 13.59 A., Z=2. G. 5.80. The name is for Radim Kettner, Professor of geology, Charles University, Prague.

M. F.

Discredited Minerals

Waltherite (=Walpurgite)

E. Fisher, Identität von Waltherit und Walpurgin. *Chemie der Erde,* **17,** 341–345 (1955).

X-ray study of 8 samples of waltherite (presumably a bismuth carbonate) from the type locality showed that it is identical with walpurgite (bismuth uranium arsenate). Microchemical tests showed Bi, U, As, and P, and CO_2 (admixed bismutite?) Other properties including physical properties and c_0 (5.42 waltherite, 5.49 walpurgite) are in good agreement. The name waltherite (1857) has priority over walpurgite (1877), but the description was so inadequate that the name waltherite should be dropped.

M. F.

Alushtite (=Dickite+hydrous mica)

L. V. Logvinenko, and V. A. Frank-Kamenetskii, On the so-called alushtite. *Doklady Akad. Nauk SSSR*, **105**, 554–557 (1955) (in Russian).

Alushtite was described by Fersman in 1907 as a hydrous aluminum silicate from Alushta, Crimea. It is now shown by chemical, optical, *x*-ray, and *D.T.A.* study to be dickite with admixed hydrous mica.

M. F.

Avalite (=chromian illite)

Douchan Stangatchilovitch (Dusan Stangačilović), Sur la présence d'illite chromifère dans le gisement de cinabre d'Avala, près de Belgrade. *Compt. rend.*, **242**, 145–147 (1956).

Avalite was described in 1884 by Losanitch (*Dana's System*, 6th Ed., p. 617) as a chromium-bearing mica, and has since generally been classed as a chromian muscovite (fuchsite). A new analysis gave SiO_2 50.05, Al_2O_3 22.83, Cr_2O_3 12.38, Fe_2O_3 2.33, FeO, MnO none, MgO 0.14, CaO 0.43, K_2O 2.16, Na_2O 0.24, TiO_2 0.40, P_2O_5 tr., H_2O^+ 9.43; sum 100.39%. *X*-ray powder data show the strongest lines at 10.13, 4.91, and 3.68 Å; a line at 7.1 Å indicates the presence of a little kaolinite. Dehydration and *D.T.A.* data also indicate that the material is to be classed as an illite. The mineral was formed by the hydrothermal alteration of a serpentinite.

M. F.

Staszicite (=Olivenite)?

C. Guillemin, Contribution a la minéralogie des arséniates, phosphates et vanadates de cuivre. I. Arséniates de cuivre. *Bull. soc. franc. minéral. crist.*, **79**, 7–95 (1956).

Staszicite was described by Morozewicz (1918) as $(Cu,Zn,Ca)_2AsO_4(OH)$. It was classed in *Dana's System*, Vol. II, p. 806, as a zincian conichalcite, $Ca(Cu,Zn)AsO_4(OH)$. Guillemin, on a sample from the type locality, Miedzianka, Poland, finds the *x*-ray powder pattern to be that of olivenite, $Cu_2AsO_4(OH)$. The sample gave a microchemical test for zinc and is considered to be a zincian olivenite.

Discussion: Guillemin does not comment on the fact that the only analysis of staszicite showed 20.80% CaO, with Ca:(Cu+Zn) nearly 1:1, as in conichalcite.

Further study is needed.

M. F.

Arsentsumebite (=Duftite-α)

C. Guillemin, *op. cit.* *X*-ray study of the original specimen (*Bull. soc. franc. mineral.*, **58,** 4 (1935)) showed it to be duftite-α mixed with a little bayldonite. (See abstract of duftite under New Data.)

M. F.

Parabayldonite (=Plumboan Conichalcite)

C. Guillemin, *op. cit.* Parabayldonite (Biehl, 1919) is shown by analysis and *x*-ray study to be a plumboan conichalcite $(Ca, Pb)CuAsO_4(OH)$, part of the duftite-β-conichalcite series.

M. F.

Cuproplumbite (=Bayldonite)

C. Guillemin, *op. cit.* Cuproplumite (Biehl, 1919) has generally been considered to be bayldonite. This is now verified by *x*-ray powder data on material from Tsumeb.

M. F.

Trichalcite (=Tyrolite)

C. Guillemin, *op. cit.* Trichalcite (Hermann, 1858), supposedly $Cu_3(AsO_4)_2 \cdot 5H_2O$, is found by *x*-ray study of material from the type locality, Turginsk, Ural Mts., to be identical with tyrolite, $Cu_9Ca_2(AsO_4)_4(OH)_{10} \cdot 9\text{–}10H_2O$, as had previously been suggested by Berry, *Am. Mineral.*, **33,** 193 (1948). Material from Shoshone County, Utah, described by Shannon, *Proc. U. S. Natl. Museum*, **62,** art. 9 (1922) as trichalcite is found by *x*-ray study to be the sulfate langite.

M. F.

NEW DATA

Duftite

C. Guillemin, Contribution a la minéralogie des arséniates, phosphates et vanadates de cuivre. I. Arséniates de cuivre, *Bull. soc. franc. minéral crist.*, **79,** 7–95 (1956).

Guillemin finds that there are two minerals of the composition $PbCuAsO_4(OH)$. The type material, here called duftite-α, is orthorhombic and the *x*-ray powder pattern is very similar to those of descloizite and mottramite, so that the space group is probably *Pnma.* Duftite-β is orthorhombic, disphenoidal, space group $P2_12_12_1$ and forms a complete series of solid solutions with conichalcite, $CaCuAsO_4(OH)$. Analyses, optical data, and *x*-ray powder data are given.

Discussion: It would be preferable to drop the terms duftite-α and duftite-β, to restrict the name duftite to what is called here duftite-α, and to rename duftite-β.

M. F.

Lavendulan (Freirinite =Lavendulan)

C. Guillemin, *op. cit.*

Lavendulan was described by Breithaupt in 1837 from Annaberg as a hydrous cobalt-nickel-copper arsenate, and was found by Vogel in 1853 at Joachimsthal, and by Goldsmith in 1877 from San Juan, Chile. Foshag (*Am. Mineral.*, **9,** 29–31 (1924)) found that the Chilean material differed optically from that of Joachimsthal and his analysis of the Chilean mineral led to the formula $Na_3(Cu,Ca)_3(AsO_4)_2(OH)_3 \cdot H_2O$. He therefore decided that the Chilean material was not identical with lavendulan and he gave it the new nmae freirinite.

Guillemin now finds by *x*-ray study that lavendulan and freirinite from the type localities give identical *x*-ray powder patterns. Analyses of a sample from Chile (impure) and of synthetic material show the presence of Cl and lead to the formula $Na(Cu,Ca)_6(AsO_4)_4Cl \cdot 4\text{–}5H_2O$ with Ca:Cu variable, about 1:5 (probably better written $NaCaCU_5(AsO_4)_4Cl \cdot 4\text{–}5H_2O$ *M.F.*). H.$=2\frac{1}{2}$, G.$=3.54$. Orthorhombic, $a=9.73$, $b=41.0$, $c=9.85$ Å, isostructural with sampleite, $NaCaCU_5(PO_4)_4Cl \cdot 5H_2O$.

M. F.

Lindackerite

C. Guillemin, *op. cit.*

New analyses of lindackerite show that the 1853 analysis, which gave the formula $Cu_6Ni_3(AsO_4)_4(SO_4)(OH)_4 \cdot 5H_2O$, was in error. No sulfate was found. Two new analyses gave the formula $H_2Cu_5(AsO_4)_4 \cdot 8\text{–}9H_2O$ with a little Co and Ni replacing Cu. Optical and x-ray powder data and data on dehydration are given. Lindackerite is monoclinic with $a=3.95$, $b=8.02$, $c=6.277$ Å, $\beta=100°30'$.

M. F.